

THE UNIVERSITY OF YAOUNDE I

FACULTY OF SCIENCE

POSTGRADUATE SCHOOL OF
SCIENCES, TECHNOLOGY AND
GEOSCIENCES



UNIVERSITÉ DE YAOUNDÉ I

FACULTÉ DES SCIENCES

CENTRE DE RECHERCHE ET DE
FORMATION DOCTORALE EN
SCIENCES, TECHNOLOGIES ET
GÉOSCIENCES

DEPARTMENT OF EARTH SCIENCE

DÉPARTEMENT DES SCIENCES DE LA TERRE

LABORATORY OF GEOSCIENCE FOR INTERNAL FORMATIONS

AND APPLICATIONS

LABORATOIRE DE GÉOSCIENCES DES FORMATIONS

PROFONDES ET APPLICATIONS

**RECENT STRUCTURAL DATA ON METASEDIMENTS IN
THE WESTERN PART OF YAOUNDE (CAMEROON)**

***NOUVELLES DONNEES STRUCTURALES SUR LES
METASEDIMENTS DE YAOUNDE-OUEST (CAMEROUN)***

A dissertation presented in partial fulfillment of Master's degree in Earth science

Option: Petrology and Structural Geology

By

GOUDJOU NANTCHOU NJIPS LILIANE

Registration number: 18A2142

Bachelor degree in Earth Science



Supervised by

METANG VICTOR

Associate professor

Academic year:2023/2024

DEDICATIONS

To my Parents

ACKNOWLEDGEMENTS

A man's desire to achieve success is totally dependent on him. I would like to express my gratitude to the people who accompanied me and contributed to the completion of this work.

I would like to thank God, for letting me through all the difficulties. I have experienced his guidance day by day. He has been the one who let me finish with my academic degree. His guidance and support lit the path to my success.

Prof BISSO Dieudonné, Head of Earth Sciences Department of the University of Yaounde I for constantly forcing the coat of duty consciousness on all in the department

Prof NZENTI Jean Paul, Head of laboratory of Geosciences for internal Formation and Application of the University of Yaounde I, who accepted my stay in this laboratory. His advice and his rigor are qualities that boosted me during my work from classroom and laboratory.

Prof METANG Victor, for supervising every step of this work. I'm grateful for the opportunity to work with you and learn under your guidance. Thank you for being such a great leader, the way you lead our team is admirable and constantly inspires me to do great work, I know that under your supervision, I will continue to grow in my academic background.

I extend my sincere thanks to all the lecturer of the Earth Sciences Department of the University of Yaounde1, in particular those with advanced training, notably the professors: NKOUMBOU Charles, NJILAH KONFOR Isaac, TCHOUANKOUE Jean Pierre, GANNO Sylvester, NUMBEM TCHAKOUNTE Jacqueline, NOMO NEGUE Emmanuel, TCHATO TCHAPTCHET DE Pesquidoux I; and Doctor's: NGO BELNOUN Rose Noël, TENE Joelle.

I would like to recognize the efforts of my academic elders, members of the Geosciences Laboratory for internal formations and Applications for the numerous scientific exchanges which have contributed to improved this work. Amongst PhD students, special thanks are due to WANDJI-BAMOU Franck Steve, TEDA SOH Arnaud Cédric, KOUAYEP Lysiane, TSASSE NGANNO Achilles Simplicie, FOMEKONG TATANG Carlyle, DIALLO Mamadou Mouctar, Domkam Brigitte, BEFOLO EDOU Guy Gerard for coaching, following up and their trust in me.

I wish to extend my special thanks to my senior, NJUME EWANG Modest, TOYI TCHOUTA Boris, YEMKEU MANFO Berthol, SIMO TATE Boris Joresse for their collaboration during field work and in the laboratory for their help in each step of this work. Whishes a great thanks to all my classmates: SIMO FOSSO Abigaëlle, TANKWA stévie caré, NJIKI BIKOI Suzanne Mathias, MASSOP Clair Durance, MBOU GUEKEU Fabiola Leticia, NDEUGUE TCHOUASSI Raphael Armel, NGUILA Parfait Aimé, ABOUBAKAK OUMAROU, LEUHA Brandon Dyny and MANGAH FONTAH Henry, who contributed in shearing materials and ideas for the building of my academic background over which this work reveals and to my friends: NGONTIE TCHEGNIA Faustin, Kaptchaoung Suzi Phalone, AWANA TIMBA Carine, MAFFO Carlone, KAMWA Steve, Kanna anne for their encouragement and advised.

A special thanks to my sisters: NJIPGANG NJIPSEU Brinda Rotesse, YOUMBI NJIPSEU Linda Vanessa, NONO NJIPSEU Marianne, MEWEBO Myrande, NANKAP NJIPSEU Sandrine Diane, MASSO TAMEGHE Sylvanie, Makoudjou Pricille Luresse, MAFFEUSI Christelle, MAFOGNE Loridane, MAKUNE Ruth Marie, MAWE Naomie Justicia and to my brothers KOUANGO NJIPSEU William, NJOMO NJIPSEU Idriss, and GOBEHI PADJOUÉ Etienne for their love and encouragement in each step of this works.

A special thanks to my uncle KWANGO Jacquard for his financial support through out my academic work, for his advice and love towards my person.

To all my present and past loved ones for all your encouragement and gestures from near and far have enable the development of this dissertation, I thank you from the bottom of my heart.

TABLE OF CONTENTS

DEDICATIONS	i
ACKNOWLEDGEMENTS	ii
TABLE OF CONTENTS	iv
LIST OF FIGURES	vii
LIST OF TABLES	ix
LIST OF ABBREVIATIONS	x
ABSTRACT	xi
RESUME	xii
GENERAL INTRODUCTION	1
CHAPTER I : NATURAL SETTING	4
I.1 .GEOGRAPHICAL SETTING	5
I.1.1. Location.....	5
I.1.2. Climate	6
I.1.3. Orography.....	7
I.1.4 Hydrography and Drainage pattern	8
I.1.5. Vegetation	9
I.1.6. Life stocks/Fauna	10
I.1.9. Economic activities	11
I.2. GEOLOGICAL SETTING	11
I.2.1. Congo craton	12
I.2.2. Pan-African North Equatorial Fold Belt (PNEFB)	13
I.2.3. Previous work of the target site.....	17
CHAPTER II : MATERIAL AND METHOD	19
II.1. MATERIAL	20
II.2. METHOD	21
II.2.1. Field studies	21
III.2.2. Laboratory works.....	21

CHAPTER III: FIELD WORK AND PETROGRAPHY.....	Erreur ! Signet non défini.....
III.1. METASEDIMENTARY UNIT	25
III.1.1. Paleosome	25
III.1.2. Neosome	33
III.2. META-IGNEOUS UNITS.....	33
III.2.1. Amphibolite	35
III.2.2. Staurolite-cordierite gneiss	37
CHAPTER IV: GEOMORPHOLOGY AND STRUCTURAL ANALYSIS.....	40
IV.1. GEOMORPHOLOGY	41
IV.1.1. Orography.....	41
IV.1.2. Hydrographic patterns	44
IV.1.3. Slope identification and analysis.....	46
IV.1.4. Lineament analysis	48
IV.1.5 Fracturing lineament.....	49
IV.2. STRUCTURAL ANALYSIS	51
IV.2.1. D ₁ deformational phase	51
IV.2.1.1. S ₁ Foliation.....	51
IV.2.1.2. B ₁ boudins	51
IV.2.1.3. F ₁ fold	51
IV.2.2. D ₂ deformational phase	53
IV.2.2. 1.S ₂ foliation	53
IV.2.2.2. B ₂ boudins.....	53
IV.2.2.3. F ₂ folds	54
IV.2.2.4. Lm ₂ mineral lineation.....	54
IV.2.2.5 .C ₂ shear	54
IV.2.3. D ₃ deformational phase	55
IV.2.3.1. S ₃ foliation	56
IV.2.3.2. C ₃ . shear.....	56
IV.2.3.3. F ₃ fold	56
IV.2.3.5. F ₃ fracture	56
IV.2.3.4. V ₃ veins.....	57

IV.2.4. D ₄ deformational phase:.....	59
IV.2.4.1. F ₄ fractutre	Erreur ! Signet non défini.
V.2.5. D ₅ deformational phase.....	60
V.2.5.1. C ₅ shear:	60
VI.2.6. D ₆ deformational phase.....	61
VI.2.6.1. F ₆ fracture	61
VI.2.6.2. F ₆ joint.....	61
CHAPTER V : INTERPRETATION AND DISCUSSION	64
V. 1. PETROGRAHY	65
V.2. NATURE OF THE PROTOLITH.....	65
V.3. TECTONIC EVOLUTION.....	66
V.4. CONTEXT AND GEODYNAMIC EVOLUTION OF THE TARGET SITE	67
GENERAL CONCLUSION AND PERSPECTIVES	68
GENERAL CONCLUSION.....	69
PERSPECTIVES	69
REFERENCES	70
ANNEXES	85

LIST OF FIGURES

Figure 1 : Localization map of the target area.....	5
Figure 2 : Ombrothermic diagram in relation to the target site.....	7
Figure 3 :The 3-digital elevation model of the target site	8
Figure 4 : Hydrographic map of the target site presenting the dominant drainage pattern.....	9
Figure 5 : The Pan-African belt of Central Africa.	16
Figure 6 : Sampling map of the target area	24
Figure 7 : Field occurrence of pygmatitic structure	Erreur ! Signet non défini.
Figure 8 : Macroscopic character of migmatites of western-Yaounde	26
Figure 9 : Macroscopic and microscopic character of garnet-biotite gneiss	28
Figure 10 : Macroscopic and microscopic character of kyanite-garnet gneiss	30
Figure 11 : Macroscopic and microscopic character of garnetite	32
Figure 12 : Macroscopic and microscopic characters of quartzite.....	33
Figure 13 : (A-C) Macroscopic character of amphibolites seened at the Mvolye quarry and at the artisanal quarry of Fam-Assi	34
Figure 14 : Microscopic character of amphibolites.....	36
Figure 15 :Microscopic characters of amphibole-biotite gneiss	38
Figure 16 : The orographic map of the target area	41
Figure 17 : The topographic map showing the cross section of the target site	43
Figure 19 : the hydrographic pattern of the target area	45
Figure 20 : The hydrographic lineament of the Target site and the directional rosette of hydrographic lineaments extracted from the SRTM image	46
Figure 21 : The slope map of the target area and its surrounding digitalize from an SRTM image	47
Figure 22 : Lineament analysis map of the target site and the directional rosette of the lineament of map extracted from an SRTM images.	48
Figure 23 : The ridge line map of the sector and its surrounding and the directional rosette of the ridge line map extracted from an SRTM image	49
Figure 24 : The fracturing line map of target area and the directional rosette of the fracturing line map digitalize from an SRTM image.....	Erreur ! Signet non défini.
Figure 25 : Structural elements observed at the D1 deformatal phase	52
Figure 26 : Stereographic representation of the F1 foliation planes of the target sitecyclographic traces.....	53
Figure 27 : Structural elements related to the D ₂ deformational phase	55

Figure 28: Rosette directional diagram of F₃ fracture. 57

Figure 29: Structural elements observed at the D₃ deformational phase 58

Figure 30: structural elements related to the D₄ deformational phase..... 59

Figure 31: Stereographic representation of F₄ fracture 60

Figure 32: Structural elements related to the D₅ deformational phase..... 61

Figure 34: Structural elements related to the D₆ deformational phase found at the Nomayos quarry and the hill of Mvogt-Betsi and Oyomabang 59

LIST OF TABLES

Table 1: Average climatic data of the Mbankomo station taken over a period of 10 years 6
Table 2: Summary of the different rock type of the study area 39
Table 3: Summary of the different phases of deformation of the target site. 63
Table 4: Summary table of the different sample collection coordinates. 86
Table 5: Foliation planes measurements and some fractures direction 87

LIST OF ABBREVIATIONS

Abbreviation of minerals (after Whitney and Evans, 2010)

Amp	: Amphibole
And	: Andalousite
AP	: Apatite
Bt	: Biotite
Cd	: Cordierite
Grt	: Garnet
Kfs	: Alkaline feldspar
Ky	: Kyanite
Mc	: Microcline
Ms	: Muscovite
Opq	: Opaque mineral
Px	: Pyroxene
Py	: Pyrite
Qtz	: Quartz
Spn	: Sphene
Std	: Staurolite
Tur	: Tourmaline

OTHER ABBREVIATIONS

CAF B	: Central Africa Fold Belt
CC	: Congo Craton
CCSZ	: Cameroon Central Shear Zone
GPS	: Global Positioning System
PABB	: Pan-African Brazilian Belt
PNEFB	: Pan-Africa Nord Equatorial Fold Belt
SF	: Sanaga Fault
SIG	: Geographic information system
SRTM	: Shuttle Radar Topography Mission
TBF	: Tibati Banyo Fault
TTG	: Tonalite-trondjemite-granodiorite
WGS84	: World Geodetic System (1984 revision)

ABSTRACT

This study presents the western part of Yaounde as a portion of the southern domain, found within the PNEFB. It aims to bring new structural information concerning the tectonic evolution of the western part of Yaounde, based on the combined field survey, lithological and satellite image processing methods.

Petrographic study revealed two lithological units: (i) the metasedimentary units (migmatites) composed of Kyanite-biotite gneiss, Garnet-biotite gneiss, garnetite and quartzite and (ii) the meta-igneous unit (metadiorites) composed of amphibolites. Mineralogical assemblages range from amphibolite facies ($\text{Amp} + \text{Kfs} + \text{Qtz} \pm \text{Grt}$, $\text{Kfs} + \text{Qtz} + \text{Amp} + \text{Bt} + \text{Pl} + \text{Spn} + \text{Grt} \pm \text{Cd} \pm \text{Std}$) to granulite facies that is Kyanite-biotite gneiss ($\text{Bt} + \text{Grt} + \text{Qtz} + \text{Ky} + \text{And} + \text{Kfs} \pm \text{Px}$), biotite–garnet gneiss ($\text{Bt} + \text{Grt} + \text{Kfs} + \text{Qtz} + \text{Pl}$), garnetite ($\text{Grt} + \text{Bt} + \text{Qtz} + \text{Ky} + \text{And} + \text{Kfs} + \text{Pl} \pm \text{Px}$) and finally quartzite ($\text{Qtz} + \text{Bt} \pm \text{Op}$). These assemblage shows that the target site is characterized by medium-pressure (MP), medium-temperature (MT) to high temperature (HT) metamorphic facies. The target site where emplaced during continental Syn-collisional zone preceded by subduction.

Analysis of the metamorphic rocks based on structural information, characterized the rocks as an imprint of poly-phased progressive deformation with 6 phases of monocyclic tectonic evolution. Here, D_1 and D_2 showed two major events of ductile deformation in which the D_1 characterize compression that led to an S_1 horizontal to sub horizontal foliation, B_1 intra-foliated boudins, on one hand while the D_2 marked transposition of D_1 structures by dextral C_2 shears, symmetrical F_2 folds. The ductile-brittle D_3 is marked by the development of dextral C_3 shear, F_3 fold. While D_4 consist of F_4 fracture, C_4 shear. The D_5 deformation phased is characterized by a brittle-ductile deformation which is composed of C_5 shearing and finally, a D_6 deformation phase characterized by vertical brittle deformation.

Key word: Metasediments, Deformation stage, western-Yaounde, southern domain

RESUME

Cette étude présente la partie Ouest de Yaoundé comme une portion du domaine sud, retrouvé au sein de la ceinture plissée Panafricaine. Elle vise à déterminer des informations structurales récentes concernant l'évolution tectonique de la partie Ouest de Yaoundé, sur la base des méthodes combinées d'enquête de terrain, lithologiques et de traitement d'images satellitaires.

L'étude pétrographique a révélé deux unités lithologiques : (i) L'unité méta-sédimentaire composée de (gneiss à disthène et biotite, gneiss à grenat et biotite, grenatite et le quartzite) et (ii) l'unité meta-ignéé (metadiorites) composé d'amphibolites. Les assemblages minéralogies vont du faciès amphibolites (**Amp +Kfs +Qtz ±Grt, Kfs +Qtz +Amp + Bt+ Pl+ Spn + Grt ± Cd ± Std**) au faciès granulite c'est-à-dire gneiss à disthène et biotite (**Bt+ Grt+ Qtz+ Ky+ And +Kfs ± Px**), gneiss à biotite et grenat (**Bt + Grt+ Kfs + Qtz + Pl**), grenatite (**Grt + Bt +Qtz+ Ky+ And+ Kfs+ Pl± Px**), et le leucosomes (**Qtz +Bt ± Op**). Ces assemblages montrent que le secteur d'étude est caractérisé par des faciès métamorphiques à moyenne pression (MP) moyenne température (MT) à haute température (HT). Les roches du secteur d'étude ont été mis en place dans un context continentale de pré-collisionnel précédée d'une subduction. L'analyse des roches métamorphiques basée sur les informations structurales montre une empreinte de déformation progressive polyphasée avec 6 phases d'évolution tectonique monoclinique. Ici, la D_1 et D_2 ont montré deux évènements majeurs de déformation ductile dans lesquels la phase D_1 est caractérisée par une compression qui a conduit à une foliation horizontale à subhorizontale (S_1), des boudins intra-foliaux, d'une part, tandis que la phase D_2 est marquée par la transposition des structures D_1 par des cisaillements dextres C_2 , des plis symétriques P_2 , La phase D_3 est ductilo-fragile et est marquée par le développement d'un cisaillement dextre C_3 , d'un pli P_3 , tandis que la D_4 est caractérisée par une fracturation F_4 , d'un cisaillement C_4 . La D_5 est progressive et est caractérisé par une déformation fragile-ductile qui est composé de cisaillements C_5 et enfin la D_6 qui est marqué par une déformation fragile verticale.

Mot clés : Métasédiments, Phase de déformation, Yaoundé-Ouest, domaine sud.

GENERAL INTRODUCTION

Geologically, Cameroon is characterized by two large lithostructural Precambrian bedrock: (i) the Ntem complex representing the northern part of the Congo Craton which extends into the central republic with the Bomu complex and (2) the Pan-African Nord Equatorial Fold Belt in Central Africa (Penaye et al., 1993; Toteu et al., 2001, 2004).

The Congo craton is a sub-circular mass with sectional area of about 5,711,000 km², covered by a Paleozoic to recent formations which makeup the Congo basin (Shang et al., 2010). The Kaapvaal, Zimbabwe, Tanzania, and the West African craton, which is made up of part of the modern tectonically stable continent of Africa formed about 3.6-2.0 Ga, bounded by younger fold belts (Toteu et al., 2001). This craton extends from the central southern Africa, in the Kasai region (D.R.C), towards Sudan and Angola, cropping as part of Gabon, Cameroon and Central African Republic, with a small portion prolonging towards Zambia named the Bangweulu block (Ernst et al., 2013). The aforementioned craton and its counterpart, the Sao Francisco craton, are resulting from a rigid Gondwana that splitted, leading to the opening of the south Atlantic Ocean (Barbosa et Sabate., 2002; Pedrosa- Soares., 2008; Babinski., 2012).

The PNEFB belongs to a major Neoproterozoic continent-scale orogenic structure extending from Brazil (Sergipano Fold Belt) to Sudan (Oubanguides) and considered to result from the collision of several continental blocks including the Sao Francisco and Congo Craton to the south, the West-African Craton and the Latea and Saharan metacraton to the north (Toteu et al., 1991 ; Castaing et al., 1994; Abdelsalam et al., 2002; Liégeois et al., 2003; Oliveria et al., 2006 ; Ngako et al., 2008 ; Nkoumbou et al., 2014) The PNEFB in Cameroon is subdivided into three lithotectonic domain : the Northern, Central and Southern domains (Nzenti et al., 1992, 1994; Ngnotue et al., 2000; Toteu et al., 2004; Tchakounte et al., 2017; Tchakounte et al., 2021). The southern domain in which the target site belongs has been the subject of numerous works such as Nzenti et al. (1988), Metang et al.(2022a), Metang et al. (2022b), Mvondo et al. (2007), Betsi et al. (2020). Also known as the southern group of the Pan-African Nord Equatorial Fold Belt in Cameroon, the domain comprises the lower Dja and Yakadouma series (Vicat et al., 1997), the low-grade Ayos-Mbalmayo-Bengbis series, and the medium- to high grade Yaounde series (Nzenti et al., 1988). This domain covers the center-south of the country and is located in the equatorial rain forest zone Metang et al, (2014) and consists of metasedimentary and meta- igneous rocks recrystallized under medium and high pressure conditions (600-800°C; 9-12kb) Metang et al. (2022a). The work of Mvondo et al. (2007); Owona et al. (2011); Metang et al. (2014) present 4 Phases deformational that affected the metasediments of Yaounde.

Recent work like that of Bissaya et al. (2023) mentions a multistage deformation of the Yaounde metasediments with 6 phases of deformation. These inconsistent results on the structural data of the metasediments obviously raise questions about the tectonic evolution of the PNEFB. With this in mind, the detailed field work on the metasediments of western Yaounde could certainly shed light on the number of deformation phases. The opening of several artisanal and industrial quarries would be an asset for making more observations and taking a lot of measurements.

The main objective of this study is to determine the exact number of deformation phase that affected the metasediments of the western portion of Yaounde. The specific objectives include:

- The inventory of the different petrographic types.
- The taking of structural measurements.
- The classification of structural measurements in the deformation phase.
- Mapping of all the outcrop points of the metasediments of western-Yaounde

Apart from a general introduction and conclusion, this master's dissertation consists of five chapters.

- Chapter I: Natural setting;
- Chapter II: Equipment and Methodology;
- Chapter III: Fields work and Petrography;
- Chapter IV: Geomorphology and Structural analysis;
- Chapter V: Result and Interpretation;

CHAPTER I : NATURAL SETTING

I.1.2. Climate

Records obtained from the meteorological station of Mbankomo presented in table 1 shows that the average annual precipitation and temperature of the sector are 1540/ mm and 23.3°C, respectively. Based on the graph obtained from this table, the highest precipitation peak falls in the month of October, indicating a great deal of rainfall (290 mm). while the almost linear horizontal brown bar of temperature, defined an almost constant level of heat and or cold although the year. This variation in precipitation and slight modification of the temperature may account for the dense equatorial rainforest in the sector. Following this data, (Tab. 1) an ombrothermic diagram (Bagnoul and Gaussen, 1957) was plotted to show the annual variations in precipitation and a relative slight modification of temperature concurrent to the target sites provides a four seasonal climatic regime (Fig. 2).

- an extensive dry season comes December to February;
- while a short rainy season, from March to June;
- then a short dry season from July to August
- and finally, an extensive rainy season from September to November;

The aforementioned interpretation helps us to conclude that the governing climate in this site is the equatorial climate (Olivry, 1986). Note that the minimum and maximum portions of the ombrothermic diagram may account for both the respective dry and humid periods within the year.

Table 1: Average climatic data of the Mbankomo station taken over a period of 10 years (2013-2023).

Month	Jan	Feb	Mar	Apr	May	Jun	Jul	Aug	Sep	Oct	Nov	Dec	Average
P (mm)	20	60	140	180	200	150	50	70	200	290	120	20	1540=Accumulation
T(°C)	48	48	48	46	46	44	44	44	44	44	46	46	46,66=Average temperature

Source: www.Weather base.com, consulted on the 8/11/2023 at 3.42 PM.

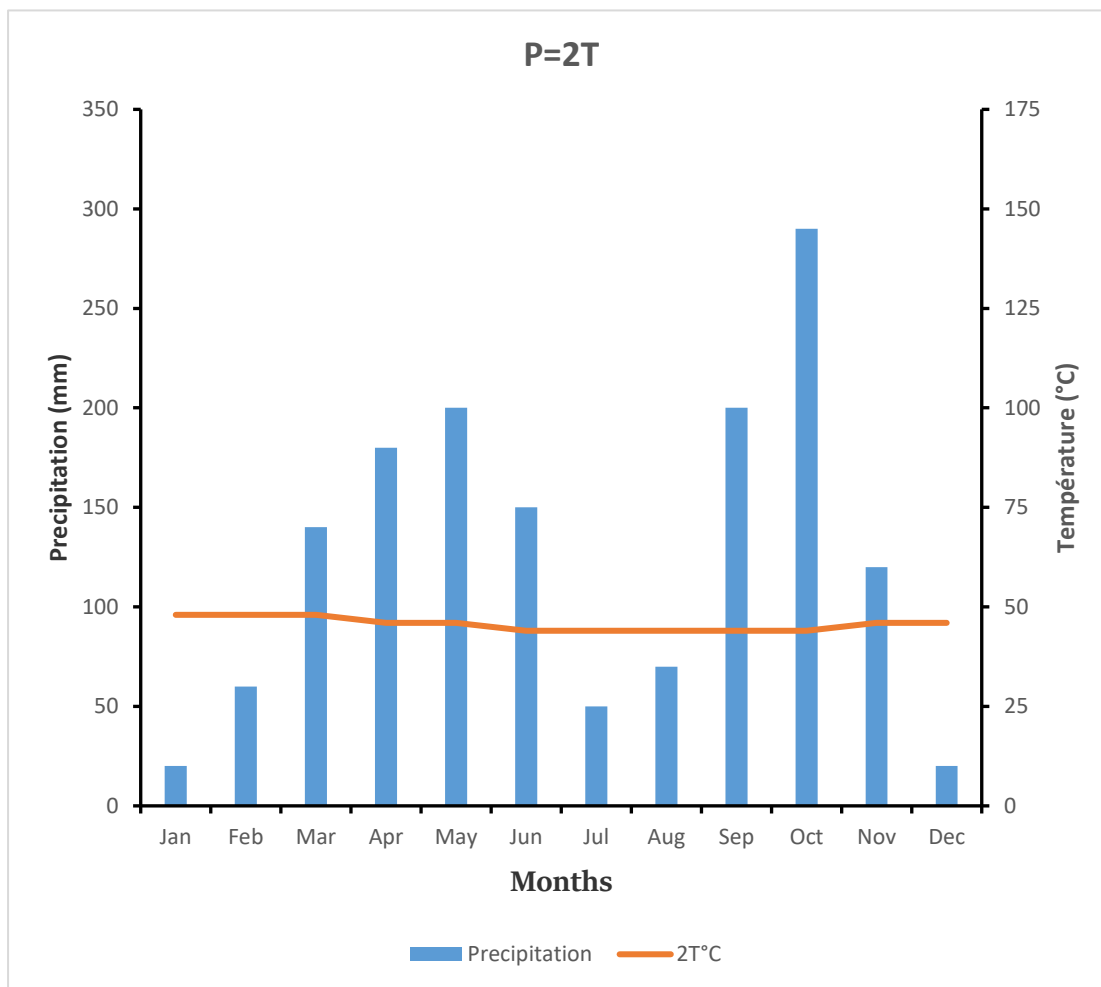


Figure 2: Ombrothermic diagram of (Bagnoul and Gaussen , 1957) in relation to the target site

I.1.3. Orography

A sketch on the geomorphology of Cameroon distinguishes three major characteristic reliefs; low altitudes, intermediates and mountainous reliefs (Kamgang Kabeyene, 1998). Based on this classification, the target site which is characterized by altitudes varying between 650 – 1130 m belongs to low (650 – 680 m), intermediate (680 – 800 m) and mountainous- land (800 – 1130 m) respectively.

The 3D geomorphological block (Fig.3) presents a gentle sloping of the relief from SE where we have the intermediate altitudes covered by streams and rivers to some extent, then a continuous elevation of elongated, semi orange, dome to flattened hills concentrated towards NW of the block. At the lowest intermediate altitudes (< 680 m) are found low lying areas which are in some parts occupied by streams and or rivers (e.g., the Mfoundi and Mefou Rivers). High altitudes consist of aligned sub-circular (semi orange-like) to elongated circular

hills following the NNE-SSW direction, with the sub-circular hills dominating and unequally distributed within the environment.

Comparing with the work of Bitom (1982), the relief are characterized by morphological units such as the Inselbergs, sub-circular and flat topped hills at altitudes from 800 m, 900 m to >1130 m respectively and seated on a Precambrian bedrock. The Inselberg barrier is represented towards northwest by Mount Nkoldom (122 km) and the south-west by Mount Eloundem (1169 m).

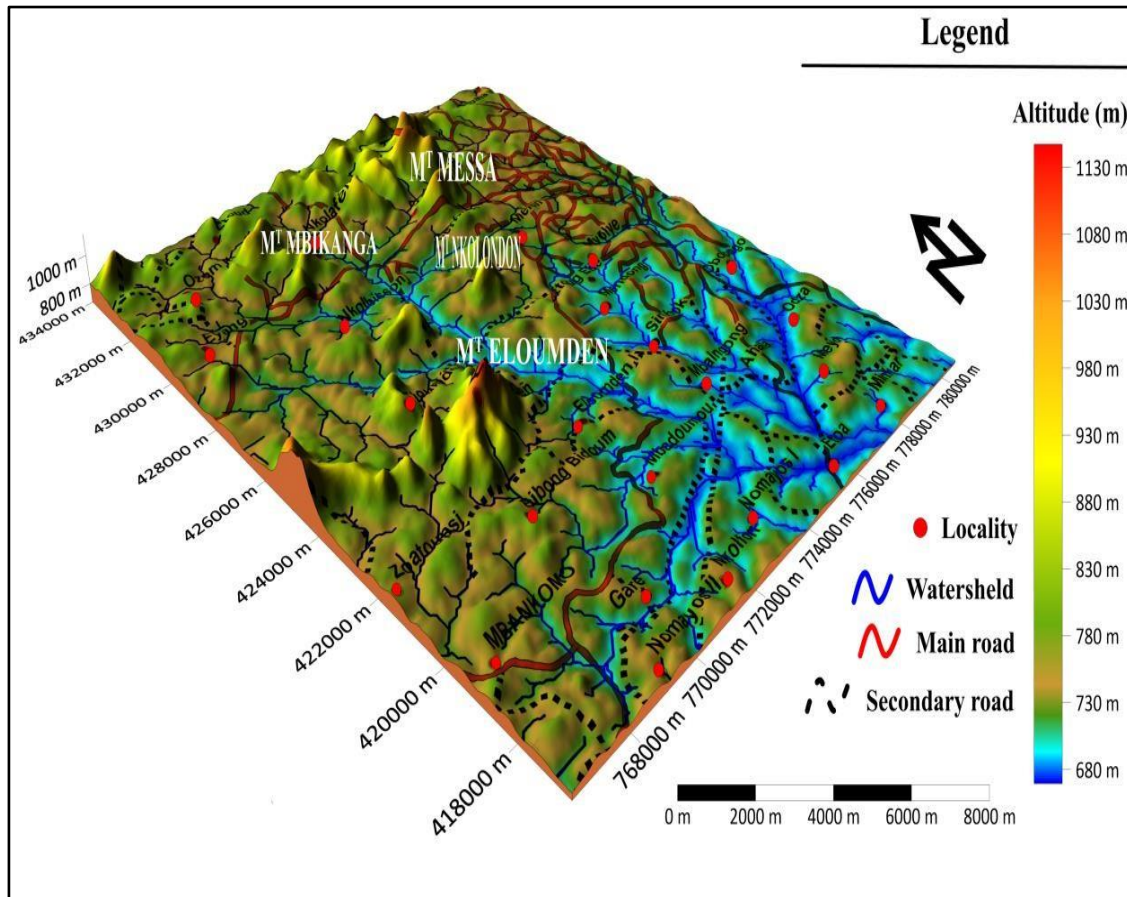


Figure 3: The 3-digital elevation model of the target site

I.1.4. Hydrography and Drainage pattern

The target area consist of main rivers to which are attached secondary streams (Fig.4) that together connects at zones of confluences, forming structures related to the dendrites of trees thus, termed dendritic patterns, as the secondary streams like Nkoumou tends to empty their materials and charges into river Nga, then to the Mefou and finally in the Mfoundi where they are carried away into the Sanaga river. Materials carried through this movement are usually sediments and charges of different values and sizes, rendering the hydrographic transportation as supple as through suspension, corasion and abrasion, dependent on the sizes

forest, covering 28% of the total forest. The dense semi-deciduous forest, in which the aforementioned target is located consist of abundant tall trees called skunk tree or hazel sterculia (*sterculiaceae foetida*) concentrated around areas such as Mbankomo and Leboudi, while the short to almost herbaceous trees called elm (*Ulmaceae*) are found around the premises of Mvogt-Betsi, Nomayos and Akouandoue. This vegetation is said to be secondary as there is intense exploitation and deforestation of the various lands respectively for agricultural purposes. In effect, this lands are said to be very fertile, since they provide crops like cassava, plantains, maize, potatoes, beans and cocoyam for consumption or for sell. Areas not affected by such vegetation within the target site are highly urbanized and are claimed to be those areas where the access to market for such products harvested from the farmlands are sold. It should be noted that the target site and Yaounde or the center region as a whole is progressively being urbanized in terms of habitation and the rapidly growing population.

I.1.6. Life stocks/Fauna

The study area, just like other villages in Cameroon has varieties of animals, from domestic to wild and small to big species such as mouse (*Mus musculus*), black mamba snakes (*Dendroaspis polylepis*), porcupine (*Hystrix cristata*) and Buffon's kob antelopes (*Kobus kob kob*) for wild, cats (*Felix catus*), dogs (*Canis lupus familiaris*), pigs (*Sus scrofa domesticus*) and goats (*Capra aegagus hircus*), for domestic. Birds such as pigeon (*Columba livia*), garden snail (*Cornu aspersum*) and coq (*Gallus gallus domesticus*) are equally found in this area.

I.1.7. Soils

The soils of the target site, just like the Centre region primarily lie on Precambrian metamorphic varieties of basement rocks, (gneiss, migmatites, and schists) which generally incorporate with organic materials after weathering to form lateritic soils. soils here are widely spread, topographically ranging in thicknesses on slopes and lowlands, obtaining red to reddish brown colors due to iron from the makeup, thus are essentially Ferrallitic (Yongue Fouateu, 1986). Around marshy areas, are some minor concentrations of orthic to hydromorphic soils derived from colluvium and river alluvium giving them an essentially kaolinitic composition highly rich in quartz, goethite, and hematite (Bachelier., 1959; Ngon Ngon et al., 2009).

I.1.8. Infrastructures and economic activities

The study area consists of administrative and public blocks such as a council, gendarmerie, hospitals and schools performing function in separate specialties and performances based on their training skills and commitments in the various domains. The gendarmerie is there to bring peace and security of the population, ensuring they respect and maintain the laws and order, following their rights as any other citizen in the country, while hospitals provides adequate services to make sure the health conditions of the population is improved, in as much as patience are concerned and finally schools such as primary, secondary and high schools provide the necessary basic, moderate and advanced educational levels for national and international institutions. Thus, preparing the youths for a competent carrier in job markets.

I.1.9. Economic activities

The main activities in the study area are commercial, agricultural and industrial exploitations. Buying and selling mainly takes place at the Mendong, Acacia, Mbankomo and Mbankolo markets, as products such as cocoyam's, yams, cassava, plantains, potatoes and banana from farm lands are transported to these main markets for commercial activities. Agriculture is practiced in large farm lands that vary from an acre to hectares, where crops such as palms, plantains, cassava, perishables are cultivated for consumption and commercial purposes. Industries such as ARAB CONTRACTORS mainly carryout quarry activities as machines at work keeps grinding larger volumes of rocks into varying shapes and sizes, after firing the source with dynamites. The Materials (gravel, sand) obtained are mainly used for construction of infrastructures.

I.2. GEOLOGICAL SETTING

The geology of Cameroon is almost universally Precambrian metamorphic and igneous basement rock, formed in the Archean as part of the Congo craton and the Central Africa Mobile Zone and covered in laterite, recent sediment and soils. Some part of the country has sequences of sedimentary rocks from the Paleozoic, Mesozoic and Cenozoic as well as volcanic rock produced by the 1600 km Cameroon volcanic line, which include the still active Mount Cameroon. The country is notable for gold, diamonds and some onshore and offshore oil and gas. The basement can be divided into two lithostructural units: (i) The Congo craton (CC) (Maurizot et al., 1986; Pouclet et al., 2007) found in the southern part of the country

under the designation of ‘Ntem Complex ‘and (ii) The Pan-African North Equatorial Fold Belt (Nzenti et al., 1984, 1988) or Oubanguides belt (Poidevin, 1983; Trompette, 1994), covering about two third (2/3) of the country, from the Yaounde group to far north.

I.2.1. Congo craton

The Congo craton in Cameroon also known as the Ntem complex is structurally subdivided into two main groups, namely the Ntem and Nyong group (Owona et al., 2021; Soh Tamehe et al., 2021).

The Ntem Group (>2.5 Ga) is an ancient granito-gneissic basement found northwest of the Congo craton, consisting of Archean TTG suites, high grade metamorphic rocks and narrow to elongated greenstone-BIFs, all intruded by extensively late K-rich granitoids (Tchameni et al., 2000; Shang et al., 2010; Thieblemont et al., 2018; Akame et al., 2020, 2021). Together with the greenstone-BIFs, the basement is crosscut by dolerite dykes striking N-S to NE-SW, while presenting a late magmatic event seen by the late highly potassic granitic intrusion (ca. 2666-2628 Ma) in Ebolowa (Tchameni et al., 2000; Akame et al., 2020, 2021). The supracrustal formations in this group were deposited between 3.04 to 2.88 Ga (Chombong and Suh, 2013; Thieblemont et al., 2018), while U-Pb on zircon dating gave ages between ca. 3,266 and ca. 2,850 Ga, corresponding to a TTG and charnockites emplacement, respectively (Takam et al., 2009; Tchameni et al., 2010). Mafic rocks (metagabbro and amphibolite) from the Ntem group revealed a crystallization age of their protoliths at ca. 2.86 Ga (Li et al., 2016; Akame et al., 2021). Available structural data indicate that the Ntem group was affected by two Archean deformational stages (D₁, D₂) and a late D₃ Paleoproterozoic event (Tchameni et al., 2000; Owona et al., 2011; Akame et al., 2019). D₁ is characterized by a N080E to N120E and NNW-trend sub vertical foliation developed during the horizontal shortening coeval with high-grade metamorphic conditions Akame et al. (2020). D₂ deformation is represented by F₂ isoclinal folds and C₂ ductile shear zones. Finally, the Archean structural trends were reworked by N045 to N–S D₃ brittle shear zones during the Eburnean/Paleoproterozoic orogeny (Owona et al., 2011; Akame et al., 2020, 2021).

The Nyong group is an Archaen to Paleoproterozoic portion located north-west of the Congo craton (Lerouge et al., 2006; Owona et al., 2021; Soh Tamehe et al., 2021). While Feybesse et al. (1986) thought this group represented a reactivated portion of the Congo craton throughout the Eburnean/Trans-Amazonian to Pan-African/Brazilian orogenic cycles, many authors Kankeu et al. (2018), Loose et Schen (2018), Bouyo Houketchang et al. (2019), Nga Essomba et al. (2020), Owona et al. (2021), Soh Tamehe et al. (2021,2022) proposed

the Nyong group represents a Paleoproterozoic sutured zone sharing the Congo and Sao Francisco cratons. This group is structurally categorized by three deformational stages (Ganno et al., 2017; Kankeu et al., 2018; Moudioh et al., 2020). The S_1 foliation, L_1 stretching lineation and β_1 boudins characterize the first compressional deformation event (D_1). The S_1 foliation is outlined by a compositional layering and a preferred orientation of pyroxene, epidote, chlorite, amphibole and needle-like quartz crystals. It mainly trends NW- SE and secondarily NE-SW with gentle (15° – 20°) to steep ($\sim 70^\circ$) dips, towards the NE and SW. The related L_1 stretching lineation is visible and trends N044E and plunge 10° SW. The D_2 event is characterized by heterogeneous deformation associated with the development of C_2 ductile shear planes and F_2 isoclinal folds with mean fold axis attitude of N016E 84° NNE. The latest D_3 deformation event is mainly brittle producing veins and joints. The tectono-metamorphic evolution reveals that D_1 event is associated with the granulite facies metamorphism, while D_2 and D_3 are related to retrograde metamorphism under amphibolite and greenschist facies, respectively (Ndema Mbongue et al., 2014; Moudioh et al., 2020).

1.2.2. Pan-African North Equatorial Fold Belt (PNEFB)

This domain is bordered west by the Trans-Saharan belt, south by the Congo craton and extending towards Borborema province in NE Brazil, forming the Pan-African-Brazilian belt (Brito de Neves et al., 2001, 2002). The PNEFB is the most important geologic unit in Cameroon (Nzenti et al., 1994). The specificity of this fold belt is the Central Cameroon Shear Zone which resulted from the horizontal movement following the multistage collision Toteu et al. (2004). This was the collision between the West African Craton, the Saharan meta-craton and the Congo-Sao Francisco craton. (Fig. 5a) during the west Gondwana assemblage (Casting et al., 1994; Abdelsalam et al., 2002; Ngako et Njonfang, 2011). Geodynamically, the PNEFB consists of three domains, which are the Northern, Central and Southern domains (Fig. 5).

The Northern Domain extends along the western edge of Cameroon, and into Poli (Toteu et al., 2006) and Mayo Kebi regions, SW of Chad (Penaye et al., 1988). It consist of : (i) metasediments (greywackes, carbonate argillites, iron argillites) and metavolcanites (830Ma; U/Pb age on metarhyolites zircon, (Toteu et al.,1887)); (ii) a gneissic (amphibole, biotite and garnet gneiss) and amphibolitic assemblage alternating with retromorphosed granulite bands(800-900°C, 13-14 kb) after Bouoyo-Houketchang et al.(2015) associated with a tectono- metamorphic history related to Paleoproterozoic granulite units (2100Ma; U/Pb age

on zircon, Penaye et al.(1988) all crosscut by diorites, granodiorites and calc- alkaline tonalities dated at 630Ma(U/Pb age on zircon, Toteu et al.,1987); (iii) Neoproterozoic orthogenesis whose petrography and geochemistry are compatible with a continental arc domain associated with a subduction zone Bouoyo-Houketchang et al. (2015).

The Central Domain is a transition between the northern and the southern domain. It stretches towards the southern domain and bounded by the Bafia group and towards the northern domain to the south of Poli where it is limited by the Tcholliré-Banyo Fault (Toteu et al., 2001). The protoliths of orthogenesis from this domain were emplaced during three distinct periods, Tonalite-trondjemite-Granodiorite (TTG) suites in the makénéne area intruded at ca. 3.0-2.5Ga, and were affected by partial melting at ca. 2,08-2,07Ga, during the Eburnean orogeny, and by a magmatic event with a metamorphic overprint at 0.64-0.61Ga, during the Pan-Africa orogeny Tchakounte et al. (2017) .This domain is characterized by the presence of large faults and shear such as the Central Cameroon Shear Zone (CCSZ) of N30°E and N30°E directions (Ngako et al., 2003),and the Fouban-Tibati-Banyo fault which are ductile transcurrent shears (Nzenti et al., 1988;Ngako et al., 1991,2003), the Sanaga Fault (SF) which is a brittle shear Dumont,(1986) and the Betare-Oya fault which is a ductile brittle shear (Kankeu et al.,2009,2010). Structural studies highlight four (04) stages of deformation (D₁, D₂, D₃ and D₄) (Ganno et al., 2010, Kouankap Nono et al., 2011 and Ntieche et al., 2017). The D₁ phase is associated with medium-grade amphibolite facies assemblages: Qtz+Kfs+Bt+Hbl+Spn/Qtz+Kfs +Bt+Pl+Spn/Qtz+Kfs+Bt+Spn/Qtz+Kfs+Bt+Spn+Grt+Ox. It is marked by the tangential movement that led to the development of S₁ foliation, L₁ lineation, and F₁ folds. The D₂ phase associated with amphibolite metamorphic facies is a phase of transcurrent tectonics with D₂ intrusion, which are set up parallel with the regional structures. The D₂ is characterized by the heterogeneous deformation marked by simple shear in dextral transpressive context which has superpose the D₁ deformation. D₂ deformation is associated with the development of axial plane foliation S₂, a mineral stretching lineation L₂, F₂ folds, and C₂ shears: The D₃ phase of deformation is typically a phase of sinistral transpressive tectonics and superposed folding. Structures associated to this phase of deformation are, S₃ foliation which overprints the S₂, L₃ stretching lineation and C₃ shear planes. The essentially brittle phase D₄ is characterized by the establishment of fractures and granitic veins. This last phase of deformation is also manifested at the regional scale and contemporaneous with the central Cameroon Shear Zone.

The Southern Domain or the Yaounde group (Nedelec et al., 1986; Nzenti et al., 1988) is limited by the central domain in the north, the Congo craton or the Ntem complex in

the south, the Kribi Campo Fault in the west and continues eastward into the Central African Republic in the Bole and Gbaya series (Pin et al., 1987). The metasedimentary rocks are less than 700Ma with a distinct local Eburnean (~ 2.0Ga) and tonian-Cryogenian (~1.0-0.7 Ga) source (Owona et al., 2021). This group consists of three series (Nedelec et al., 1986; Nzenti et al., 1988; Vicat et al., 1986; Yonta-Ngoune et al., 2010) which are from east to west: the yakadouma series made up of low-to high-grade metamorphic rocks (schist, gneiss, and migmatites), the Ayos-Mbalmayo-Bengbis series made up of low-to medium-grade metamorphic rocks (schist) and the Yaoundé series (Nzenti et al., 1988; Toteu et al., 2004) into which belongs the study area. The Yaounde series is made of two medium- to high-grade lithological units that have thrust onto the Congo craton during the Neoproterozoic (Nzenti., 1998; Ngako et al., 2003; Mvondo et al., 2007; Ngako et Njonfang., 2011; Metang et al., 2022): (i) a metasedimentary unit consisting of garnet- Kyanite gneisses, garnet-plagioclase gneisses, and garnet micashists into which calc-silicate rocks; locally quartzites and talc- schists are inserted (Stendal et al., 2006; Mvondo et al., 2007). (ii) a meta-igneous unit consisting of orthogneiss, metadiorites or pyriclasites, metagabbro, pyroxenites, talc-schists, amphibolites, and amphibole gneisses (Nzenti et al., 1988; Nzenti, 1998 ; Yonta-Ngoune et al., 2010; Li et al., 2017; Nkoumbou et al., 2014). The latest unit would represent distinct magmatic events associated with the evolution of the Yaoundé sedimentary basin from opening and oceanization to convergence and closure (Nkoumbou et al., 2014).

The tectonic evolution in the Yaoundé group is characterized by four main deformational phase (D₁-D₄) of ductile deformation (Mvondo et al., 2003, 2007; Metang et al., 2014). The D₁ and D₃ phases correspond to East-West to Northwest-southeast shortening (or contraction) and crustal thickening by nappes stacking. The D₂ stage corresponds to the North-South to Northeast-Southwest extension occurring during the orogenic collapse and exhumation of the Yaoundé series. D₁ represent the nappe stacking stage associated to prograde metamorphism that culminates in high-pressure granulite condition. In reverse, D₂ represents a decompressional stage that occurred as orogeny parallel extension. It was associated with intense magmatic underplating and large- scale foliation boudinage and (or)gneissic strongly doming that transposed D₁ fabrics to form regional strain flat-laying ones. The latter was refolded by D₃ deformation into F₃ folds representing the regional strain pattern developed consistently with the East-West trans-saharian convergent system. The D₄ folding stage is tentatively attributed to lateral flow subsequent to a diachronous crustal extension. Both D₃ and D₄ are thought to be contemporaneous events defining a bulk at

630Ma under granulite facies condition. Ages below 630Ma are attributed to retrograde metamorphism associated with crustal exhumation

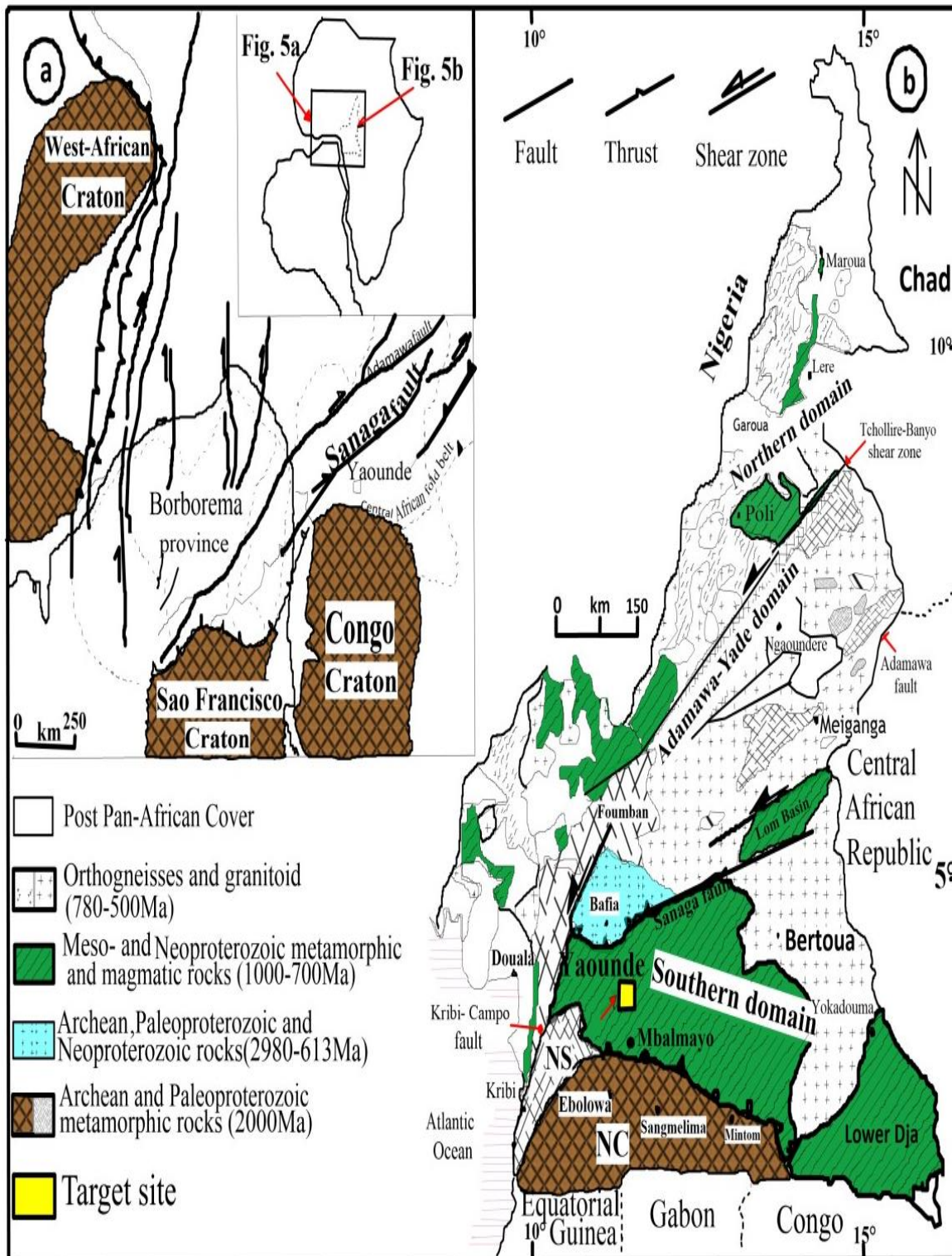


Figure 5: The Pan-African Nord Equatorial Fold Belt of Central Africa: (a) Continent scale geodynamic reconstruction (Oliveira et al., 2006); (b) Map of the different lithotectonic units of Cameroon with localization of the target site (Tchakounte et al., 2017 modified in Metang et al., 2022b).

I.2.3. Previous work of the target site

Pioneer researches of Champetier de Ribes et Aubague (1956) as well as recent studies of (Mvondo et al., 2007; Owona et al., 2011; Nkoumbou et al., 2014; Fuh et al., 2021) reveal the existence of the NNW-SSE-trending faults, which split the Yaounde series indeed, this structural discontinuity would represent one of the driving forces related to the history of the Pan-African orogeny and the deformation history and mechanisms. Nzenti et al. (1988) proved that the Yaounde group is composed of medium-to high-grade series and the low- grade Mbalmayo-Ayos-bengbis series while (Nedelec et al., 1986) thrust onto both the Archean Ntem complex, Dja and Yakadouma series, in which the high-grade metamorphic rocks (e.g. gneisses) are of calc-silicate composition were rocks like marble, quartzite and migmatites-rich orthopyroxenites (Nzenti et al., 1988; Stendal et al., 2006; Owona et al., 2011; Yonta-Ngoune et al., 2010), further said that the metamorphic (typically metasedimentary and meta-igneous) rocks recrystallized under medium-to high-regional metamorphic conditions which could probably be progressive in nature. Then (Nedelec et al., 1986; Nzenti et al., 1988; Vical et al., 1998; Yonta-Ngounet et al., 2010) shows that the Yaounde group consisted of three metamorphic rock categories making up three series, running east to west: the low to high-grade rocks (the Yakadouma series), the low-to medium-grade rocks (highlighting the Ayos-Mbalmayo-Bengbis series) and finally, the Yaounde series (Nzenti et al. 1988; Toteu et al., 2004 ; Owona et al., 2011) reveal that metapelites and meta-psammopelites of the Yaounde group experienced a multiphase deformation history in which the syn-tectonic deformation stages D₁-D₂ was progressive, leading to a regional dominant foliation S₂ in the metamorphic rocks that outcrops the sector. Ngnotue et al. (2012) attest that within the metasedimentary unit, two types of granitic leucosomes series were distinguished, displaying In situ leucosomal calc- alkaline and high-k calc-alkaline (peraluminous S-types granitoids derived from the partial melting of a host metamorphosed pelite) to injected shoshonitic leucosomal series (I-to S-type peraluminous granitoids issued to the partial melting of metamorphosed greywackes) respectively.

Mvondo et al. (2003, 2007), Metang et al. (2014) explained that the tectonic evolution in the Yaounde group is characterized by four main deformation stages: (D₁-D₂) represent an E-W ductile phase seen by the presence of foliation for example, the D₃ and D₄ phases correspond to a NW-SE shortening (or contraction) and crustal thickening by nappe stacking. The D₂ phase corresponds to N-S to NE-SW extension occurring during the orogenic folding

and exhumation of the Yaounde series. Meta-igneous and metasedimentary unit of the Yaounde series display migmatitic feature (Lasserre., 1979; Nzenti et al., 1988; Penaye et al., 1993).

Bineli et al. (2020) for the first time, robust rutile LA-ICP-MS. U-Pb dates were obtained showing that the Neoproterozoic rutile in the Yaounde group occurs in four main generation of crystals dated at $719\pm 32\text{Ma}$, $661\pm 21\text{Ma}$, $630\pm 6\text{Ma}$, and $561\pm 8\text{Ma}$ alongside tectono- metamorphic cycle. Ages older than 620Ma ca. date the prograde metamorphic conditions accompanying deformation whose onset is $> \text{ca. } 719\text{Ma}$. In contrast. Younger ages ($> \text{ca. } 620\text{Ma}$) are attributed to retrogression and crustal exhumation, with $522\pm 6\text{Ma}$ illustration lead loss attributed to Ediacaran tectonism. The Yaounde group is dominantly composed of Neoproterozoic crustal material with subordinate contribution from older crusts. Their deposition age is older than ca. 632Ma . Finally, Metang et al. (2022c) shows that the metasediments rocks of the Yaounde group comprise Grt chlorite schists, Grt micaschists and Grt-ky migmatites displaying granoblastic to granolepidoblastic texture and mineral assemblages of green schist, amphibolite and granulite facies, suggesting prograde metamorphism. The geochemical data reveal wide range of $\text{Fe}_2\text{O}_3+\text{MgO}+\text{Tio}_2$ contents, from 7.3 to 33.6%, probably reflecting to diversity of lithological units. The protoliths of these metasediments are post-Archean shales and greywackes deriving mostly from the Congo craton and, or the Adamawa-yadé andesite and granulite. The eroded materials are from the upper continental crust source, and were emplaced in an active margin context and / or Oceanic Island arc. Bissaya et al. (2023) exposed that four ductile (D_1 - D_4) and two ductile-brittle (D_5 - D_6) deformation events dominate the structural evolution of the Neoproterozoic orogeny in Yaounde zone. D_1 features S_1 shallow dipping foliation and F_1 isoclinal folds which illustrate a simple shear regime, within the early tangential southward movement. D_2 showed a S_2 gentle-dipping foliation and a $\sim\text{N-SL}_2$ lineation associated to $\sim\text{N-S}$ C_2 striking shears, illustrating the general flattening, within the late southward tangential movement. D_3 featured $\sim\text{N}$ -trending and $\sim\text{E-W}$ - shortening folds, whereas D_4 featured $\sim\text{E-W}$ and $\sim\text{N-S}$ - shortening folds, denoting the transcurrent tectonics. D_5 and D_6 took place-continuously to earlier D_3 and D_4 transcurrent tectonics with flexural-slip folding features which would be overprinted by post-orogeny stress regime later.

CHAPTER II : MATERIAL AND METHOD

To obtain detailed petrographic and structural information of the western part of Yaounde, it is advisable to carry out field work and research studies. Reason why as objective in this chapter, it would be wise to present and describe the materials used and their methods of adaptation in accordance to fieldtrip, and then present the best and convenient methods viable to the observation, description, interpretation and result obtained. In this effect, the chronology of this chapter start from:

II.1. MATERIAL

Field and laboratory studies are very important for a convenient geological work. To accomplished these studies, the following equipment facilitated the work:

- Topographic map: It enables us to locate the study area using its geographical coordinates. Several information including the relief (hills, valleys and slopes), watersheds, roads and tracks were generated from the topographic map.
- Geological map: The geological map of the sector was generated with the help of those of Champetier de Ribes et Aubargue (1956), Weeck Steen (1957), Owona et al. (2011, 2013) and Mvondo et al. (2007). This map aided to best comprehend and obtain knowledge concerning the assimilation of the previous geologic history in the Target site, to better reconstruct the area base on the recent structural data and information obtained from the western Yaounde metamorphic terrains.
- Compass-clinometer permitted us to measure the directions (strike) and dip of various structures. These structures (fold, schistosity, shear zone, foliation) provided valuable clues about the deformation history of the study area.
- Garmin 64s GPS (global positioning system) was used in the field to collect geographic coordinates for cutting of the specific area under studies on a map and for waypoint plotting, thereby identifying the sector in question. This gives a profound identification of the area for good studies as outcrops were equally coordinated following the same format of identification.
- Digital camera helped to provide photographs of the various vegetations, outcrops and fresh rock samples to appreciate geologic phenomena and ease mega and mesoscopic descriptions of the study area.
- A Geologic hammer was used to crack and split out rock sample on the field for better study.

- A Note book was used to take some important information on the field, like strike and dips, description of some features, rock textures, predictive mineral compositions, nature and sketching some important features to avoid confusion and forgetful mind.
- Sample bag used to collect fresh rock samples for laboratory use.
- Pencil used to take notes on the field and to draw some features.
- Cutlass used to clear roads and outcrops to ease movement and give clear access to field studies.
- Pen, bold marker and coins were used as a scale on the different outcrops and fresh samples
- Cement paper help us to tight fresh rock sample collected on the field to avoid contamination. In addition to that it equally helps to avoid confusion between the different samples, as a code were assign to each sample.

II.2. METHOD

II.2.1. Field studies

We carried out a field work campaign lasting 14 days during the month of April 2023. On the field, the best and convenient survey method was on mapping, then outcrop to sample scale observations that is, appreciating the general characteristic structures and lithology of the outcrops after coordinating them geographically. Outcrops were further studied on the basis of their petrology (origin, types and occurrence of rocks) and structural inventory and analysis. Fresh archetypal samples of the diverse outcrops were identified and described following the lithological types, whilst structural aspects were concerned in identifying and describing geologic structures seen on the outcrops. Systematic data were gotten with the help of a compass-clinometer, a GPS and a marker as they were all used each time a structure was observed. After placing the instruments to obtain data, sketches were made to keep a good record of the studied structures. Field studies ended with sample cracking, describing, coding, collecting and transportation to the laboratory for petrographic studies

III.2.2. Laboratory works

In the laboratory, studies began by some bibliographic research on previous works of the resulting researched theme. Macroscopic studies of the various samples were done to determine the petrographic types while fourteen (14) thin section were prepared for microscopy at the Geoscience Laboratory of Deep Formations and Applications, Department of Earth Sciences, University of Yaoundé I. The prepared thin sections were observed and described, to determine

the textures, mineralogical associations and assemblages. The relationship between the different rock entities were established in order to deduce their tectonic evolution. Nevertheless, micrographs were equally taken to appreciate thin section and illustrate the description given for the slide.

Structural studies were based on two major methods, including morpho-structural analysis and field analysis. (i) Geomorphologic work consisted of studying reliefs and drainage based on topographic and hydrographic maps respectively. Then lineaments from SRTM images were sketched and interpreted to provide the relationship between streams, crest lines and geologic lineaments to develop field numerical model and produce thematic map. Extraction, processing and sketches were realized from softwares like ArcGis10.8, Global Mapper 15 and Surfer 16. (ii) Structural studies consisted of identifying and describing field observed structures, to provide a relative chronology for their occurrences.

**CHAPTER III: FIELD WORK AND
PETROGRAPHY**

Petrographic studies were done by a complete description of the textures or microstructures, inclusions, reactions textures, and mineralogical makeup, to enhance the possible paragenesis, mineral associations and characterize the deformations occurring at the microscopic scale, in thin section formed from the rocks of this area, to better appreciate recent structural (geologic) data within the premises of the western Yaounde.

III.1. METASEDIMENTARY UNIT

These rocks are migmatites, they crop out in dome, block and slabs and are observed on the hill of Vogt-betsi, Oyomabang, Eloudern, and at the Mbankolo, Nomayos and Leboudi quarries (Fig. 8B). These rocks are heterogeneous and present two parts: (1) the paleosome which shows a gneissic foliation (Fig. 8A, D) (marked by an alternation of light and dark beds) and composed of biotite, alkaline Feldspath, plagioclase, quartz, kyanite and pyroxene, and (2) the neosome which is composed of lightly colored bed (leucosomes) (Fig. 8C) and dark bed (melanosome) has a massive structure and is visibly made of quartz and Feldspath showing no preferential orientation (Fig. 8C). The leucosomes appears in the form of a boudins, a fold and veins of variable thickness (centimetric to decametric), (Fig. 8 D, F).

III.1.1. Paleosome

The paleosome is the part of the rock which has not undergone partial melting. It has retained its gneissic particularity which presents a foliation marked by an alternation, often discontinuous, of light (quartzo-feldspathic) and dark (rich in ferromagnesian minerals) beds, which is mesocratic in color. On the basis of the mineralogical composition, the paleosome has 3 metamorphic facies including biotite-garnet gneiss, kyanite-garnet gneiss and garnetite.

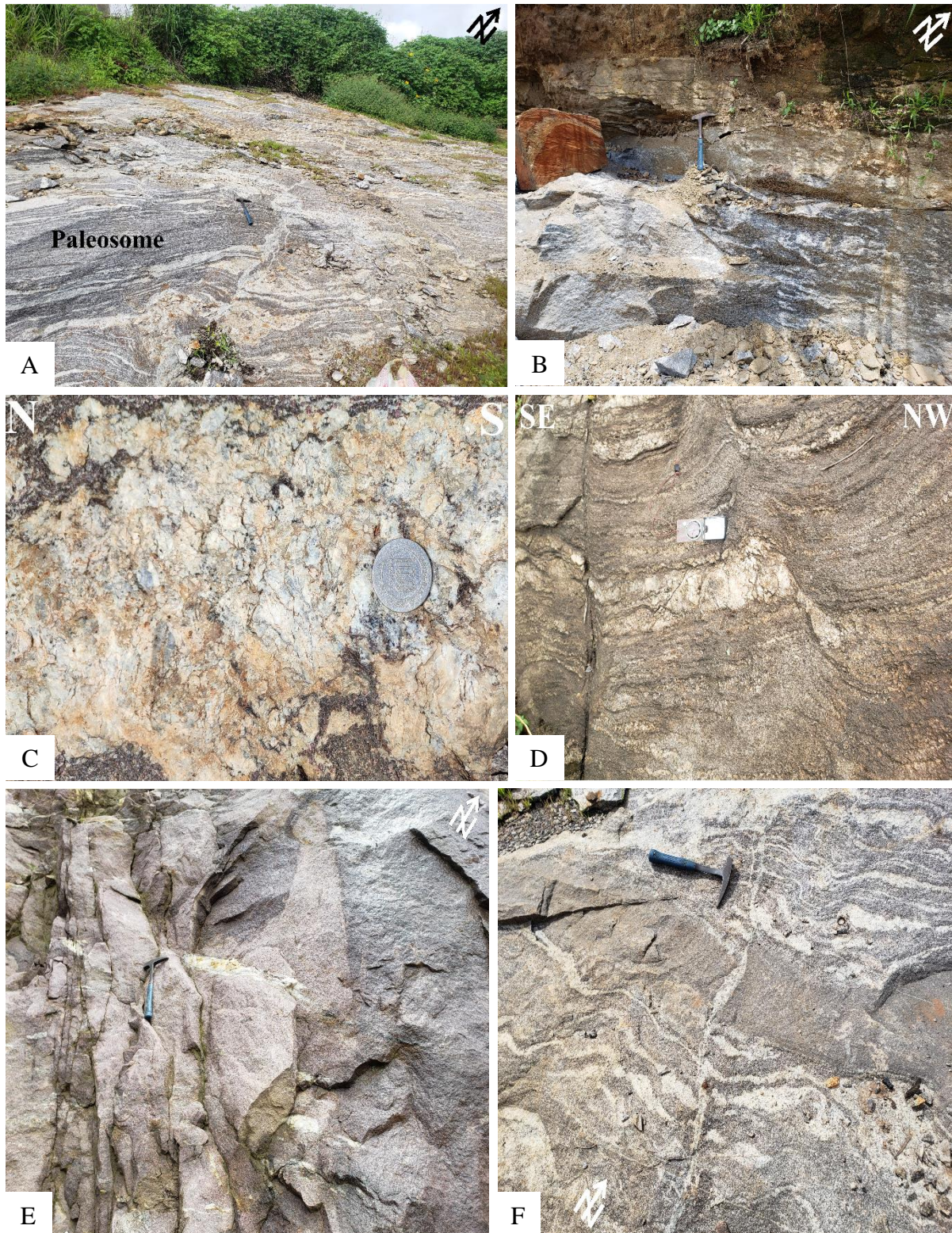


Figure 8: Mesoscopic character of migmatites of western-Yaounde: (A) slab outcrop of migmatites showing the paleosome bed;(B) blocky outcrop showing pods of metadiorites at Fam-Assi; (C) dommy outcrop of migmatites at the Leboudi quarry (D) migmatitic outcrop showing banding plane: (E) dommy outcrop garnetite at the Nomayos quarry; (F) outcrop in slab with boudined and folded quartzofeldspathic band at the artisanal quarry of Mbankolo.

❖ Garnet- biotite gneiss

The outcrop is light gray in color, occurring as slab shaped structure that ranges to about 4 km. They occur at altitude ranging to about 799 m and geographical coordinates 03°53' 45.35" northern and 11° 29' 40,45" eastern in the Mbankolo quarry.

Based on the macroscopic observation, this rock is light gray in color. Minerals, which are distinguished with the naked eyes are biotite, garnet, feldspar, quartz and kyanite (Fig. 9A).

Under the light microscope the rock displays a grano-lepidoblastic texture richly composed of garnet, quartz, biotite, feldspar, and plagioclase.

Garnet (40%) crystals are euhedral to anhedral within this rock. This mineral has grain sizes that measure 0.2×2.3 mm. This garnet is associated to biotite, quartz and feldspar. Some of the garnet are globular in form (Fig. 9C) with no inclusion but shows alteration products (Fig. 9B).

Quartz (20%) elongated to anhedral crystals. Ranging from 0.2×2.3 mm, showing smaller to large crystal grains. Associated to feldspar, biotite and garnet, in which some of the quartz shows no inclusion but alteration product. (Fig. 9B).

Biotite (15%) tabular anhedral to subhedral shaped crystals with 0.1×0.7mm in dimension. It is associated with several minerals such as garnet, feldspar, plagioclase quartz (Fig. 9B). Some crystals have been altered into sericite. (Fig. 9B).

Feldspar (10%) appear as anhedral to subhedral in form. Measure 0.1×1.1 mm in association with biotite, garnet and quartz. Some of the feldspar are altered into sericite. (Fig. 9B).

Plagioclase (5%) it is elongated to subhedral in forms. This mineral has grain sizes that measure 0.3×1.1 mm and it is associated to biotite, quartz and feldspar.

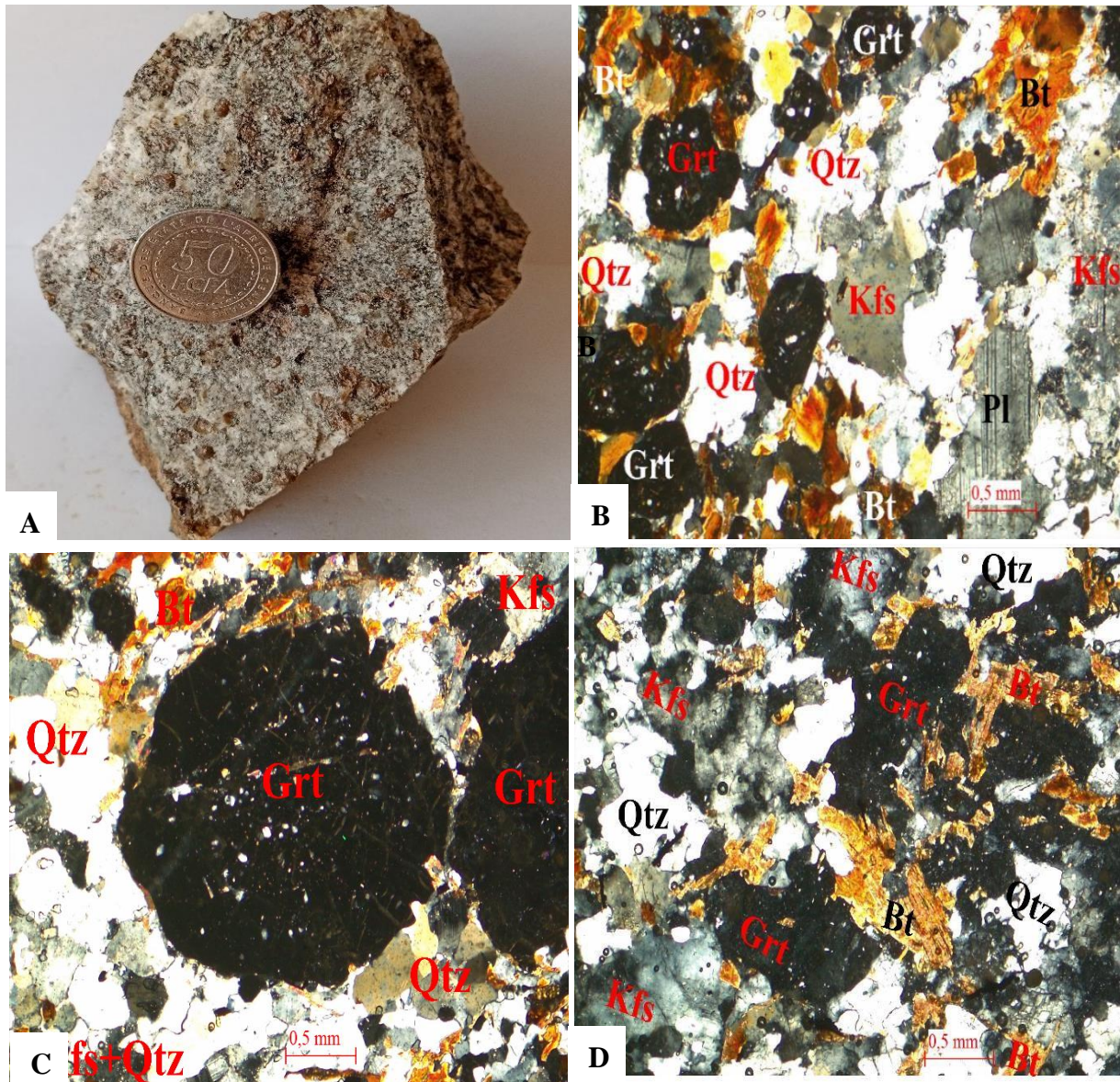


Figure 9: Macroscopic and microscopic character of garnet-biotite gneiss: (A) fresh rock sample; (B) granolepidoblastic texture; (C) mineral association and globular garnet; (D) transformation of garnet to biotite.

❖ Kyanite –biotite gneiss

The kyanite-biotite gneiss bodies in the field outcrop in the form of slabs of about several centimeters to few meters. It occurs at altitude of 799 m with geographical coordinates N03°53' 45.35" and E11° 29' 40,45" in the western portion of the Mbankolo quarry.

On the macroscopic scale, it has a dominantly light gray colored with a medium to coarse-grained nature. Distinguishable minerals are biotite, garnet, feldspar, quartz and kyanite (Fig. 10A).

Based on the microscopic observations, it shows a lepidogranoblastic texture abundantly composed of biotite, kyanite, quartz, garnet, feldspar, andalusite, staurolite, muscovite and accessory mineral such as tourmaline and apatite.

Biotite (30%) crystals are needle-like to anhedral in form. These grains have dimension that varies to about 0.2×1.2 mm. Some of these crystals are associated to staurolite, quartz, kyanite and garnet (Fig. 10B). It has minute inclusion of quartz (Fig. 10C).

Kyanite (20%) appears as subhedral to anhedral in form which is most stable at high pressure, ranging from 0.7×1.3 mm. Associated to biotite, andalusite, feldspar and garnet (Fig. 10C). Showing some finger-like inclusion of biotite (Fig.10E), certain crystals are showing evidence of alteration. (Fig. 10C).

Garnet (15%) is subhedral to anhedral in shaped and has 0.2×1.9 mm as grain sizes. This garnet are elongated and in association with biotite, kyanite, andalusite, feldspar (Fig. 10C). Moreover, some garnets are skeletal in shaped (Fig.10E).

Quartz (10%) elongated to anhedral crystals in shaped. Rranging from 0.2×0.6 mm which is associated to biotite, kyanite, staurolite and garnet. It has minute inclusion of garnet and apartite (Fig. 10B).

Feldspar (10%) crystals has dimension that measure to about 0.2×1.1mm. They are subhedral to anhedral with inclusion of quartz and muscovite (Fig. 10D). It is associated to biotite, garnet and quartz (Fig. 10C).

Andalusite (5%) has grain sizes that measures 1.1×2.0 mm. Most of these grains are euhedral to subhedral and are associated with kyanite, feldspar, biotite and garnet (Fig. 10C).

Staurolite (5%) are subautomorphic to xenomorphic and has 0.5×1.0 mm as grain sizes. Occur as inclusion within quartz and biotite. Also, they are in association with kyanite, feldspar, biotite as well as quartz.

Muscovite (2%) Needle-like to anhedral shaped crystals, ranging from 0.05-0.7mm in diameter, associated to biotite, feldspar, quartz and kyanite. Muscovite is in inclusion in feldspar (Fig. 10D).

Microcline (2%) found in little quantity in thin section. Occurring as anhedral crystals in form and has variable grains ranging from 0.02×0.4 mm. It is associated to biotite and quartz, certain crystal like biotite shows alteration product (Fig. 10B).

Tourmaline (½%) displaces variation in grains sizes ranging from 0.03×0.5 mm. They are subautomorphic to automorphic in form and associated with kyanite and apatite. It is in inclusion in quartz (Fig. 10D).

Apatite (1/2%) rounded to subhedral crystals in form with 0.02×0.4 mm in dimension. It is associated with several minerals such as tourmaline, biotite and quartz. Some of the apatite are in inclusion in quartz (Fig. 10D).

The sample present a mineral assemblage as Bt + Ky + Grt + Qtz+ Std+Tur which are characteristics of medium grade metamorphic conditions. The foliation bounded around the garnet porphyroblast lead to the development of a pressure shadow zone and the formation of a structure in the form of an eye (Fig. 10F).

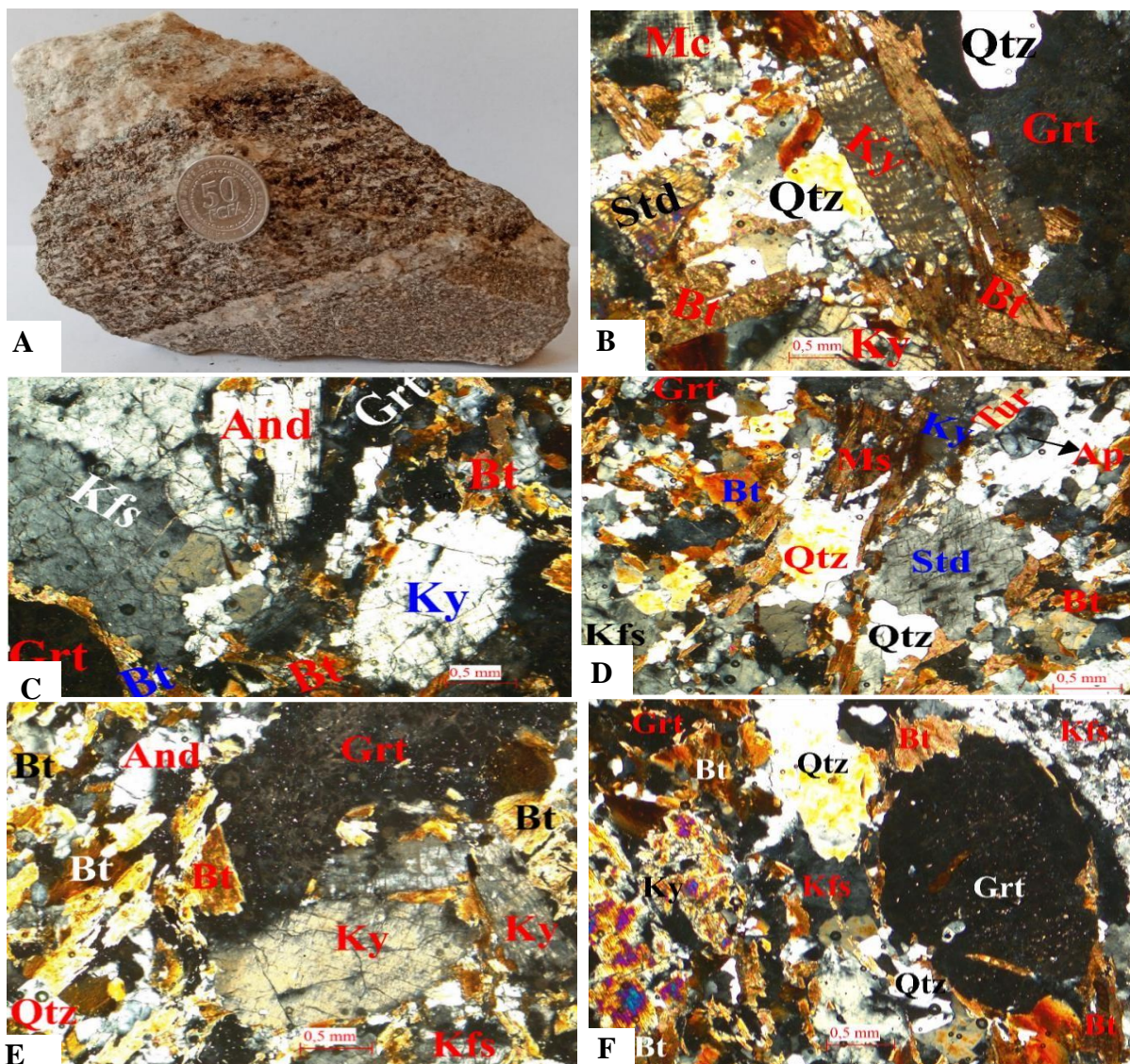


Figure 10: Mesoscopic and microscopic character of kyanite-garnet gneiss: (A) fresh specimen sample; (B) grano- lepidoblastic texture; (C-D) elongated garnet and transformation of garnet to biotite showing coronitic structure ;(E) longitudinal and basal section of kyanite, inclusion of biotite in kyanite; (F) garnet showing coronitic texture.

❖ Garnetite

The garnetites rock samples in the field outcrop in the form of blocks and domes of about several centimeters to few meters. They occur at an altitude of 745 m with coordinates $03^{\circ} 46' 40.46''$ northern and $11^{\circ} 24' 47.36''$ eastern in the Kamlang-Nomayos quarry.

Based on the macroscopic observation, this rock is light gray in color. Distinguishable minerals are biotite, garnet, feldspar, quartz, kyanite and pyrite (Fig. 11A).

Microscopically, the rock displays a granolepidoblastic texture richly composed of garnet, biotite, quartz, kyanite, andalusite and feldspar.

Garnet (45%) crystals are abundantly subhedral to anhedral in form, comprises 0.08×2.8 mm in terms of dimension. Associated to andalusite, kyanite, biotite and feldspars, forming curved and wormy contacts. They are mostly being included by quartz inclusions. Here, there is irregular intergrowths, formed as a result of the incomplete reaction of skeletal to polygonal garnets transforming to wormy (vermicular) biotites that provide reaction textures as in (Fig. 11.B, F).

Biotite (15%) leaf-like anhedral elongated crystals. It has grain sizes that measure 0.2×1.6 mm in association with kyanite, andalusite, quartz and feldspars, forming concave convex contacts. Most of this oriented biotites are seen tapered from garnets as a result of intergrowth while some are generally included by quartz and feldspar inclusions.

Quartz (10%) subhedral to anhedral crystals. Ranging from 0.08×1.1 mm in diameter in association with quartz, biotite, feldspar and garnet (Fig. 11C).

Kyanite (10%) appear as subhedral to anhedral elongated crystals. Which ranges from 1.1×2.4 mm in sizes and is in association with biotite, andalusite, quartz and feldspar (Fig. 11D). The mineral is seen transforming to its polymorph andalusite probably by loss of water as a result of decrease in temperature and pressure conditions, forming exsolution microstructures around their edges as in (Fig. 11D).

Andalusite (7%) is elongated to subhedral shaped crystals. Ranging from 0.2×0.8 mm and it is associated to garnet, biotite, quartz and kyanite. It has minute inclusion of garnet.

Feldspar (6%) anhedral crystals. Its grains vary between 0.2×2.0 mm and is associated to muscovite, garnet and quartz. It shows no inclusion.

Plagioclase (4%) crystals are anhedral to subhedral. Ranging from 0.05×1.1 mm which is in association with biotite and garnet, biotite is included in plagioclase (Fig. 11E).

Pyroxene (2%) seems as subhedral crystal. Ranging from 0.4×0.8mm. Some of these crystals are associated with garnet, quartz and feldspar.

Accessory minerals (1%) are represented by opaque minerals which are elongated and found in inclusion in biotite and Sphene. It is euhedral in forms.

The rock in general shows foliation (schistosity) similar to preserved parental sedimentary bedding planes, as minerals are oriented following biotite direction, probably indicating deformation formed after metamorphism. Symplectic reactions are equally observed around the garnet. The rock shows a paragenesis to be that of Grt + Bt +Qtz + Ky+ +And +Kfs +Pl+Px and a grano-lepidoblastic texture.

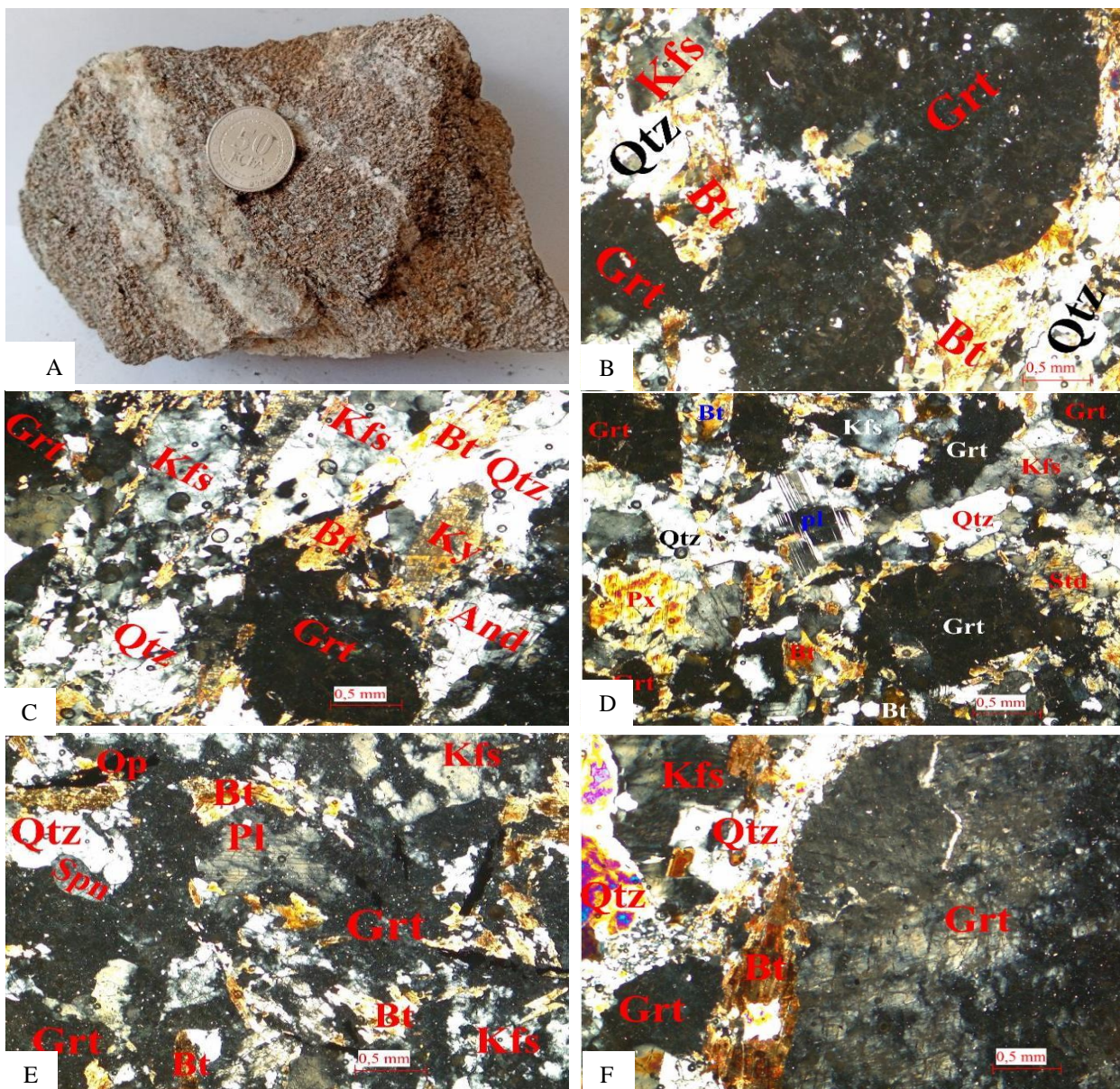


Figure 11: Macroscopic and microscopic character of garnetite; (A) hand specimen of pods of garnet showing the alignment of kyanite; (B) skeletal garnet; (C-F) Grano-lepidoblastic texture.

III.1.2. Quartzites

The quartzites rock samples is constituting the surrounding body, which in the field outcrop in the form of metric domes. It occurs at altitude of 784 m with geographical coordinates N03° 53' 4.87" and E11° 28' 01.94" in the western border of Afeumenor.

On the macroscopic scale, it has a dominantly whitish colored aspect with a medium to coarse-grained nature (Fig.12). It is subdivided into two that is: Restite and Mobilizer, in which the restites is melanocratic in color richly compose of mineral such as biotite and the mobilizer is leucocratic in color abundantly made of mineral such as quartz

Under the light microscope, this rock presents a granoblastic texture and encompasses the following minerals: Qtz +Bt+Op (Fig. 12).

Quartz (95%) is the most abundant mineral phase in the thin section. It is coarse-grained with 0.4×2.2mm in dimension and forms an aggregate of megacrystals. Quartz Crystals are subhedral to anhedral in form. Some of these crystals are associated with biotite and opaque mineral and it has minute inclusion of biotite and opaque mineral (Fig. B).

Biotite (4%) measure 0.03×0.7 mm. This ferromagnesian mineral has a needle-like subhedral to anhedral habit. It has no inclusion and in association with mainly quartz and opaque mineral.

Opaque mineral (1%) crystals are anhedral to subhedral with 0.01×0.5 mm in dimension. It is associated with minerals such as quartz and biotite and it has no inclusion.

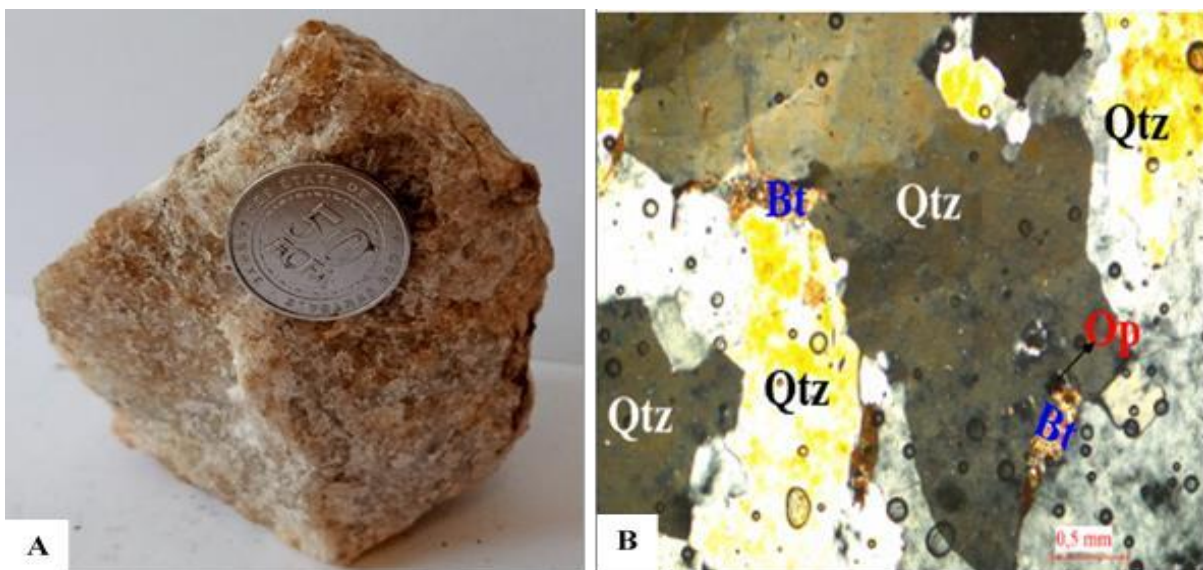


Figure 12: Mesoscopic and microscopic characters of mobilizer and restite;(A) fresh rock sample (B) minute inclusion of biotite and opaque mineral in quartz.

III.2 META- IGNEOUS UNITS

The meta-igneous rocks of the target site are metadiorites, outcropping as dome and slab. This rock is dark to light gray depending on the mineralogical composition observed in the field. At the naked eyes and under the microscope minerals are medium grained in texture. The rock is made of quartzo-feldspathic bands that alternate with ferromagnesian bands or beds (compositional foliation) (Fig. 13.A, B and C), accompanied with some pockets concentrated in garnets, amphiboles and eye shaped feldspars within the Mvolye and Leboudi quarry.

Macroscopically, feldspars, muscovites, biotites, amphiboles, quartz and garnet were observed scattered throughout the rock and occasionally as pods of amphibole and garnet (Fig.13D, E). Biotite occurs in centimetric to decametric layers in some areas of the rock and sometimes making up veins cutting across the bed rock, some amphibole crystals are in association with quartz and garnet in the form of sigmoidal coils.

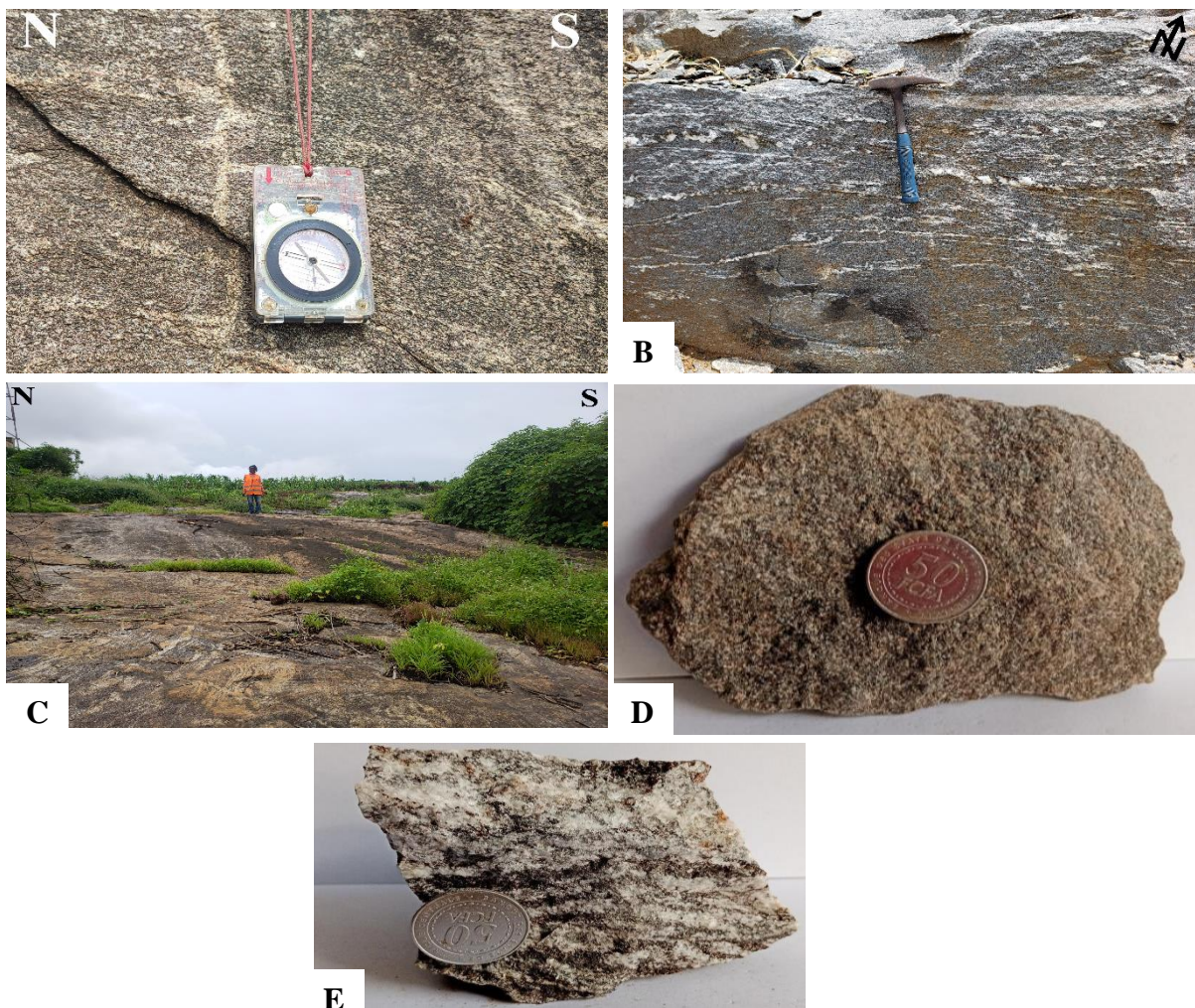


Figure 13: (A-C) Macroscopic and mesoscopic character of amphibolites seened at the Mvolye quarry and at the artisanal quarry of Fam-Assi;(D-E) fresh hand specimens of amphibolites.

III.2.1. Amphibolite

Amphibolite is exposed as pavement on the bedrock at the premises of the Mvoyle and Leboudi I quarry. The rock is fine-grained, light gray in color, with no visible minerals to the eye except plagioclase and garnet crystals unevenly spotted all over the rock. Situated at an altitude of 832 m with geographical coordinates 03° 53' 48.57" northern and 11° 26' 21.32" eastern.

Under the microscope the rock has a nemato-granoblastic texture made up of amphibole, feldspar, quartz and garnet.

Amphibole (40%) shows subhedral elongated crystals, with size varies from 0.2 to 4.0 mm in dimension (Fig. 14C). This minerals are associated with quartz, garnet and feldspars and Some sections contain inclusions of quartz while other show alteration in biotite (Fig.14D). Minerals are oriented following amphibole (Fig.14C).

Feldspar (25%) crystals are subhedral to anhedral in form. The dimension of crystals is variable in sizes 0.1× 0.8 mm and it is frequently associated with quartz and amphibole.

Quartz (20%) elongated to subhedral crystals. The grains size of quartz is up to 0.2×0.8 mm in forms and is associated in certain cases with amphibole, garnet and feldspar (Fig.14B). Sometimes quartz occurs as inclusion within amphibole and alkali feldspar crystals (Fig.14D).

Garnet (10%) skeletal subhedral to anhedral crystals in shaped, comprises 0.2×1.2 mm in terms of dimension. It is associated with amphibole and quartz and it shows minute inclusion of quartz (Fig. 14A).

Biotite (5%) sub-automorphic in form, can be seen with grain sizes that measures 0.03×0.2 mm. it is in association with amphibole, quartz and feldspars and shows no inclusion.

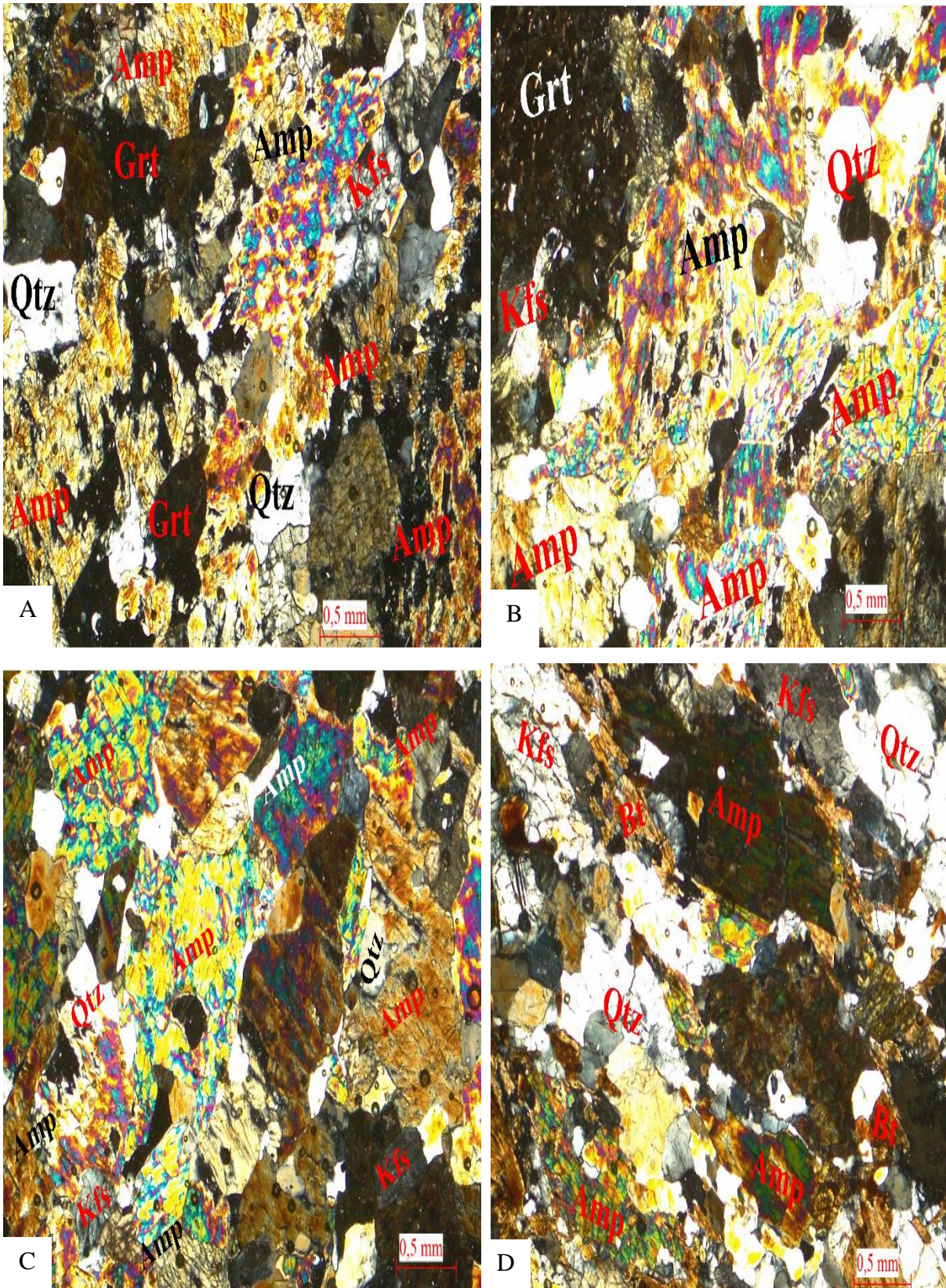


Figure 14: Microscopic character of amphibolites: (A) dommy outcrop ;(B) fresh sample ;(C-D) nemato-granoblastic texture and mineral association.

III.2.2. Staurolite-cordierite gneiss

The outcrop is light gray in color, occurring as slab shaped structure that ranges to about 40km. It occurs at altitude of about 753 m and geographical coordinates $03^{\circ}47' 57.59''$ northern and $11^{\circ} 26' 20.92''$ eastern at the Bibong Bidoum Antenne area.

Based on the microscopic observation, distinguishable minerals are garnet, biotite, muscovite, kyanite, quartz and feldspar.

Under the bright microscope, the rock displays a grano-lepido-nematoblastic texture abundantly composed of quartz, biotite, plagioclase, kyanite, garnet, muscovite and pyrite.

Feldspar (25%) occurs as subhedral to anhedral crystals. This grains measure 0.1×1.0 mm and it is associated with quartz, amphibole and biotite (Fig. 15 D).

Quartz (20%) crystals are subhedral in form, comprises, 0.1×2.2 mm in terms of dimension. It is associated with plagioclase, biotite, feldspar and amphibole, it has minute inclusion of biotite. Quartz is transforming itself to plagioclase (Fig. 15A).

Amphibole (15%) elongated to subhedral crystals and ranging from 0.2×2.6 mm. It is in association with quartz and feldspar where it has minute inclusion of biotite and feldspar (Fig. 15B).

Biotite (15%) seems as anhedral elongated crystals. It has grain sizes that measure 0.4×3.1 mm in association with biotite, feldspar, cordierite and quartz, and showing alteration product. Biotite is seen included in amphibole (Fig. 15B).

Plagioclase (10%) has a subhedral to anhedral habit. It has 0.3×2.0 mm grain sizes and is in association with biotite, quartz and amphibole, forming triple points and contacts. The contact between the associated minerals above are uneven and rough. Biotite and quartz are seen in inclusions in plagioclase.

Garnet (7%) crystals occurring as subhedral to anhedral in form, can be seen with grain sizes that measure 0.3×0.7 mm. It is in association with quartz, feldspar and biotite forming triple points and contacts (Fig. 15A). The contact between feldspar and the other minerals (biotite and feldspar) are rough and uneven.

Cordierite (4%) euhedral shaped crystals, comprises 0.4×0.9 mm. It rarely has inclusion and is associated with biotite and feldspar.

Staurolite (3%) appears as anhedral crystals, ranging from 0.3×0.6 mm in sizes. Associated to plagioclase, quartz, biotite and feldspar.

Pyrite (1%) it is euhedral in form, ranging from 0.2×0.4 mm. Which associated to biotite, garnet, quartz and feldspar and it shows alteration product (Fig. 15A).

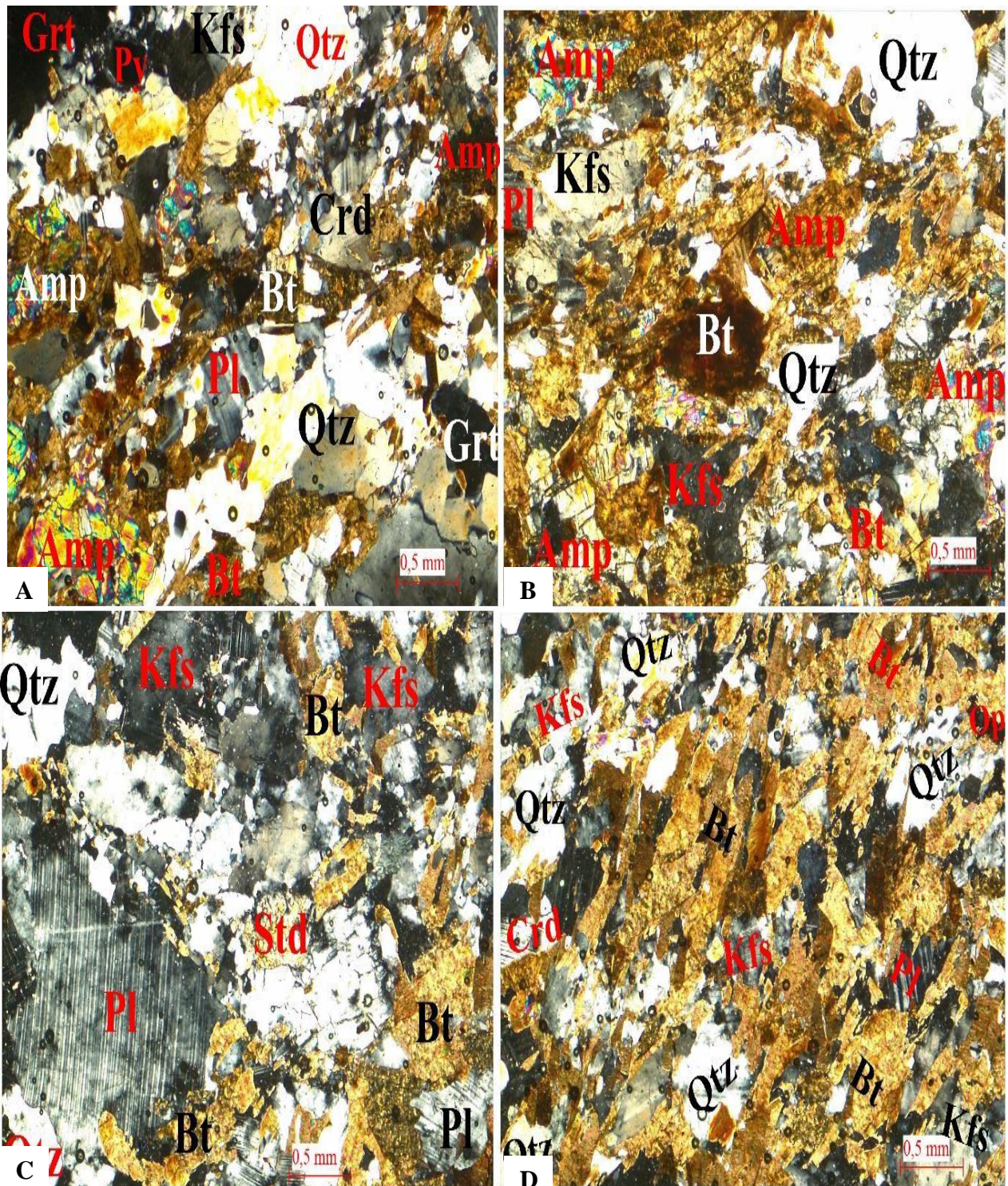


Figure 15: Microscopic characters of Staurolite-cordierite gneiss (A, B) grano-nematolepidoblastic texture and inclusion of biotite in amphibole; (C) transformation of plagioclase to biotite; (D) mineral orientation following biotite

Petrographic characteristics of rocks in the target site.

Table 2: Summary of the different rock type of the study area

Metasedimentary unit				
Rock name	Occurrences	Microstructures	Mineral assemblages	Metamorphic Facies
Kyanite-Biotite gneiss	Slab	Grano-lepidoblastic	Bt+Grt+Qtz+Ky+And+Ky	Granulite
Garnetite	Dome	Grano-lepidoblastic	Grt + Bt +Qtz+ Ky+ And+ Kfs+ Pl± Px	Granulite
Garnet-Biotite gneiss	Slab	Grano-Lepidoblastic	Grt +Qtz +Bt+ Kfs± Pl	Amphibolite
Quartzites	Dome	Granoblastic	Qtz +Bt ± Op	Amphibolite
Meta-igneous units				
Amphibolite	Slab and block	Nemato-Granoblastic	Amp+Kfs+Qtz±Grt	Amphibolite
Staurolite cordierite gneiss	Slabs	Grano-Nemato-Lepidoblastic	Kfs+Qtz+Amp+Bt+Pl+Grt ±Cd±Std	Amphibolite

CONCLUSION:

The detailed field mapping and petrographic description of samples from the study area helped in classifying these samples as a purely multi-facial metamorphic lithological set (Tab. 2) composed of migmatites (biotite-garnet gneiss, kyanite-garnet gneiss, garnetite and leucosomes) and metadiorites (amphibolite and staurolite-Cordierite gneiss). These rocks are generally characterized by a granoblastic heterogranular texture. Some garnet porphyroblasts in garnet gneiss exhibit poeciloblastic microstructures. Helicitic texture was identified in amphibolite, while the foliation bounded around the garnet porphyroblast lead to the development of a pressure shadow zone and the formation of a structure in the form of an eye structure.

**CHAPTER IV: GEOMORPHOLOGY AND
STRUCTURAL ANALYSIS**

This chapter present the geomorphology which aim is to highlight the relationship between the shapes of the relief and lithology of the study area, to determine the tectonic evolution imprinted on metamorphic rocks and associated formation through geometric, kinematic and dynamic analysis of structural elements on the megascopic, macroscopic and microscopic scales.

IV.1. GEOMORPHOLOGY

IV.1.1. Orography

The orographic map (Fig.16) of the sector highlight two portions, a SE low lying river characterized area, justified by low altitude contour lines that widens and spaces out from a WSW-ENE direction and the NW hilly to mountainous environment in which hills and/or mountains trends toward the NE-SW directions and noticed by the presence of tight, chunked up or compact concentric high altitude contours (750-1050 m) for exemple around Eloumdem, Centre and Oyomabang.

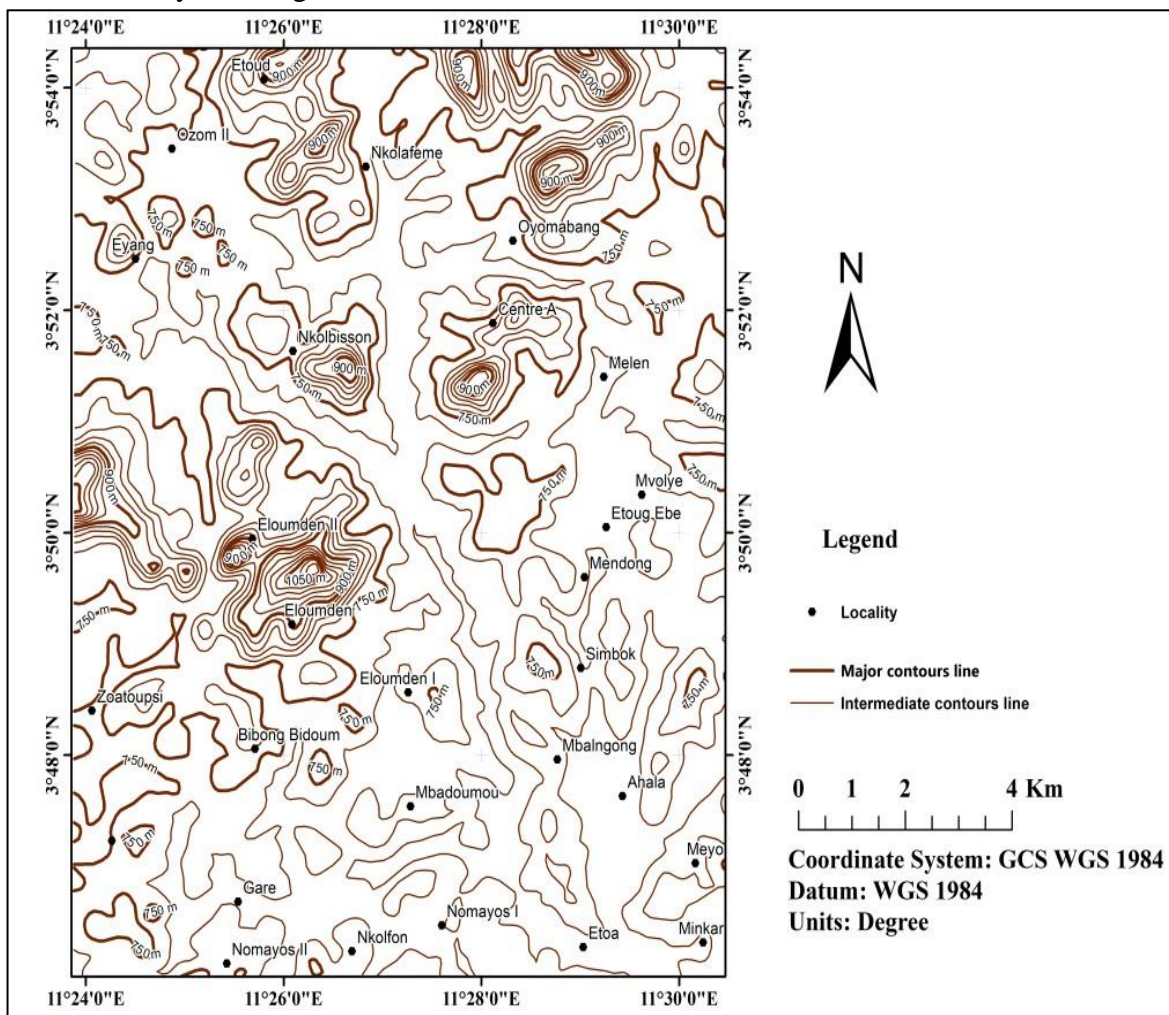


Figure 16: The orographic map of the target area.

This map was designed or constructed from an SRTM image of the centre region of Cameroon, that provides information on the different altitudes of the target area, showing variations in the elevation of relief models drawn from 4 sectional profiles (Fig.17: A-B, C-D, E-F and G-H) that exhibits 3 geomorphological units (Fig. 18).

- The low altitude units (shown at the right part of profile A-B and E-F) which occupies the SE and extend towards SSW, ranging from about (600 - 700 m), consisting of U-shaped valleys, occupied by streams, rivers (e.g. Ngaa) or run offs that takes their sources up slope transporting in regolith and other fragments from highlands through intermediate to lowlands. The regolith may later incorporate with organic matter to form soils, reason why the low lands are abundant with soils.
- Intermediate altitudes regroup elevations ranging from 700 to 950 m consisting of a chain-like sub-circular hills to elongated domes in the NW-SE (profile G-H), NNW-SSE, (profile E-F) and NNE-SSW (profile C-D) directions. The hills are characterized by varieties of metamorphic rocks like gneisses, amphibolites etc designed with structures.
- High altitude units which extends from 950 to more than 1100 m towards NW-SE (profile C-D) direction. They are characterized by cone and dome shaped chain-like summits on one hand and U-V shaped valleys on the other hand. They are equally composed of metamorphosed rocks of different varieties having fascinating structures like folds, bandings, and shear structures.

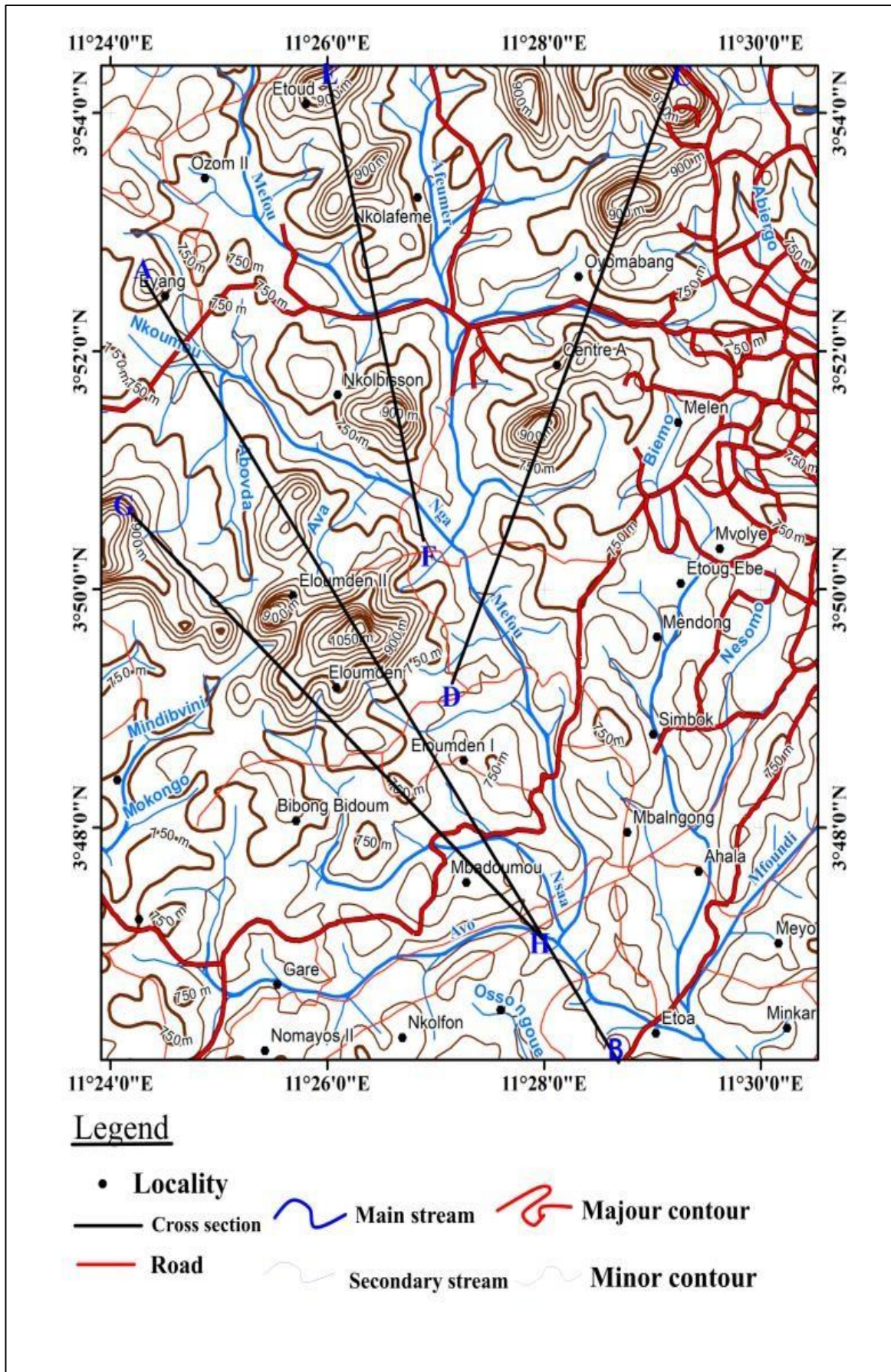


Figure 17: The topographic map showing the cross section of the target site

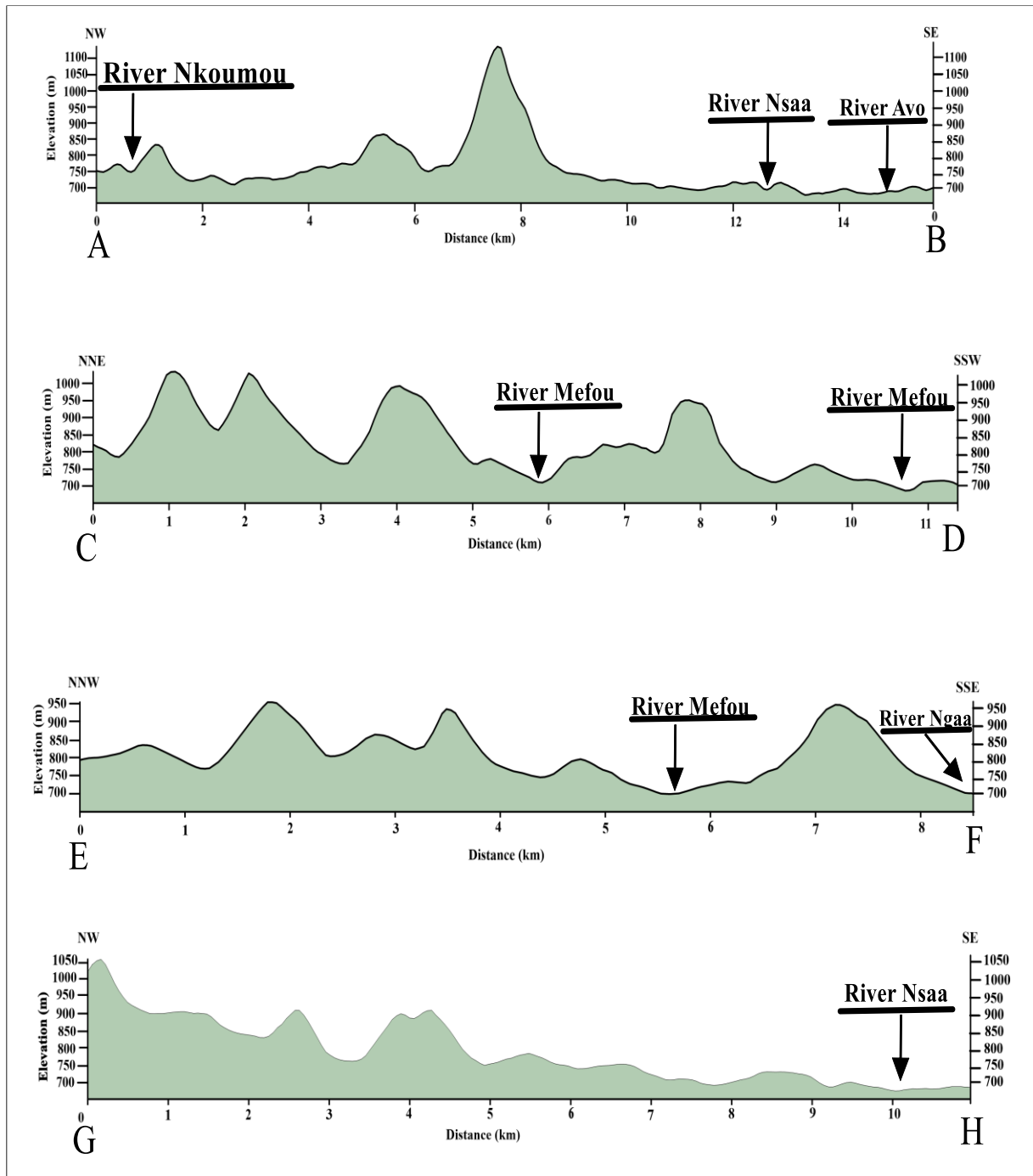


Figure 18: Cross section of the target site showing 4 profiles

IV.1.2. Hydrographic patterns

Seeing that the low lying areas or altitudes composes of lowlands that are generally characterized by rivers (Mefou river), a hydrographic lineament (Fig. 19) of the sector was drawn from the hydrographic SRTM, to foster a map that shows the hydrographic networks as a dendritic pattern, with dendrites trending in all directions. Based on this map, a

The hydrographic lineament map (Fig. 20A) provided rosettes that confirms the general directions (E) of the hydrographic network in relation to the river sources that correlates to the fracture types. Thus, this data helped to correlate and distinguish between river rich fractures and dry fractures generated from normal lineaments. In a specific sense, the flow overrides the NNE-SSW trend, with the major streams showing the high peaks. The highest peak lodged in the SE takes the direction of N109E. These streams may also give an account on the formation and widening or narrow nature of fresh or water rich fractures of the target site (Fig. 20B).

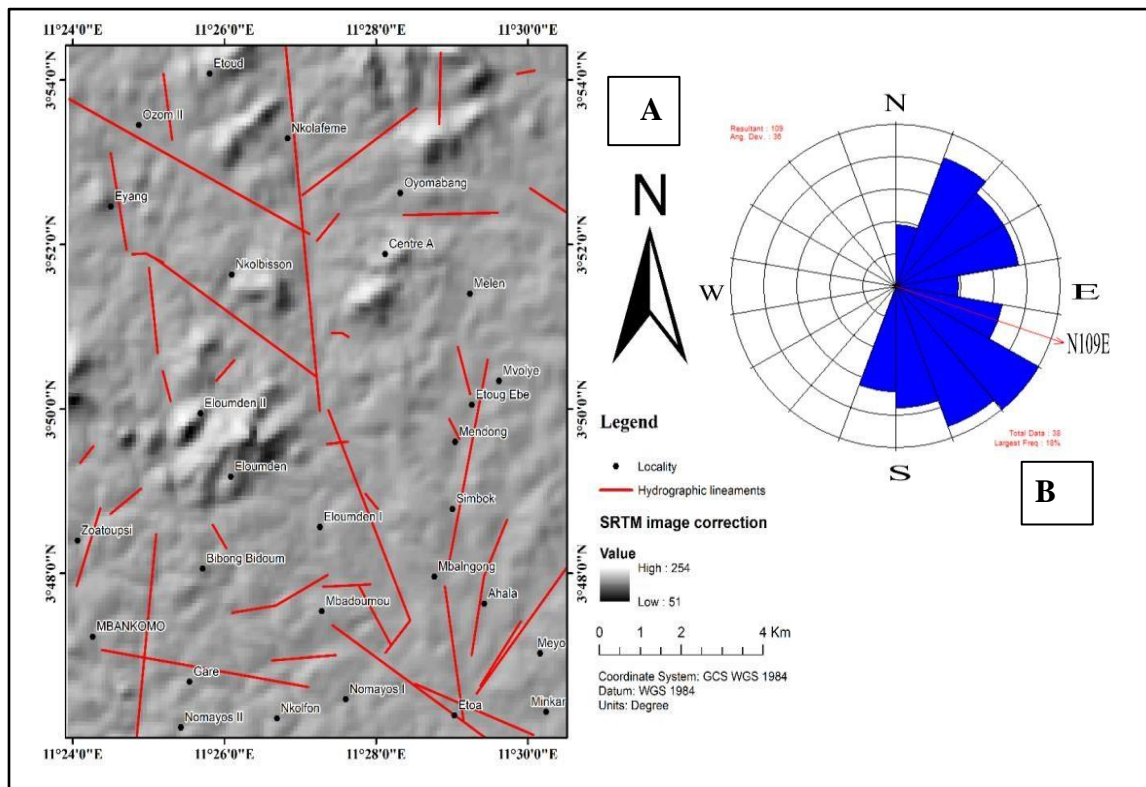


Figure 20: The hydrographic lineament of the Target site (A) and the directional rosette of hydrographic lineaments extracted from the SRTM image (B)

IV.1.3. Slope identification and analysis

The slope (Fig. 20) of the study area proves the presence of hills with positive gentle slopes recognized by concentric repeating yellow-orange or reddish brown colors (up to 47°) in the NW and trending towards NNE –SSW on the map. The gentle slopes are continuous from one hill, then a valley or lowland to the next hill and another valley or lowland, giving adulatory sensations that perhaps resembles fold chains. These slopes characterize a good transport condition that cleared them from every rigorous nature of fragments developed through weathering or human activities. Thus, even though a small portion of the slope may not be significant as of what concerns human activities, making some parts of the target site

difficult enough to be accessed. However, greater portion of the slopes in the area still have good propensity for farming at one end and at the other for construction of houses and roads as seen during fieldworks. The slope map equally highlights crest and troughs lines (whose talweg is highlighted up to 47°) with depression bottom seemingly taking U to V shapes as seen on the profiles above. Regarding the nature of the crest and trough lines, one notices a gentle to steep slope rising from 8° (yellowish green portion of the map seen on the legend) to 47° (reddish brown to orange portion), thus, defining alignments of visible hills and/or mountains as ridge lines on the map from the NNE to SSW. Below 8° are lowlands while above 47° are very high altitudes that are not accessible to man easily.

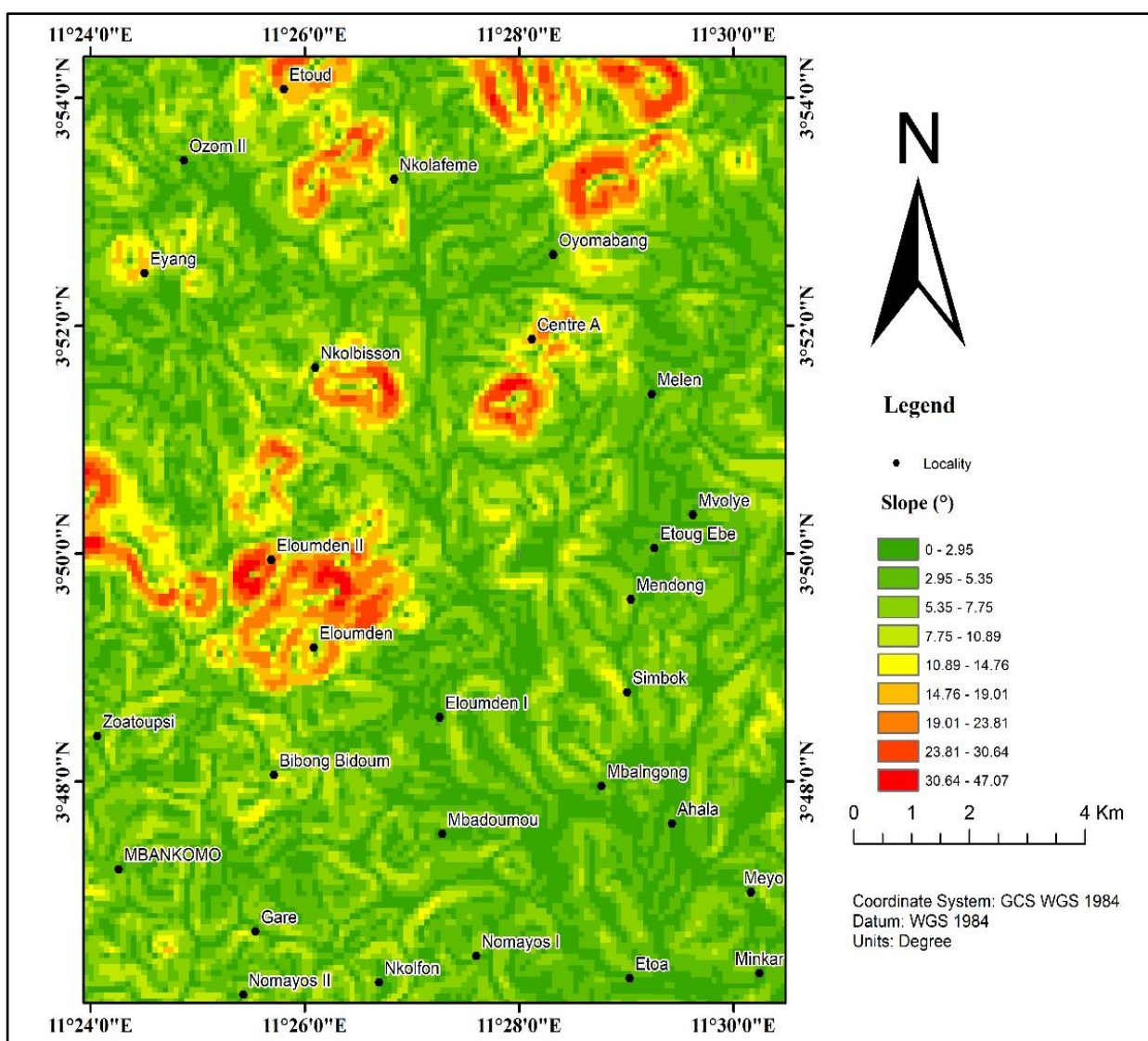


Figure 21: The slope map of the target area and its surrounding digitalize from an SRTM image

IV.1.4. Lineament analysis

The map for lineaments provides information on the regional scale arrangement of geological structures base on SIG and SRTM satellite image management. The resulting map of lineaments was made using cartographic softwares like ArcGIS 10.8. Corrections made with Hill shades were prepared according to directional scans, pre-programmed according to the position of the sun in the study site and following this corrections, 02 main filters namely: Gradient and sobel filters engered the overview of these lineaments thus, allowing identification and vectorising of all the straight bulging lined structures on the map of the target site. As shown in the map below the target area is intensely fractured with exception of the NW part of the sectors which has little fracture (Fig. 22A).

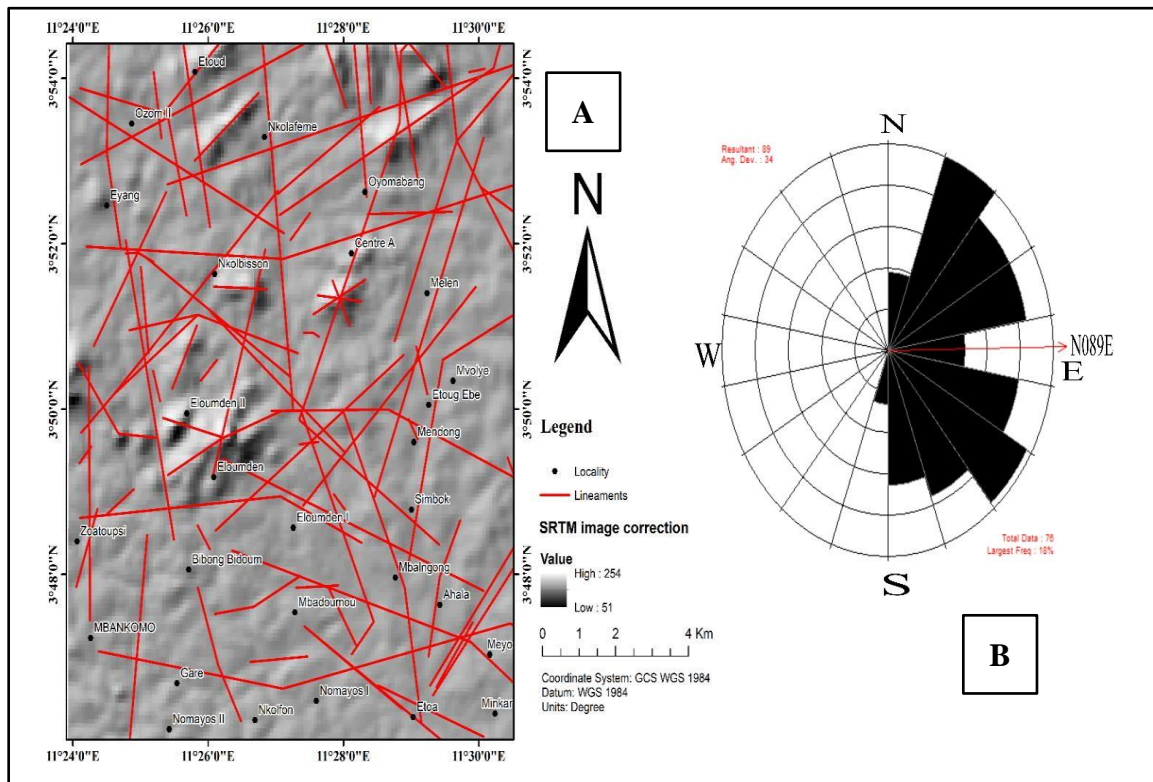


Figure 22: Lineament analysis map of the target site (A) and the directional rosette of the lineament of map extracted from an SRTM images (B).

The directional lineament rosette of the map highlights the main direction of structures in the N089E. The data obtained from the target site shows that field observed structures that ties with the lineaments are lines, schistosity, cleavages in high grade rocks, foliations and folds having preferential orientation in the NNE -SSW direction (Fig. 22 B). The ridge line map helped to identify and characterize hilly to mountain chains of the study area (Fig. 23A) by highlighting the position, shape and orientation of the mountains or hills. These lines are

concentrated toward NW on the map, indicating the density of hills/mountains along the NW border of the western part of Yaounde. These hills/mountains are elongated to sub- circular and/or circular in shape, generally aligned to the W-E direction. Thus, fostering the circulation of water in the target area downslopes and in lowlands or valleys. This could account for the good water flow of rivers like the Mefou. Rosette generated from ridge map highlights a major direction of N142°E for the hills/mountains, influencing crest lines towards NW of the sector. The rosettes also highlight the general direction of the crest line as N071°E, which roughly defines the entire crest lines of the sector that is 14 ridge lines listed (Fig. 23B).

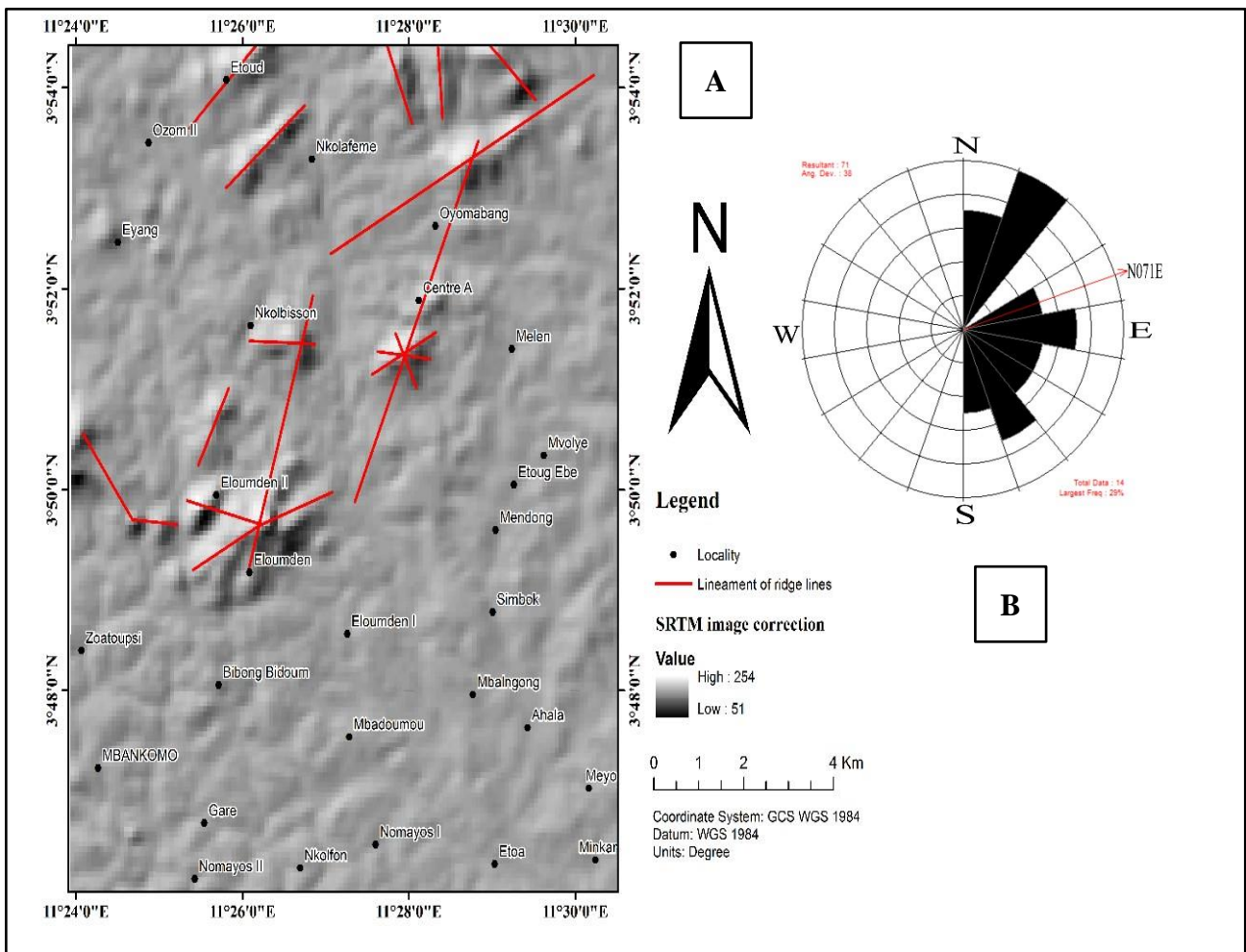


Figure 23: The ridge line map of the sector and its surrounding (A) and the directional rosette of the ridge line map extracted from an SRTM image (B).

IV.1.5. Fracturing lineament

Considered as crustal phenomena on rocks exposed as surfaces, in road cuts or stream outcrops, linear fractures are innumerable, commonly spaced fractions of a meter to a few meters apart and in different orientations. In the characterization of the study area which may have some

potentials for hosting a repository information at depth in crystalline bedrocks, it is essential to understand the existent framework of brittle deformation zones in the bedrock. The fracture lineaments of the study area were acquired around 3:30 am., local time, when sun's rays came from NW position at a moderate elevation angle. Fractures occupying depressions trending NE are shadowed on their SE side, and therefore, stand out in the image as shadow relief (Fig. 24A). Those trending NW are equally illuminated on both sides hence, largely invisible and easily missed. The directional rosette of these fractures shows directions for the linear fractures grouped at regular intervals (10°) such that the length of the tapering bar in each interval is proportional to its frequency distribution (17%) among all the lineaments in the intervals distributed over 180° ; that encompasses NNE to SSW trends. Note that the dominant direction for these fractures is N092E, with highest peaks in the NE and SE directions respectively (Fig. 24B).

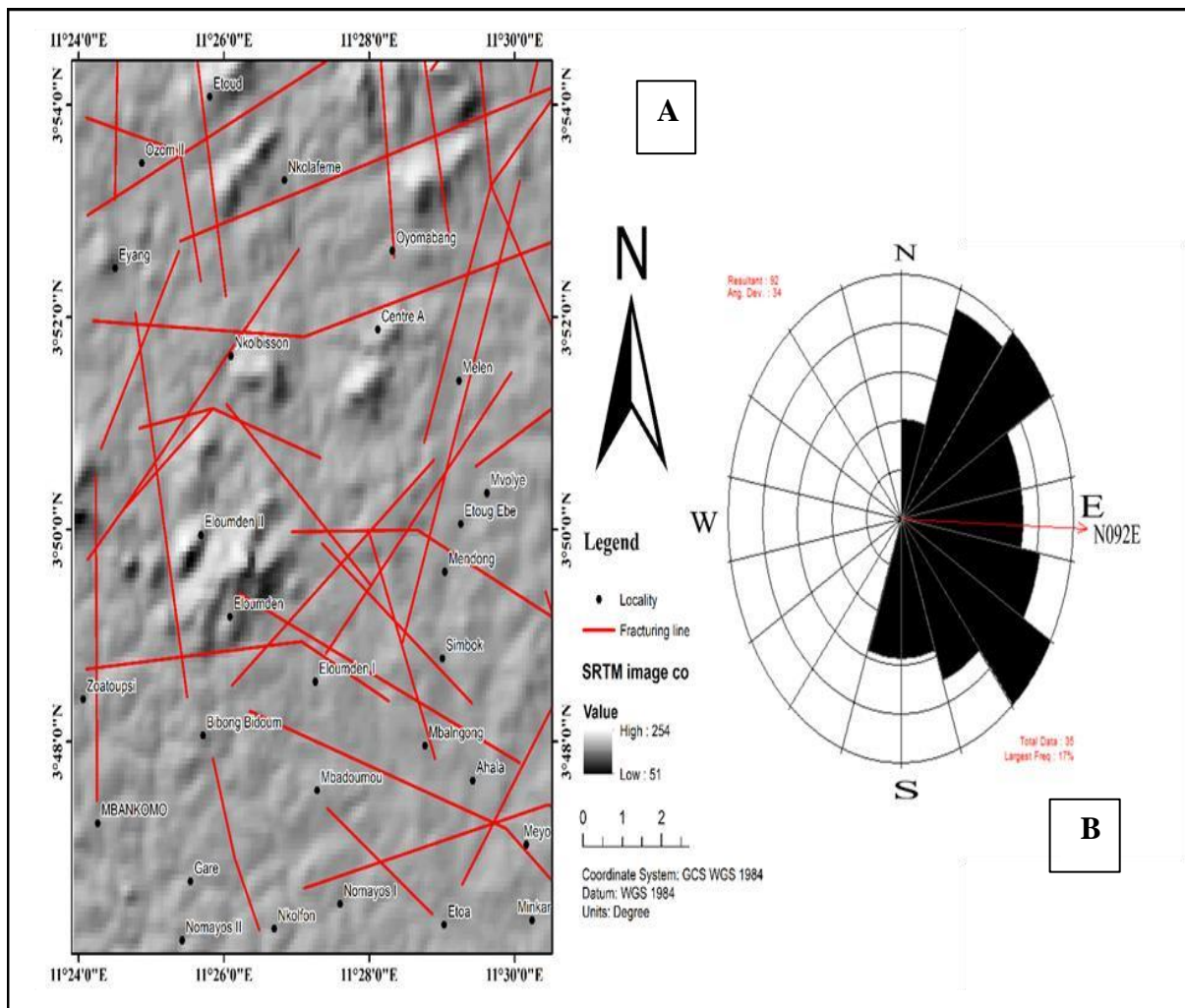


Figure 24: The fracturing line map of target area (A) and the directional rosette of the fracturing line map digitalize from an SRTM image (B).

IV.2. STRUCTURAL ANALYSIS

Western Yaounde is made up of high grade metamorphic rocks that have been affected by a multistage deformation, generally characterized on the bases of the deformational stages below.

IV.2.1. D1 deformation stage

D₁ exhibits schistosity or foliation, boudinage and fold planes selectively segmented into planar structures. These structures can be represented as follows.

IV.2.1.1. S₁ Foliation

The S₀/S₁/S₂ plane (Fig. 25A) of the study area is generally marked by preferred mineral orientation and compositional bandings in the gneisses of Akouandoue, Nkolbison, Mbadoumou, Bibong -Bidoum and Mbankolo quarry. The bandings are millimetric to centimetric, composed of ferromagnesian (mafic or dark e.g. biotite, garnet and amphiboles in a preferred orientation) layers, alternating the quartzofeldspathic (felsic or light colored e.g. quartz, feldspars) layers, forming planes generally striking from N138E 32° NE to N140E 18°NE.

V.2.1.2. B₁ boudins

The B₁ boudins are intra-foliated and contemporary with the S₁ schistosity, they are mostly observed in the quartzofeldspathic layers of the migmatites striking toward SE and seen as complete boudins on one hand, while others show pinch and swell on the other hand due to much compression around the edges and less extension towards the swelled areas (Fig. 25 B). In some area like Nkolbison synschistose intra-foliated boudins are consist of minerals such as biotite, quartz, feldspar, biotite and kyanite (Fig. 25 C), probably resulting from concentrated hydrothermal fluids that crystalized at the time of compression and extension (Fig. 24C).

IV.2.1.3. F₁ fold

The F₁ fold are observed in the quartzo-feldspathic layer. They are intra-foliated and syn-schistose, in some area within the migmatites of the Mbankolo quarry. They are mostly observed at the Mbankolo quarry and at the hill of Vogt-betsi of direction N045E (Fig. 25A).

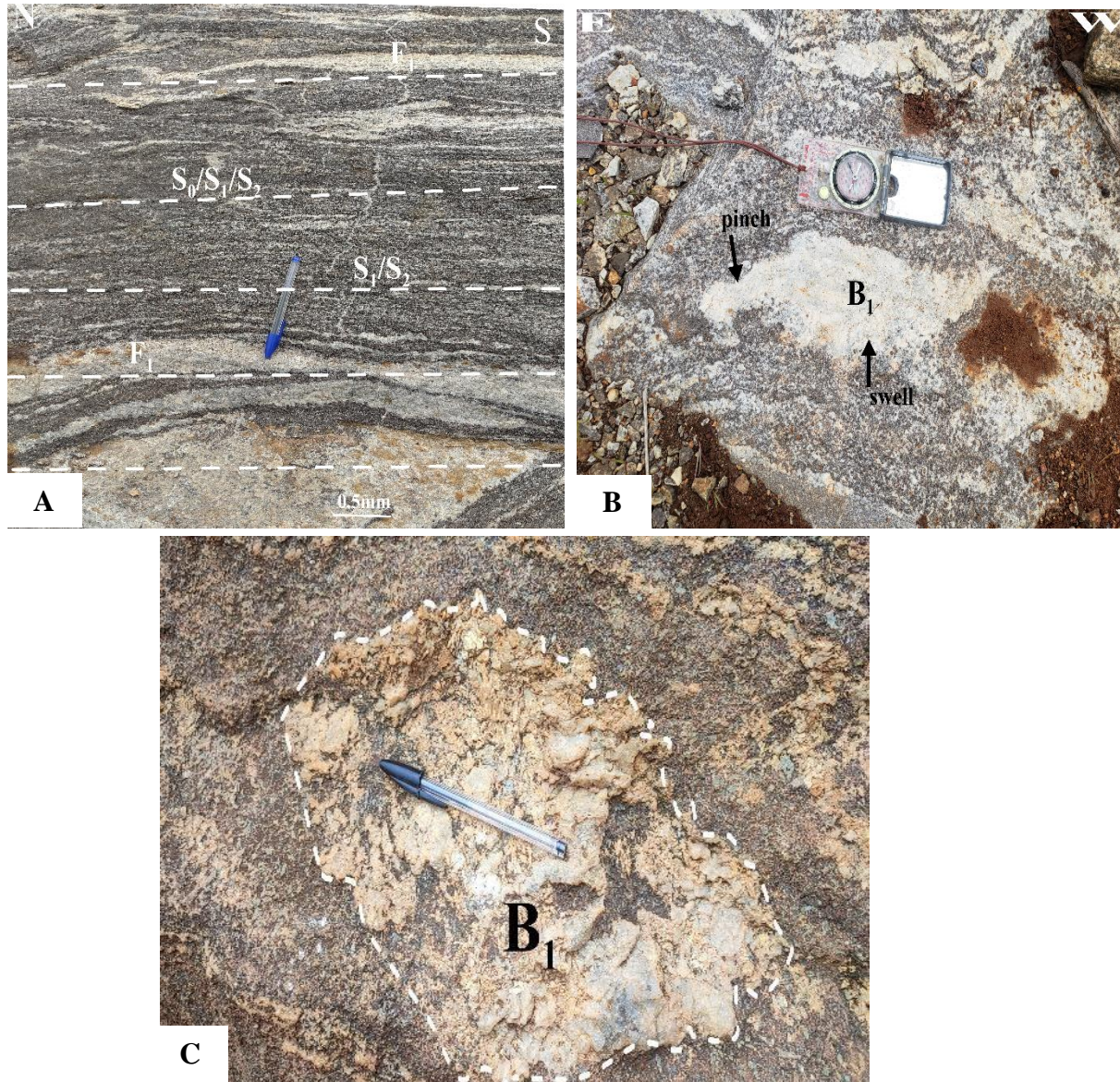


Figure 25: Structural element observed in the target site related to the D1 deformational phase: (A) F_1 foliation; B) B_1 pitch and swell boudins; C) quartzofeldspathic B_1 boudins.

The stereographic projection (Fig. 26A) of S_1/S_2 foliation planes indicates that the cyclographic traces are more compact in the NW-SE and NE-SW directions with contradictory dips. The planes foliation dips mainly in the NW. Thus, interpreting the existence of folds. Poles concentrated SE of the stereogram may account for compression (shortening) and slight extension (slight elongation) following the NE-SE directions. Stress axes (Fig. 26B) that probably results from such deformation provides orientations: σ_1 (N124. 72°), σ_2 (N281.17°) and σ_3 (NO13. 6°). Thus, we have $\phi\sigma_1 > \phi\sigma_2 > \phi\sigma_3$ indicating that the D1 deformation would be a flattening induced by a shortening NE-SE.

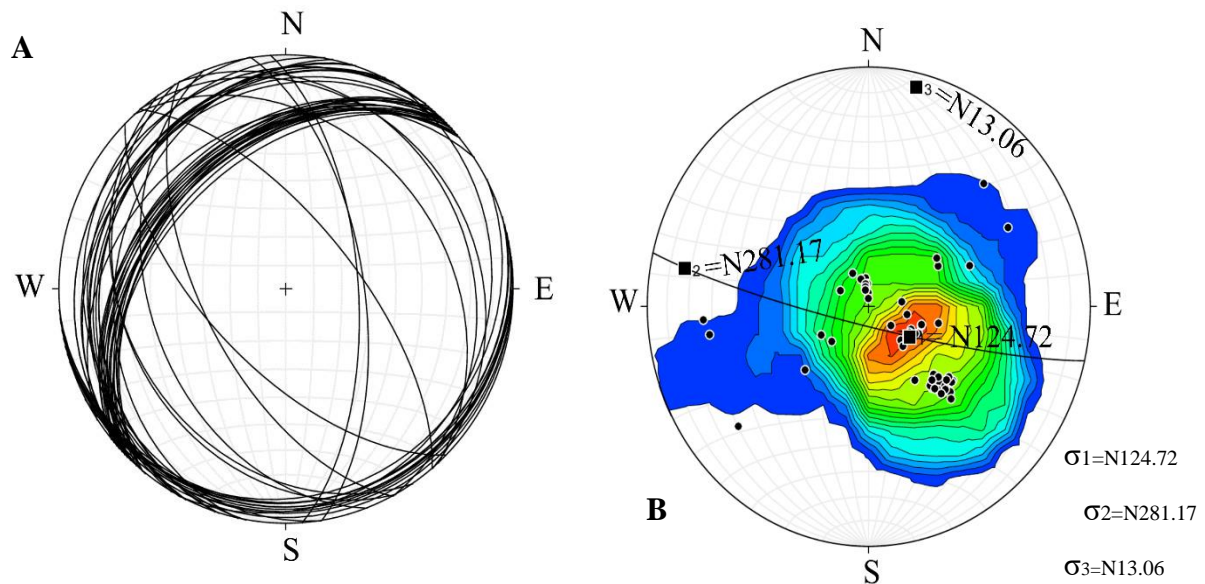


Figure 26: Stereographic representation of the F1 foliation planes of the target site: (A) cyclographic traces; (B) polar diagram

IV.2.2. D₂ deformation stage

The D₂ phase is ductile-brittle and affects the gneisses of the study area. The result of D₂ phase are structures such as S₂ foliation, B₂ boudins, F₂ fold, C₂ shear and L₂ lineation designed on both the metasedimentary and meta igneous units of the western Yaounde.

IV.2.2. 1.S₂ foliation

Probably developed from S₁ in the course of the progression of D₁ to D₂ and are parallel to the C₂ shear which may have engendered the process, thereby producing F₂ joints (Fig. 27B). This structure can be confirmed by the presence of the S₂ crenulation cleavages at Vogt-betsi, formed as a result of continual stress initiation and are then developed by further dissolution of quartz in the fold limbs (Fig. 27D).

IV.2.2.2. B₂ boudins

They are observed in the migmatites of Mbankolo quarry. These boudins are in the form of complete and incomplete sausage filled with quartzo-feldspathic minerals only (Fig. 27B). They occur as continuous asymmetrical series, each developed due to compression and extension, forming pinch at their junctions. The sausages encountered in the study area are of size variation cm, pointing in the NE direction, with a sinistral movement.

IV.2.2.3. F₂ folds

F₂ fold formed by continuous compression of the S₂ foliation on the metasediments and metadiorites of the Nkolbison quarry and the of Mvogt-betsi outcrops respectively, where S₁ exist as relics. The fold type here is symmetrical inclined levo-rotatory sinistral, oriented NNW-SSE and dipping 10° NE (Fig. 27D). It is important to note that the rock composition and competence play a vital role in the formation of the F₂ fold. F₂ folds are 2cm in diameter, having axial planes running parallel to the fold direction. Large folds commonly have smaller-scale folds in their limbs and crest formed during flexure of layered rock where slip occurs between rocks layers known as parasitic folds are mostly common in the metasedimentary rock of western Yaounde mainly made of M-fold (Fig. 27 A) in which the hinge line are symmetrical dipping at NE direction and the S-fold in which the short limbs appear to have been rotated counterclockwise (Fig. 27B) which are asymmetrical dipping in the northern direction.

IV.2.2.4. Lm₂ mineral lineation

Rocks of the study area contain lines or lineations that are widely oriented in different directions depending on their spatial positions and dispositions which is formed by the alignment of kyanite crystals in biotite-garnet gneiss, kyanite-biotite gneiss and garnetite following straight to needle-like paths, thus, attributing the name mineral lineation (Fig. 27E).It is sub-horizontal (2 to 20°) with Lm₂ that strike from NW-SE observed at the Nkolbison, Mbankolo quarry and at the hill of Mvogt-betsi.

IV.2.2.5 .C₂ shear

The C₂ shear planes are rare (Fig. 27 F) were mainly observed in kyanite-biotite gneiss and biotite-garnet gneiss of the Mbankolo quarry and the hill of Akouandoue. These shears are responsible for the slight curling of the quartzo-feldspathic veins and the ferromagnesian dark bands which transposed F₁ foliation with either sinistral or dextral movement dipping towards N160E.

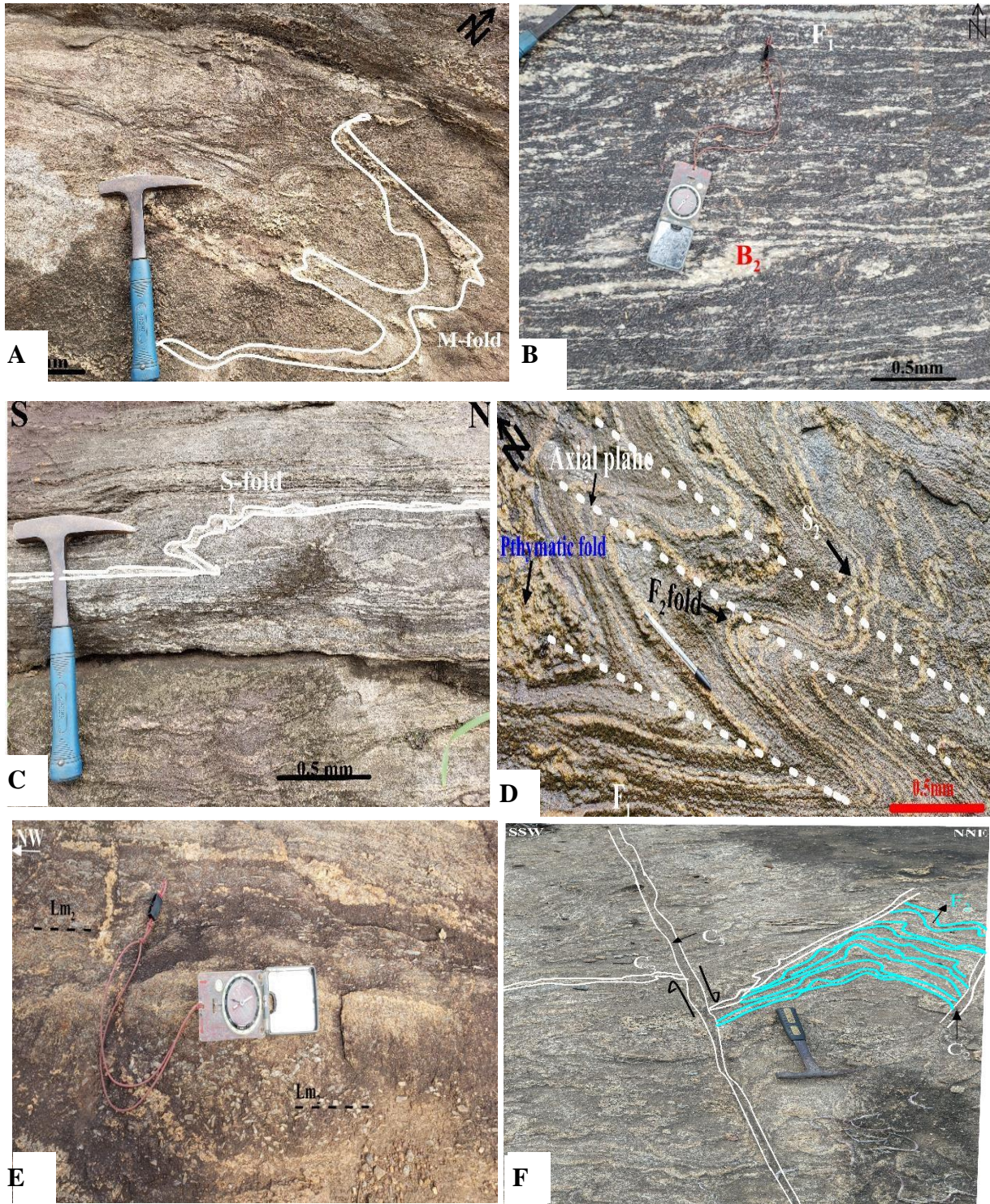


Figure 27: Structural element related to the D₂ deformational phase D₂: A) F₂ M- fold; B) F₂ symmetrical fold; C) S-fold; D) S₂ crenulation; E) Lm₂ mineral lineation F) C₂ shearing and F₂ fold.

IV.2.3. D₃ deformation stage

The D₃ are characterized by transposition of D₂ structures. The structures which develop here are as follow,

IV.2.3.1. S₃ foliation

The S₃ schistosity grows in C₃ shear joints showing minerals alignment of quartz and feldspar mostly observed at the Mbankolo quarry (Fig. 28B). S₃ foliation is outlined by a lithological banding and a compositional and is locally sheared and folded .in general one orientation od S₃ plane have been identify as ENE-WSW with an average dip of 45°ENE,50°WSW recorded respectively in kyanite-biotite gneiss and biotite gneiss.

IV.2.3.2. C₃ shear

The C₃ shear is mostly observed on the gneisses at Vogt-Betsi, Mbankolo and at fam-Assi. C₃ are sinistral (Fig. 29A, C), striking N014E and formed as result of progressive deformation inherited from a D₂, shown by a quartzo-feldspathic vein that cuts across F₂ folds.

IV.2.3.3. F₃ fold

The f₃ fold are mostly observed in the metadiorites and metasediments in the study area found at Bibong-Bidoum and Mbankolo quarry, the V₃ veins which crosses, intersecting the F₂ foliation and then a F₃ fold is being formed, the F₃ fold are either dissymmetrical upright folds with sheared limbs or kink fold (Fig. 29B), the altitude of the F₃ fold lies between N038E and N044E.

IV.2.3.5. F₃ fracture

In the kyanite-garnet gneiss, the F₃ fractures are oriented NO68E and it cuts the S₁ foliation including the C₂ shear in the biotite-garnet gneiss of Bibong-Bidoum Antenneire which were caused by stress exceeding the rock strength, causing the rock to lose cohesion along its weakest plane (Fig. 29C). The F₃ fracture planes altitudes are of various directions testify the fact that the rock has undergone a great deformation in time with a fairly high pressure; as direction, we have NE-SW, NNE-SSW, ENE-WSW, E-W thus indicated by the directional rosette diagram (Fig. 28)

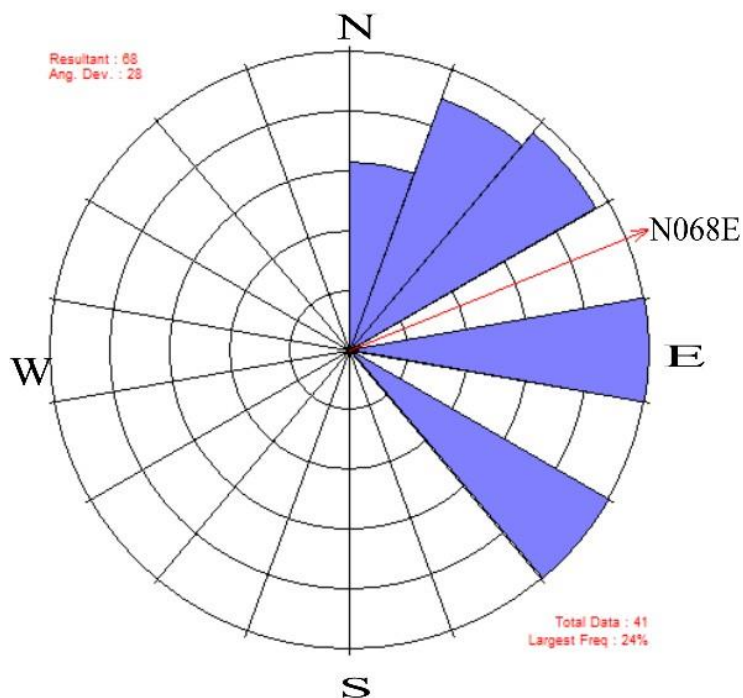


Figure 28: Rosette directional diagram of F3 fracture.

IV.2.3.4. V₃ veins

The V₃ veins is sub-vertical and observed at the Mbankolo quarry (Fig. 29A) The V₃ vein cut across the f₂ foliation and F₂ fold. The V₃ veins are filled with minerals such as quartz and Feldspath formed when the mineral constituents where carried out by an aqueous solution within the rock mass which were deposited through precipitation due to hydrothermal circulation.

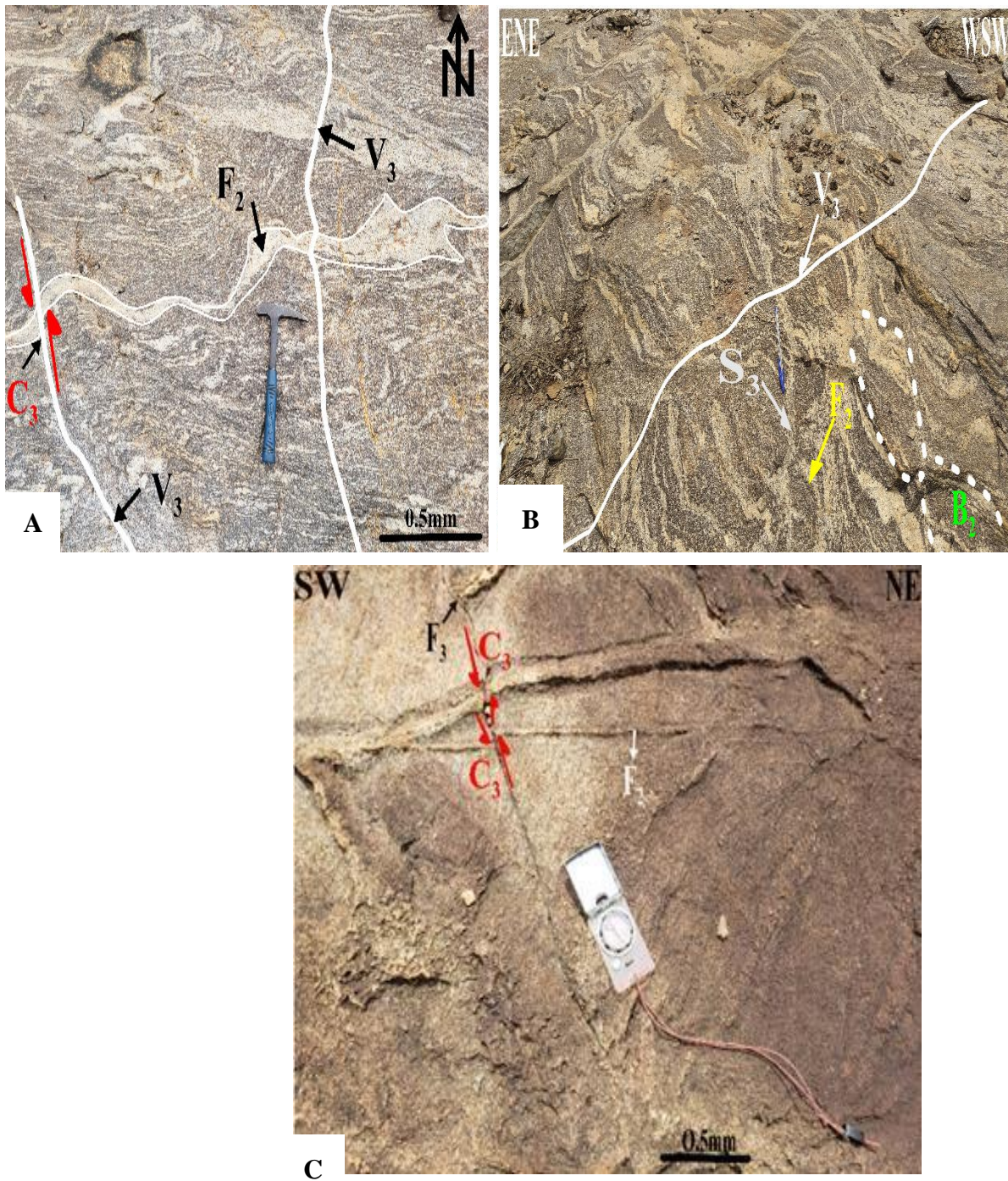


Figure 29: Structural elements observed at the D3 deformational phase: A) V_3 veins and C_3 shear found at the Mbankolo quarry; B) F_3 fold, S_3 schistosity; C) C_3 shear and F_3 fracture found at the hill of Oyomabang.

IV.2.4. D₄ deformation Stage:

The D₄ deformation stage is characterized by a brittle deformation phase resulting to the fracturing of rock. The fractures are infilled by powder cemented material.

IV.2.4.1. F₄ fracture

At Oyomabang almost all the outcrops are highly fractured throughout the zone showing a family of fracture cross-cutting in different directions, with a major dip that is N050E. some of the fractures are filled with minerals and while others are completely dry, and then the rocks can easily be broken due to the fracture found in it, therefore giving access to water to circulate easily (Fig. 30A).



Figure 30: Structural element related to the D₄ deformational phase: (A) F₄ fracture field with quartzo- feldspathic minerals.

The stereographic projection obtained in the D₄ deformation stage show that the cyclographic traces are more compact in the NNW-SSE and NNE-SSW directions (Fig. 31A.). The polar diagram which defines this F₄ fracturing (Fig. 31B) characterizes the stress axis that probably results from such deformation provides orientation: σ_1 (N014. 15°), σ_2 (N120. 44°) and σ_3 (N270 .41°). Thus, we have $\phi\sigma_3 > \phi\sigma_2 > \phi\sigma_1$ indicating That the D₄ deformation would therefore be an elongation induced by σ_3 stress towards the E-Wdirectin.

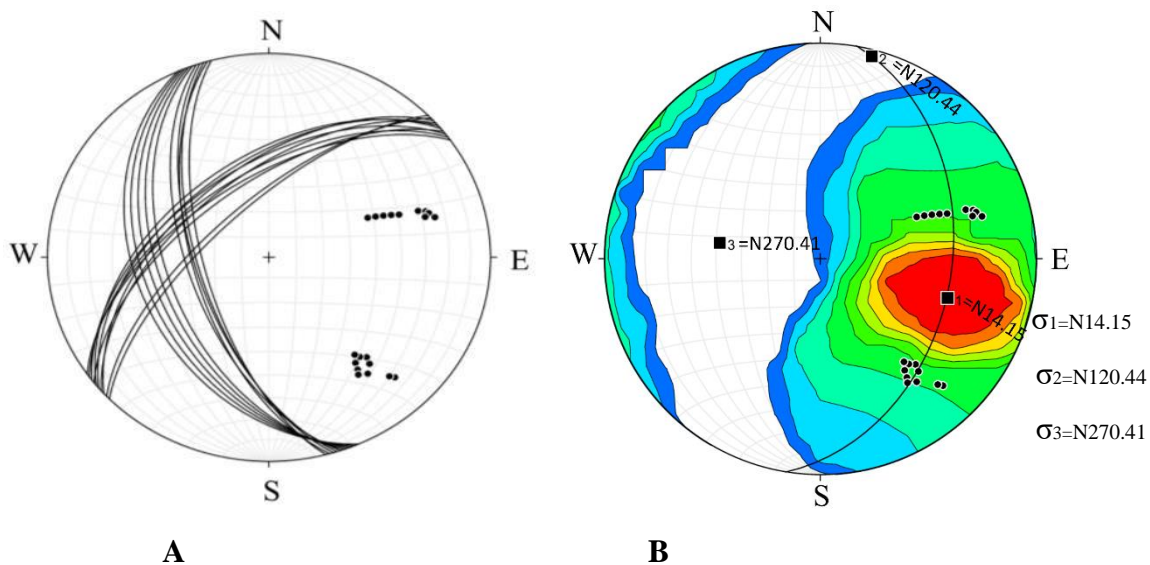


Figure 31: Stereographic representation of F₄ fracture: (A) F₄ cyclographic traces.; (B) F₄ polar diagram.

V.2.5. D₅ deformation stage

The D₅ deformation phase is characterized by a brittle deformation phase resulting to the fracturing of rocks, its consist of C₅ shearing and F₅ fractures.

V.2.5.1. C₅ shear:

The C₅ shearing is characterized by brittle deformation with a dextral behavior mostly found at the Mbankolo quarry in which the outcrop is in the form of a slap and then it is cutting the D₁, D₂, D₃ and D₄ deformational phase.it is also found at the hill of Vogt-betsi in the form of a dome in gneisses which dip direction is N160E.

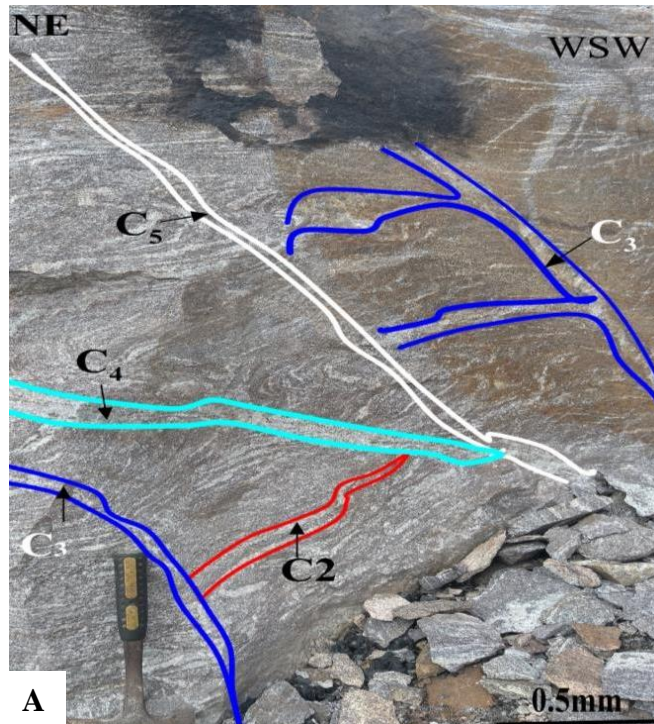


Figure 32: Structural element related to the D₅ deformational phase: A) C₅ dextral shear

VI.2.6. D₆ deformation stage

The D₆ deformation is the last phase of deformation, which is characterized by a brittle deformation, consisting of an F₆ fracture and F₆ joint respectively.

VI.2.6.1. F₆ fracture

The F₆ fracture is cross cutting the dome shaped garnetite of the Nomayos quarry, and the hill of Oyomabang presenting conjugate fractures dipping N160E, N146E, N142E with an angle of 29°SW. The fracture varies from mm to cm, with some occupied by quartzo-feldspathic minerals, while others are dry (Fig. 33A and C).

VI.2.6.2. F₆ joint

The F₆ joint is the last stage of deformation which cross-cut all the rest of the deformational phases in all the outcrop of the western part of Yaounde, it is mostly common kyanite-garnet gneiss of the Mbankolo quarry and at the Vogt-betsi dome shaped outcrop (Fig. 33B). They strike towards N130E and vary in dimension from mm to m.

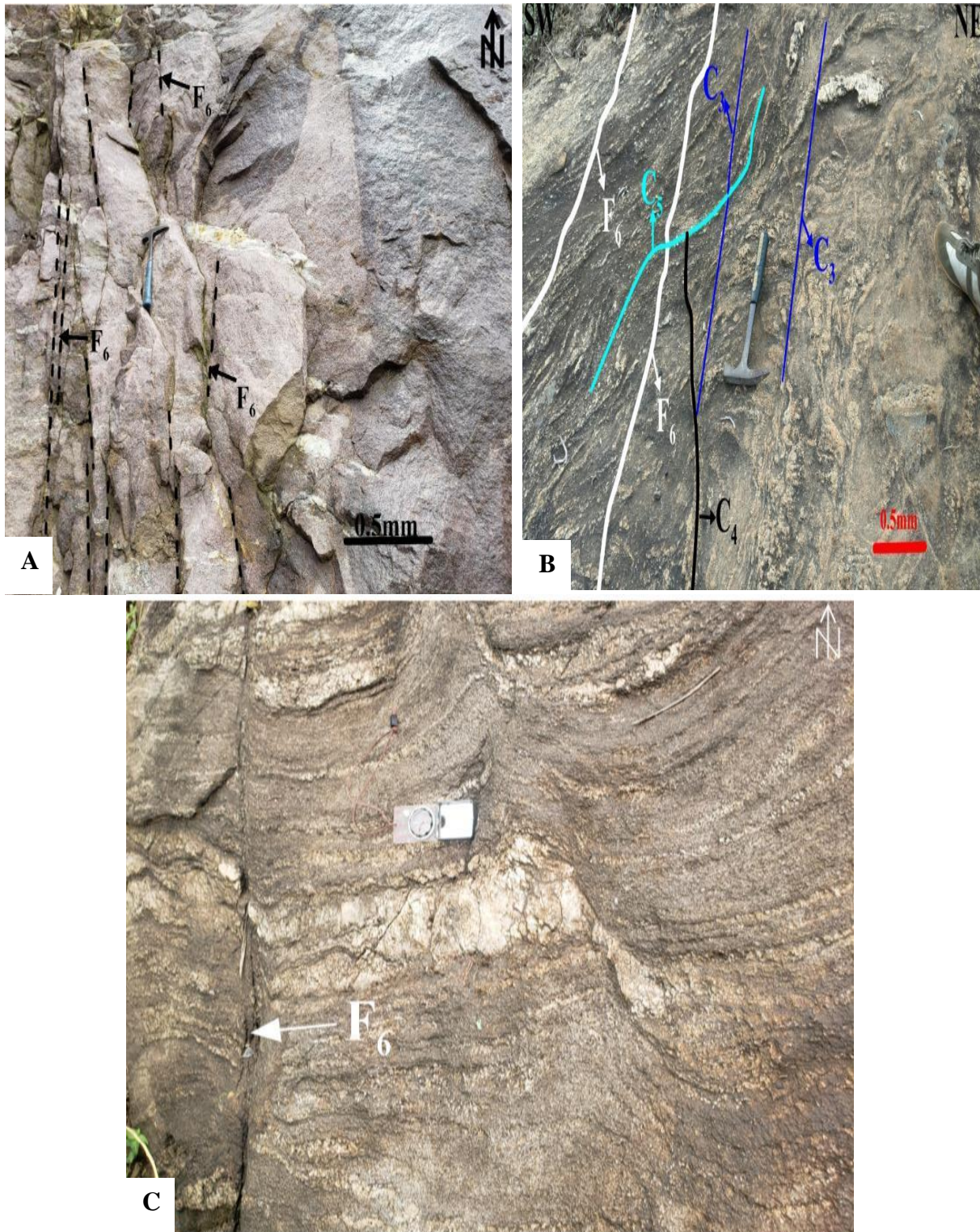


Figure 33: Structural element related to the D₆ deformational phase found at the Nomayos quarry and the hill of Mvogt-Betsi and Oyomabang: (A-C) F₆ vertical fracture found in garnetite and kyanite-garnet gneiss; (B) F₆ vertical joints found at the hill of Mvogt-betsi.

Table 3: Summary of the different phases of deformation of the target site

Deformation	Mechanism	Structure	Localities
D ₁	Ductile behaviour	S ₁ ,F ₁ ,B ₁	Mvogt-betsi Nkolbison Mbankolo
D ₂	Ductilo-Fragile	S ₂ , B ₂ ,F ₂ , C ₂ , Lm ₂	Nomayos, Mbadoumou BibongBidoum, Mvolye
D ₃	Translation of Ductilo-Fragile	S ₃ ,C ₃ ,F ₃ ,V ₃ veins	Fam-Assi,Leboudi quarry1, Mvolye
D ₄	Fragile behaviours intense	F ₄ fracture	In all the locality
D ₅	Ductilo-fragile	C ₅ shearing	Mont Oyomabang, Nomayoquarry Mbankolo
D ₆	Fragile behaviours	F ₆ fracture F ₆ joint	Nomayos quarry Mvogt- betsi

CHAPTER V : INTERPRETATION AND DISCUSSION

V. 1. PETROGRAHY

The western portion of Yaounde to which the study area belongs to revealed two lithological units: (i) the metasedimentary units (migmatites) composed of Kyanite-biotite gneiss, Garnet-biotite gneiss, garnetite and quartzite and (ii) the meta-igneous unit (metadiorites) composed of amphibolites. Mineralogical assemblages range from amphibolite facies (**Amp + Kfs + Qtz ± Grt** , **Kfs + Qtz + Amp + Bt + Pl + Spn + Grt ± Cd ± Std**) to granulite facies that is Kyanite-biotite gneiss (**Bt + Grt + Qtz + Ky + And + Kfs ± Px**), biotite–garnet gneiss (**Bt + Grt + Kfs + Qtz + Pl**), garnetite (**Grt + Bt + Qtz + Ky + And + Kfs + Pl ± Px**) and finally quartzite (**Qtz + Bt ± Op**). These assemblage shows that the target site is characterized by medium-pressure (MP), medium-temperature (MT) to high temperature (HT) metamorphic facies, locally reaching the granulite facies (T=750-800°C and P=10-12kbar; Nzenti et al., 1988; Penaye et al., 1993; Toteu et al., 2004; Owona et al., 2011) of the Yaounde series in the southern domain . They underwent partial melting to the migmatitic/gneissic level (Nzenti et al., 1988) producing paragenesis that generally fall in **Kfs + Qtz + Amp + Bt + Pl + Grt ± Cd ± Std (metadiorites) and Bt + Grt + Kfs + Qtz + Pl + Ky** (metasediments) respectively, displaying characteristic medium to high grade metamorphism similar to that portrayed by Nzenti et al. (1988).

V.2. NATURE OF THE PROTOLITH

The metamorphic rocks of the western sector of Yaounde are generally characterized by amphibolites, quartzite and gneisses, each having peculiar petrographic, mineralogical and structural characteristics.

The amphibolites consist of mafic minerals from basic origin and characterized by **Amp + Kfs + Qtz ± Grt**, relative to magmatic protolith. These amphibolites outcrops as domes, presenting nematogranoblastic textures, with amphibole and Feldspar indicating the facies type (amphibolite) and characteristic of metamorphic zone. The rocks present characters similar to those identified in the Fomopea region Fotzing et al. (2019) of Mbe-sassa-Bersi of the Adamaoua yadé group (Saha Fouotsa et al., 2018, 2019) and that of rocks in Yaounde, notably around the western portion of Yaounde (Metang et al., 2022e). While the migmatites are garnetite and garnet-biotite gneiss presenting **Bt + Grt + Kfs + Qtz + Pl + Ky and Grt + Qtz + Bt + Kfs ± Pl**. These paragenesis are indicatives of mafic and aluminous minerals that make up the bulk rock, originally resulting from the partial melting of a basic rich magma and smooth burial of the sedimentary rocks that were metamorphosed. The meta igneous rocks of the western Yaounde have characteristics similar to that of Metang et al. (2022c), while the

metasediments are comparable to those of the Tchollire Banyo region located in the Nord-Center of the CPNE (Bouyo et al., 2013), in the Mbe-sassa- Bersi region from the central Cameroonian domain (Saha Fouotsa et al., 2019). Moreover, the occurrence of the metasediments suggest that the sediment deposition occurred in distensive intracontinental context due to a substratum made of Paleoproterozoic formations which are the source of the metasediments as suggested by Bouyo et al. (2013), Saha Fouotsa et al. (2019) indicates that the sources of the metasediments are Archaean, Paleoproterozoic and Neoproterozoic whose age of protolith deposition is located at 725 ± 12 years old.

V.3. TECTONIC EVOLUTION

Structural study of the western Yaounde highlights six major phases of deformation D_1 , D_2 , D_3 , D_4 , D_5 and D_6 , presenting different characteristics. The geological deformation phase D_1 assigned as a compressive and thrust tectonic phase under a simple shear regime characterized by the development of sub-horizontal S_1 foliation, B_1 boudins and F_1 isoclinal folds (Mvondo et al., 2003, 2007; Owona et al., 2011) developed in migmatites (kyanite-biotite gneiss, garnet-biotite gneiss) oriented mainly NE -SW direction.

The D_2 assigned as an extensive tectonic phase under a pure shear regime characterized by a ductile- brittle nature result from the tectonic transposition of structures (F_2 folds, F_2 vein joints and C_2 shear) of D_1 as proposed by (Mvondo et al., 2003, 2007; Owona et al., 2011; Mbola et al., 2014 and Metang et al., 2014). The sub-horizontal F_2 vein joint are marked by mechanical stretching of quartzo-feldspathic layer. The F_2 folds of asymmetrical/ monoclinic nature of sub-horizontal axial plane and the C_2 shear planes (of dextral polarity and directions NNW-SSE) rotates and shifted the foliation of the previous deformational D_2 stage (Metang et al., 2014).

The D_3 deformational phase transposed and reoriented the structures of the anterior D_2 stage, it represented by the C_3 shears of dextral kinematics, local fracturing of variable direction F_3 , S_3 , F_3 fold representing the regional strain pattern developed consistently with the E-W trans-saharian convergence system (Mvondo et al., 2009, Ndzana et al., 2014). The fragile or brittle deformation phase D_4 is characterized by vertical kilometeric constriction which intersect in a major sense with the other structures of previous deformation D_1 , D_2 and D_3 . The major fractures have the direction NW-SE added to secondary fracture of direction NNW-SSE. This NW-SE direction of these fracture is similar to the works of (Metang et al., 2022b; 2022d and 2022c).

The D₅ and D₆ structures are respectively shear, fractures and veins that developed due to an early progressive shear stress regime mechanism that developed to brittle behavior. However, these structures have been overprinted by post-orogenic stress regimes, thus, existing as over printings and some ones as relics (Bissaya et al., 2023)

V.4.CONTEXT AND GEODYNAMIC EVOLUTION OF THE TARGET SITE

The metamorphic rocks of the western part of Yaounde present meta-sedimentary rocks revealing an ancient sedimentary basin which result from extensional processes in the northern boundary of the Congo Craton, guided by rifting, and fragmentation. Petrographic studies of these rocks present a paragenesis similar to medium grade metamorphism of amphibolite facies on one hand, and high grade granulite facies (migmatites) on the other hand. These paragenesis are similar to those obtained by Nzenti et al. (1988). Western Yaounde is characterized by a continental Pre-collisional zone preceded by subduction (Metang et al., 2022d; Miyashiro,1961), additionally presenting quartzo-feldspathic to quartz rich veins, probably formed in an intraplate domain, reflecting the existence of an extension which lead to the establishment of a rift (Nkoumbou et., al 2014; Tchakounte et al., 2021).

GENERAL CONCLUSION AND PERSPECTIVES

GENERAL CONCLUSION

This study present petrographical and structural data of the metasedimentary and meta-igneous rocks in the western part of Yaounde, with the aims to discuss their petrogenesis and structural settings. The result obtained lead to the following conclusion:

Field mapping and petrographic description review the rocks of the study area to be the metasediments that have been migmatized (kyanite-biotite gneiss, biotite gneiss, garnet-biotite gneiss, garnetite and quartzite), and the amphibolite of the meta-igneous rocks. These rocks are generally characterized by granoblastic heterogranular texture that indicates complex tectono-metamorphic evolution mark by granulite, hornfels and amphibolite facies assemblages of plurifacial metamorphic evidence (prograde metamorphism).

The deformation feature imprinted on these rocks marks a continuous deformation from lineations through schistosity (cleavages) to foliation then folds to fractures engendered by Ductilo-brittle deformation with phases D_1 , D_2 , D_3 , D_4 , D_5 and D_6 . Were the D_6 where characterized by brittle failure thereby producing fractures and veins. This deformation shows an intraplate major deformation of the Pan-African block on which part of Cameroon rest.

Western Yaounde is characterized by a continental Pre-collisional zone preceded by subduction, additionally presenting quartzo-feldspathic to quartz rich veins, probably formed in an intraplate domain, reflecting the existence of an extension which lead to the establishment of a rift.

PERSPECTIVES

Western Yaounde is found in the southern domain of the Pan-African Nord Equatorial Fold Belt in Cameroon, Where the current studies help to understand the metamorphic evolution, protolith and deformation of the rocks to characterized the recent deformational phases. However, detailed studies on mineralogy, isotope geology and geochronology will be required to confirm the evolution of the rocks including their deformational phases within the sector. In addition, the opening of several artisanal and industrial quarries would be an asset for making more observations and taking a lot of measurements.

REFERENCES

- Abdelsalam, M.G., Liégeois, J, P.and Stern, R.J., 2002.** The Saharan Metacraton. Journal of African Earth Sciences 34, 119-136.
- Akame, J., 2021.** Évolution géodynamique à l'Archéen du complexe du Ntem (Craton du Congo, Cameroun) : Études structurales, géochimiques des terrains à granitoïdes et ceinture de roche verte de Sangmélima. Thèse de doctorat/Ph. D, Université libre de Bruxelles, 200p + annexes.
- Akame, J.M., Elson P. Oliveira., Pujol, M., Hubblet, G., Debaille, V., 2019.** The Sangmelima granite. Greenstone belts (South Cameroon): Intergration of Remote Sensing and Aeromagnetic Data for structural interpretation. The Egyptian Journal of Remote Sensing and Space Sciences 22, 37-47.
- Akame, J.M., Elson P. Oliveira., Pujol, M., Hubblet, G., Debaille, V., 2020.** LA-ICP-MS zircon U-PB dating, LU-HF, Sm-Nd geochronology and tectonic setting of the Mesoarchean mafic and felsic magmatic rocks in the Sangmelima granite-greenstone terrane, Ntem complex (South Cameroon). Lithos 372,105702.
- Babinski, M., Pedrosa-soares, AC., Ferreira da Trindade, RI., Martin, M., Mauricio Noce, C., Liu, D., 2018.** Neoproterozoic glacial deposits from the Araçuaí orogen, Brazil: Age, provenance and correlations with the Sao Francisco Craton and West Congo belt. Gondwana Research 21(2-3),451-465.
- Bachelier, G, 1959.** Etude pédologique des sols de Yaoundé : Contribution à l'étude de la pédogenèse des sols ferrallitiques. Agronomie Tropicale,14.279-305.
- Bagnouls, F. et Gaussen, H., 1957.** Les climats biologiques et leurs classifications. Annales de géographie, 66,193-220.
- Barbosa, J.S.F., Sabaté, P., 2002.** Geological features and the Paleoproterozoic collision of four Archean crustal segments of the Sao Francisco craton, Bahia, Brazil, A synthesis. Annals of the Brazilian Academy of sciences 74,343-359.
- Betsi, T.B., Ngo Bidjeck B.L.M., Mvondo H., 2020.** Rutile LA-ICP-MS U-Pb geochronology and implications for tectonometamorphic evolution in the Yaoundé Group of the Neoproterozoic Central African Orogeny. J Afr Earth Sc 171, 103939.
- Bineli Betsi, T., Ngo Bidjeck Bondje, L.M., Mvondo, H., Mama Nga, L.N.Y., 2020.** Rutile LA-ICP-MS U-Pb geochronology and implications for tectono-metamorphic evolution

in the Yaoundé Group of the Neoproterozoic Central African Orogeng. *Journal of African Earth Sciences* 171,103-939.

Bissaya, R., Boukar. M., Ngammy Kamwa. A., Onana, J.B., 2023. Deformation styles of Neoproterozoic and post-in Yaounde, southern Cameroon: the polyphaser deformation, the strike-slip fault systems, and their geodynamic implication. *Arabian journal of Geosciences*16(8) m, 457.

Bouyo Houketchang, M., Penaye, J., Barbey, P., Toteu, F. S., Wandji, P., 2013. Petrology of high-pressure granulite facies metapelites and metabasites from Tcholliré and Banyo regions: Geodynamic implication for the Central African Fold Belt (CAFB) of north central Cameroon. *Precambrian Research* 224, 412-433.

Bouyo Houketchang, M., Toteu, S.F., Mouri, H., Penaye, J., 2019. Eclogite facies metabasites from the Paleoproterozoic Nyong Group, SW Cameroon: Mineralogical evidence and implications for a high-pressure metamorphism related to a subduction zone at the NW margin of the Archean Congo craton, *Journal of African Earth Sciences* 149, 215–234.

Bouyo Houketchang, M., Zhao, Y., Penaye, J., Zhang, S.H., Njel, U.O., 2015. Neoproterozoic subduction-related metavolcanic and metasedimentary rocks from the Rey Bouba Greenstone Belt of north-central Cameroon in the Central African Fold Belt: new insights into a continental arc geodynamic setting. *Precambrian Research* 261, 40-53. zone at the NW margin of the Archean Congo craton, *Journal of African Earth Sciences* 149, 215–234

Brito de Neves, B.B., Van Schmus, W.R., Fetter, H., 2002. North western Africa, North Eastern Brazil. Major tectonic links and correlation problems. *Journal of African Earth Sciences* 34, 275-278–450.

Brito de Neves, B.D., Van Schmus., Fetter, A., 2001. North-West Africa North-Eastern Brazil. Major tectonic links and correlation problems. *Journal of African Earth Sciences* 34, 275-273.

Castaing, C., Feybesse, J.L., Thiéblemont, D., Chèvremont, P., 1994. Paleogeographical reconstructions of the panafrican/Brasiliano orogen: closure of an ocean domain or intracontinental convergence between major blocks. *Precambrian Research* 69, 327-344.

Castaing, C., Feybesse, J.L., Thiéblemont, D., Triboulet, C., Chevremont, P., 1994.

Paleogeographical reconstructions of the Pan-African/Brasiliano orogen: closure of an oceanic domain or intercontinental convergence between major blocks? *Precambrian Research* 69, 327 - 344.

Champetier de Ribes, G., Aubague, M., 1956. Carte géologique de reconnaissance à l'échelle 1/500 000 feuille Yaoundé Ouest, avec notice explicative. Direction des mines et de la géologie, Yaoundé, Cameroun : 35p

Chombong, N.N., Suh, C.E., 2013. 2883 Ma commencement of BIF deposition at the northern edge of Congo craton, southern Cameroon: new zircon SHRIMP data constraint from metavolcanics. *Episodes* 36, 47–57p.

Dumont, J.F., 1986. Identification par télédétection de l'accident de la Sanaga (Cameroun) : sa position dans le contexte des grands accidents d'Afrique Centrale et de la limite nord du craton congolais. *Géodynamique* 1, 13-19.

Ernst, R.E., Wouter Bleeker., Söderlund, Ulf., Andrew, c. Ker., 2013. Large Igneous Provinces and supercontinents: Toward completing the plate tectonic evolution. *Lithos* 174,1-14.

Feybesse, J.L., Johan, V., Maurizot, P., Abeessolo, A., 1986. Mise en évidence d'une nappe synmétamorphe d'âge Eburnéen dans la partie NW du craton Zairiois (SW Cameroon). Publication occasionnelle-Centre international pour la formation et les échanges géologique 10, 105-111.

Fozing, E. M., Kwékam, M., Dedzo, M. G., Asaah, A. N. E., Njanko, T., Tcheumenak Kouémo, J., Efon Awoum, J., Njongfang, E., 2019. Petrography and geochemistry of amphibolites from the Fomopea Pluton (West Cameroon): Origin and geodynamic setting. *Journal of African Earth Sciences* 154, 181-194.

Fuh, C. G., Nkoumbou, C., Tchakounte, N. J., Mukete, K. O., Tchouankoue, J. P., 2021. Petrology, geochemistry, Ar-Ar isotopes of an arc related calc-alkaline pluton from Mamb (Pan African Yaoundé group, Cameroon): a testimony to the subduction of a hot oceanic crust. *Lithos* 384-385, 105-973.

Ganno, S., Njiosseu Tanko, E.L., Kouankap Nono, G.D., Djoukouo Soh, A., Moudioh, C., Ngnotué, T., Nzenti, J.P., 2017. A mixed seawater and

- hydrothermal origin of superior-type banded iron formation (BIF)-hosted Kouambo iron deposit, Palaeoproterozoic Nyong series, Southwestern Cameroon: Constraints from petrography and geochemistry. *Ore Geology Reviews* 80, 860-875.
- Ganno, S., Nzenti, J-P., Ngnotué, T., Kankeu B., Kouankap Nono, G. D., 2010.** Polyphase deformation and evidence for transpressive tectonics in the Kimbi area, Northwestern Cameroon Pan-African Fold Belt. *Journal of Geology and Mining Research* 4, 1-15.
- Kamani, M. K., Wang, W., Tchouankoue, J. P., Huang, S. F., Yomeun, B., Xue, E. K., Lu, G. M., 2021.** Neoproterozoic syn-collision magmatism in the Nkondjock region at the northern border of the Congo craton in Cameroon: Geodynamic implications for the Central African orogenic belt. *Precambrian Research* 353, 106-015.
- Kankeu B., Greiling R.O., Nzenti J.P., 2009.** Pan-African strike-slip tectonics in eastern Cameroon - magnetic fabrics (AMS) and structure in the Lom basin and its gneissic basement. *Precambrian Research* 174, 258-272.
- Kankeu, B., Nzenti, J. P., Greiling, R. O., Ganno, S., Ngnotué, T., Bassahak, J., Hell, V. 2010.** Application de la technique de l'Anisotropie de la Susceptibilité Magnétique (ASM) à l'identification des structures géologiques : le cisaillement panafricain de Bétaré-Oya dans le district aurifère de l'Est Cameroun. *Annales Faculté des Sciences* 38, 1, 17–29.
- Kankeu, B., Reinhard O. G., Nzenti, J.P., Ganno, S., Danguene, P.Y., Bassahak J., Hell J.V., 2018.** Contrasting Pan-African structural styles at the NW margin of the Congo Shield in Cameroon. *Journal of African Earth Sciences*. 146, 28-47p.
- Kouankap Nono, G. D., 2011.** Etude du Cisaillement Centre Camerounais dans la région de Banefo-Mvoutsaha au NE Bafoussam, dans le domaine centre de la Chaîne Panafricaine Nord Equatoriale au Cameroun. Pétrogenèse, Géochronologie et Structurologie des formations du socle. Thèse de Doctorat/ Ph.D., Université de Yaoundé I, 118p.
- Lasserre, M., Soba, D., 1976.** Age Libérien des granodiorites et des gneiss à pyroxène du Cameroun Méridional. *Bulletin BRGM* 2, 17–32.
- Lerouge, C., Cocherie, A., Toteu, S. F., Penaye, J., Milési, J.-P., Tchameni, R., Nsifa, N. E., Fanning, C. M., Deloule, E., 2006.** Shrimp U-Pb zircon age evidence for

- Paleoproterozoic sedimentation and 2.05 Ga syntectonic plutonism in the Nyong Group, southwestern Cameroon: consequences for the Eburnean-Trans Amazonian belt of NE Brazil and Central Africa. *Journal of African Earth Sciences* 44, 413-427.
- Li, X.H., Chen, Y., Li, J., Yang, C., Ling, X.-X., Tchouankoue, J.P., 2016.** New isotopic constraints on age and origin of Mesoarchean charnockite, trondhjemite and amphibolite in the Ntem complex of NW Congo Craton, southern Cameroon. *Precambrian Res.* 276,14-23.
- Liégeois, J.P., Latouche, L., Boughrara, M., Navez, J., Guiraud, M., 2003.** The LATEA
- Loose, D., Schenk, V., 2018.** 2.09 Ga old eclogites in the Eburnian-Transamazonian orogen of southern Cameroon: Significance for Palaeoproterozoic plate tectonics. *Precambrian Research* 304, 1-11.
- Maurizot, P., Abessolo, A., Feybesse, J.L., Johan, V., Lecomte, P., 1986.** Etude et prospection minière du Sud-Ouest Cameroun. Synthèse des travaux de 1978 à 1985. Rapport BRGM, Orléans 85, CMR 066, 274 p.
- metacraton, (central Hoggar, Tuareg shield, Algeria): behaviour of an old passive margin during the Pan-African orogeny. *Journal of African Earth Sciences* 37, 161-190.
- Metang, V., 2015.** **Cartographie géologique du secteur de Matomb-Makak** (centre-sud Cameroun) implications sur l'évolution géodynamique du groupe panafricain de Yaoundé. Thèse de doctorat/Ph. D, Université de Yaoundé I, 198P + annexe.
- Metang, V., Domkam, B., Toussi, T.M., Wandji, B.S.F., Mboutchouang D.C., Kenzo, H.A., 2022e.** Contribution of remote sensing for the mapping of the Yaoundé Metadiorite. *European Journal of Environment and Earth Sciences* 3, 321.
- Metang, V., Nkoumbou, C., Tchakounté, N. J., Njopwouo, D., 2014.** Application of remote sensing for the mapping of geological structures in rainforest area: a case study at the Matomb-Makak area, CenterSouth Cameroon. *Journal of Geosciences and Geomatics*, 2(5),196 -207.
- Metang, V., Nomo, N.E., Ganno, S., Takodjou, W.J.D., Ewolo, T.A.M., Teda, S.A.C., Fossi, D.H., Mbakam, K.M.D., Tchameni, R., Nkoumbou, C., Nzenti, J.P., 2022a.** Anatexis of metadiorite from the Yaoundé area, Central African Orogenic Belt in Cameroon: implications on the genesis of in-source granodiorite leucosomes. *Arabian Journal of Geosciences* 15, 1-21.

- Metang, V., Tassongwa, B., Ngo Belnoun, R., Kenzo, H. A, T o u s s i , T.M., Nkamga Mbakam, D.M., Tene Kengne, L.G., Tchop Legrand, J., Mouafo, L., Tchouankoue, J.P., 2022d.** Petrography and Geochemistry of metasedimentary rocks from the Southwestern portion of the Yaoundé group in Cameroon; Provenance and tectonic Implications. *Earth Sciences* 11, 232-249.
- Metang, V., Tassongwa, B., Nomo, N.E., Kenzo, H.A., Wandji, B.S.F., Domkam, B., Mboutchouang, D.C., Mbakam, K.M.D., Kengne, T.L.G., Mouafo, L., 2022.** Geological study of a Mewoulou-Nkolbisson ductile strike-slip fault segment (Western Yaoundé, Cameroon): evidence of hazards related to structural landforms. *Arabian Journal of Geosciences* 15, 359.
- Miyashiro A., 1961.** Evolution of metamorphic belts. *Journal Petrology* 2, 277-311.
- Moudioh, C., Soh Tamehe, L., Ganno, S., Nzepang Tankwa, M., Brando Soares, M., Ghosh, R., Kankeu, B., Nzenti, J.P., 2020.** Tectonic setting of the Bipindi greenstone belt, northwest Congo craton, Cameroon: Implications on BIF deposition. *Journal of African Earth Sciences* 171, 103971.
- Mvondo, H., den Brok, S.W.J., Mvondo Ondoa, J., 2003.** Evidence for symmetric extension and exhumation of the Yaoundé nappe (Pan-African fold belt, Cameroon). *Journal of African Earth Sciences* 36, 215–231.
- Mvondo, H., Owona, S., Mvondo, O.J., Essono, J., 2007.** Tectonic evolution of the Yaoundé segment of the Neoproterozoic Central African Orogenic Belt in Southern Cameroon. *Canadian Journal of Earth Sciences* 44, 433- 444.
- Mvondo, O. J., 2009.** Caractérisation des événements tectoniques dans le domaine sud de la chaîne au Cameroun : styles tectoniques et géochronologie des séries de Yaoundé et de Bafia. Thèse de Doctorat/Ph. D, Université de Yaoundé I, 160 p.
- Ndema Mbongue, J.L., Ngnotué, T., Ngo Nlend, C. D., Nzenti, J.P., Suh, C. E., 2014.** Origin and evolution of the formation of the Cameroon Nyong series in the western border of the Congo craton. *Journal of Geosciences and Geomatics* 2, 62-75.
- Ndzana Mbola, P.S., Mvondo Ondoa, J., Owona, S., Sep Nlogang, J.P., Olinga, J.B., Bilong, P., 2014.** Evidence of the NE-SW extension in the Sa'a- Monatélé Region as in Bafia and Yaounde groups within the Central African Fold belt (Cameroon): Implication

- for the southern Cameroon Neoproterozoic extension. *Sciences, Technologies et Développement* 15,1-15.
- Nédélec, A., Macaudière, J., Nzenti, J.P., Barbey, P. 1986.** Evolution structurale et métamorphique des schistes de Mbalmayo (Cameroun). Implications sur la structure de la zone mobile panafricaine d'Afrique Centrale au contact du craton du Congo. *Comptes Rendus de l'Académie des Sciences de Paris* 303, II, 1, 75- 80.
- Nga Essomba Tsoungui, P., Ganno, S., Tanko Njiosseu, E.L., Ndema Mbongue, J.L., Kamguia Woguia, B., Soh Tamehe, L., Takodjou Wambo, J.D., Nzenti, J.P., 2020.** Geochemical constraints on the origin and tectonic setting of the serpentized peridotites from the Paleoproterozoic Nyong series, Eseka area, SW Cameroon. *Acta Geochimica* 39, 404-422.
- Ngako V., Njonfang E. 2011.** Plate amalgamation and plate destruction, the Western Gondwana history. In: Closson, D. (Editions), *Tectonics*. INTECH, United Kingdom, 358.
- Ngako, V., Affaton, P., Njonfang, E., 2008.** Pan-African tectonics in northwestern Cameroon: implication for the history of western Gondwana. *Gondwana Research* 14, 509 –522 *Earth Sciences* 36, 207-.214.
- Ngako, V., Affaton, P., Nnange, J. M., Njanko, T., 2003.** Panafrican tectonic evolution in central and southern Cameroon: transpression and transtention during sinistral shear movements. *Journal of African Earth Sciences* 36, 207-214.
- Ngako, V., Jégouzo, P., Nzenti, J.P., 1991.** Le Cisaillement Centre Camerounais. Rôle structural et géodynamique dans l'orogénèse panafricaine. *Compte Rendus de l'Académie des Sciences, Paris* 313, 457-463.
- Ngnotué, T., Ganno, S., Nzenti, J. P., Schulz, B., Tchaptchet Tchato, D., Suh Cheo, E., 2012.** Geochemistry and geochronology of Peraluminous High-K granitic leucosomes of Yaoundé series (Cameroon): evidence for a unique Pan-African magmatism and melting event in North Equatorial Fold Belt. *International Journal of Geosciences* 3, 525-548.
- Ngnotué, T., Nzenti, J. P., Barbey, P., Tchoua, F. M., 2000.** The Ntui-Betamba highgrade gneisses: A Northward extension of the Pan-African Yaounde gneisses in Cameroon. *Journal of African Earth Sciences* 31, 369-381.

- Ngon Ngon, GF., Yongue-Fouateu, R., Bitom, DL., Bilong, P., 2009.** A geological study of clayey laterite and clayed hydromorphic material of the region of Yaoundé (Cameroon): a prerequisite for local material promotion. *Journal of African Earth Sciences* 55(1-2), 69-78.
- Nkoumbou, C., Barbey, P., Yonta-Ngouné, C., Paquette, J.L., Villiéras, d.F., 2014.** Precollisional geodynamic context of the southern margin of the Pan-African fold belt in Cameroon. *Journal of African Earth Sciences* 99, 245-260.
- Nkwemoh Anguh, C., Tchindjang, M., Ngwatung Afungan, R., 2017.** The impact of urbanization on the vegetation off Yaounde, (Cameroon). *Int J Innov Res Dev* 6, 6-18.
- Ntieche, B., Mohan, R. M., Amidou, M., 2017.** Granitoids of the Magba Shear Zone, West Cameroon, Central Africa: Evidences for Emplacement under Transpressive Tectonic Regime. *Journal of the Geological Society of India* 89, 33-46.
- Nzenti, J. P., 1998.** Neoproterozoic Alkaline Meta-Ignous Rocks from the Pan-African North Equatorial Fold Belt (Yaoundé, Cameroon). Biotitites and Magnetites Rich Pyroxenites. *Journal African Earth Sciences* 26, 37-47.
- Nzenti, J. P., Barbey, P., Jegouzo, P., Moreau, C., 1984.** Un nouvel exemple de ceinture granulitique dans une chaîne protérozoïque de transition les migmatites de Yaoundé au Cameroun. *Comptes Rendus Académie des Science* 17, 1197-1199p.
- Nzenti, J. P., Barbey, P., Macaudiere, J., Soba, D., 1988.** Origin and evolution of the late Precambrian high-grade Yaoundé gneisses (Cameroon). *Precambrian Research* 38, 91-109.
- Nzenti, J.P, 1987. Pétrogenèse des migmatites de Yaoundé (Cameroun).** Eléments pour un modèle géodynamique de la chaîne panafricaine Nord Équatoriale. Thèse Doctorat de l'Université de Nancy I, 147p.
- Nzenti, J.P., Barbey P., Jegouzo, P., Moreau C., 1984.** Un nouvel exemple de ceinture granulitique dans une chaîne protérozoïque de transition : les migmatites de Yaoundé au Cameroun. *Comptes Rendus de l'Académie des Sciences Paris* 17, 1197-1199.
- Nzenti, J.P., Barbey, P., Bertrand, J., Macaudiere, J., 1994.** La chaîne panafricaine

au

- Cameroun cherchons suture et modèle. Abstracts 15eme RST, Nancy, Société Géologique France, édition Paris, 99p.
- Nzenti, J.P., Barbey, P., Macaudière, J., Soba, D., 1988.** Origin and evolution of late Precambrian high -grade Yaoundé gneisses (Cameroon). *Precambrian Research* 38, 91-109.
- Nzenti, J.P., Barbey, P., Macaudière, J., Soba, D., 1988.** Origin and evolution of the Late Precambrian high-grade Yaoundé gneisses (Cameroon). *Precambrian Research* 38, 91-109
- Nzenti, J.P., Barbey, P., Tchoua, F.M., 1999.** Evolution crustale au Cameroun : éléments pour un modèle géodynamique de l'orogénèse néoproterozoïque. In : Vicat, J. P. & Bilong, P. (eds) *Géologie et environnements au Cameroun. Collection GEOCAM 2*, 397-407p. ncy (France) 99p. *Geological Society of India* 89, 33-46.
- Nzenti, J.P., Ngako, V., Kambou, R., Penaye, J., Bassahak, J., Njel, O.V., 1992.** Structures régionales de la chaîne panafricaine du Nord Cameroun. *Comptes Rendus de l'Académie des Sciences* 315, 209-215.
- Oliveira, E.P., Toteu, S.F., Araujo, M.N.C., Carvalho, M.J., Nascimento, R.S., Buen, J.F., McNaughton, N., Basilici, G., 2006.** Geologic correlation between the Neoproterozoic Sergipano belt (NE Brazil) and the Yaoundé schist belt (Cameroon, Africa). *Journal of African Earth Sciences* 44, 470 - 478.
- Olivry, J.C., 1986.** Fleuves et rivières du Cameroun. Collection monographies hydrologiques. MESRES/ORSTOM, N°9, Paris 1, 733.
- Ongo, B.E., Nkoa, D. W., Tameko, T.G., 2024.** Efficiency of local public spending in Cameroon: Does population size matter. *African development review* 36, 362-376.
- Owona, S., Mbola-Ndzana, S.P., Mpesse, J. E., Mvondo-Ondoa, J., Schulz, B., Pfänder, J., Ekodeck, G.E., 2013.** Petrogenesis of amphibolites from the Neoproterozoic Yaounde Group (Cameroon, Central-Africa): Evidence of MORB and implications on their geodynamic evolution. *Comunicações Geológicas* 00(1), 5-13.
- Owona, S., Mvondo Ondoa, J., Ratschbacher, L., Mbola Ndzana, S.P., Tchoua, F.M., Ekodeck, G.E., 2011.** The geometry of the Archean, Paleo- and Neoproterozoic tectonics in the Southwest Cameroon. *Géosciences* 343, 4, 312-322.

- Owona, S., Ratschbacher, L., Ngapna, M. N., Gulzar, A. M., Mvondo, O. J., Ekodeck G. E., 2021.** How diverse is the source? Age, provenance, reworking, and overprint of Precambrian meta-sedimentary rocks of West Gondwana, Cameroon, from zircon U-Pb geochronology. *Precambrian Research* 359, 10-622
- Pedrosa-soares, C.A., Alkmim, FF., Tack, L., Mauricio Noce, C., Babinski, M., Luis Carlos da siliva., MA Martins-Neto., 2008.** Similarities and differences between the Brazilian and Africa counterparts of the Neoproterozoic Araçuaí-West Congo Craton. *Geological society, London, special publications* 294(1), 153-172.
- Penaye, J., 1988.** Pétrologie et structure des ensembles métamorphiques au Sud-Est de Poli (Nord Cameroun) : rôles respectifs du socle protérozoïque inférieur et de l'accrétion crustale panafricaine. Thèse de Doctorat de l'INP de Lorraine, Ecole Nationale Supérieure de Géologie, Nancy (France), 19 p.
- Penaye, J., Toteu, S.F., Van Schmus, W.R., Nzenti, J.P., 1993.** U–Pb and Sm–Nd preliminary geochronologic data on the Yaoundé Series, Cameroon: reinterpretation of the granulitic rocks as the suture of a collision in the “Centrafrican” belt. *Comptes Rendus de l'Académie des Sciences, Paris* 317, 789-794.
- Pin, C.H., Poidevin., J.L., 1987.** U Pb Zircon evidence for a Pan-African granulite facies Metamorphism in Central Africa Republic. A new interpretation of the high-grade series of the northern border of the Congo Craton, *Precambrian Res* 36, 303-312.
- Poidevin, J.L., 1983.** La tectonique panafricaine à la bordure nord du craton congolais : l'orogénèse des Oubanguides (abstract). 12th colloque on the African Geology, Musée Royal de l'Afrique Centrale, Tervuren, Belgium, 75p.
- Poulet, A., Tchameni, R., Mezge, K., Vidal, M., Nsifa, E., Shang, C., Penaye, J., 2007.** Archaean crustal accretion at the northern border of the Congo Craton (South Cameroon). The charnockite-TTG Link. *Société Géologique de France* 178 331-342. *Sciences* 34, 275-278.
- Saha Fouotsa A.N., Vanderhaeghe O., Barbey P., Eglinger A., Tchameni R., Zeh A., Fosso Tchunte P.M., Nomo Negue E., 2019.** The geologic record of the exhumed root of the Central African Orogenic Belt in the central Cameroon domain (Mbé - Sassa-Mbersi region). *Journal of African Earth Sciences* 15, 286-314.

- Saha Fouotsa, A.N., Tchameni. R., Nomo Negue E., Dawai. D., Penaye, J., Fosso Tchunte, P.M., 2018.** Polyphase Deformation in the Mbé - Sassa-Bersi Area: Implications on the Tectono-Magmatic History of the Area and the Tectonic Evolution of the Tcholliré-Banyo and Central Cameroon Shear Zones (Central North Cameroon). *Journal of Geosciences and Geomatics* 6, 41-54.
- Shang, C.K., Liégeois, J.P., Satir, M., Frisch, W., Nsifa, E.N., 2010.** Late Archaean highK granite geochronology of the northern metacratonic margin of the Archaean craton, Southern Cameroon: Evidence for Pb-loss due to non-metamorphic causes. *Gondwana Research* 18, 337-355.
- Soh Tamehe, L., Wei, C., Ganno, S., Rosiere, C. A., Nzenti, J. P., Ebotehouna, C. G., Guanwen Lu., 2021.** Depositional age and tectonic environment of the Gouap banded iron formations from the Nyong group, SW Cameroon: Insights from isotopic, geochemical and geochronological studies of drill core samples. *Geoscience Frontiers* 12, 549-572.
- Soh Tamehe, L., Wei, C., Ganno, S., Rosiere, C.A., Huan, Li., Soares, M.B., Nzenti, J.P., Joao Orestes S. Santos., Bekker, A., 2022.** Provenance of metasiliciclastic rocks at the northwestern margin of the East Gabonian Block: Implications for deposition of BIFs and crustal evolution in southwestern Cameroon. *Precambrian research volume* 376, 106-677.
- Stendal, H., Toteu, S. F., Frei, R., Penaye, J., Njel, U. O., Bassahak, J., Nni, J., Kankeu, B., Ngako, V., Hell, J. V., 2006.** Derivation of detrital rutile in the Yaounde region from the Neoproterozoic Pan-African belt in southern Cameroon (Central Africa). *Journal of African Earth Sciences* 44, 443-458.
- Takam, T., Arima, M., Kokonyangi, J., Dunkley, D. J., Nsifa, N.E., 2009.** Paleoarchaen charnockite in the Ntem complex, Congo Craton, Cameroon: insights from SHRIMP zircon U-Pb ages. *Journal of Mineralogical and Petrological Sciences* 104(1), 1-11.
- Tchakounté J. N., Gentry C. F., Ngamy A. K., Metang V., Mvondo J. O., Nkoumbou C., 2021.** Petrology and geochemistry of the PanAfrican High-K calc-alkaline to shoshonitic-adakitc Bapé plutonic suites (Adamawa-Yade block, Cameroon): evidence of a hot oceanic crust subduction. *International Journal of Earth Sciences* **110, 2067-2090.**

- Tchakounté, J., Eglinger, A., Toteu, S.F., Zeh, A., Nkoumbou, C., Mvondo-Ondoa, J., Penaye, J., de Wit, M., Barbey, P., 2017.** The Adamawa-Yadé domain, a piece of Archaean crust in the Neoproterozoic Central African Orogenic belt (Bafia area, Cameroon). *Precambrian Research* 299, 210-229.
- Tchameni, R., Lerouge, C., Penaye, J., Cocherie, A., Milesi, J.P., Toteu, S.F., Nsifa, N.E., 2010.** Mineralogical constraint for metamorphic conditions in a shear zone affecting the Archean Ngoulemakong tonalite. Congo craton (Sourthen Cameroon) and retentivity of U-Pb SHRIMP zircon dates. *Journal of African Earth Sciences* 58, 67-80.
- Tchameni, R., Mezger, K., Nsifa, N.E., Pouclet, A., 2000.** Neoarchean crustal evolution in the Congo craton: evidence from K-rich granitoids of the Ntem complex, southern Cameroon. *Journal of African Earth Sciences* 30, 133–147.
- Thiéblemont, D., Callec, Y., Fernandez-Alonso, M., Chène., 2018.** A geological and isotopic framework of precambrian terrains in western Central Africa: An introduction. *Geology of southwest Gondwana*, 107-132.
- Toteu S. F., Bertrand J. M., Penaye J., Macaudière J., Angoua, S., Barbey, P., 1991.** Cameroon a tectonic keystone in the pan-african network. In Lewry J.F. and Stauffer M. R. Eds., the Early proterozoic Trans-Hudson orogen of North America. Geological Association of Canada, Special Paper 37, 483-496.
- Toteu, S. F., Penaye, J., Deloule, E., Van Schmus, W. R., Tchameni, R., 2006.** Diachronous evolution of volcanosedimentary basins north of the Congo craton: insights from U e Pb ion microprobe dating of zircons from the Poli, Lom and Yaounde Series (Cameroun). *Journal of African Earth Sciences* 44, 428-442.
- Toteu, S. F., Penaye, J., Poudjom Djomani, Y. H., 2004.** Geodynamic evolution of the PanAfrican belt in Central Africa with special reference to Cameroon. *Canadian Journal of Earth Sciences* 41, 73–85. Yaound_e Series (Cameroun). *Journal of African Earth Sciences* 44, 428-442.
- Toteu, S.F., Michard, A., Bertrand, J.M., Rocci, G., 1987.** U–Pb dating of Precambrian rocks from northern Cameroon, orogenic evolution and chronology of the PanAfrican belt of central Africa. *Precambrian Research* 37, 71-87.

- Toteu, S.F., Van Schumus, W.R., Penaye, J., Michard, A., 2001.** New U-Pb and Sm-Nd data from North-Central Cameroon and its bearing on the pre-pan African history of Central Africa. *Precambrian Research* 108, 45-73.
- Trompette, R., 1994.** Geology of Western Gondwana (2000-500 Ma). Pan-African-Brasilino Aggregation of South America and Africa. A.A Balkema Press, Rotterdam, 350p.
- Vicat J.P., Leger J.M., Nsifa E., Piguet P., Nzenti J.P., Tchameni R., Pouclet A., 1998.** Distinction au sein du craton congolais du Sud-ouest du Cameroun, des deux épisodes désertiques initiant les cycles orogéniques éburnéen (Paleoprotérozoïque) et panafricain(Neoprotérozoïque) C R Academie de Science Paris 323, 575-582.
- Vicat, J.P., Leger, J.M., Nsifa, E., Piguet, P., Nzenti, J.P., Tchameni, R., Pouclet, A., 1996.** Distinction au sein du Craton congolais du Sud-Ouest du Cameroun, de deux épisodes doléritiques initiant les cycles orogéniques éburnéen (Paléoprotérozoïque) et PanAfricain (Néoprotérozoïque). *Comptes Rendus de l'Académie des Sciences Paris* Vol.323: 575-582.
- Vicat, J.P., Pouclet, A., Nkoumbou, C., Seme Mouangue, A.C. 1997.** Le volcanisme fissural néoprotérozoïque des séries du Dja inférieur, de Yokadouma (Cameroun) et de Nola (RCA) – Signification géotectonique. *C.R. Académie des Sciences Paris* 325: 671-677.
- Vicat, J.P., Ten Kam Kon, N., Maurin, J.C., 1992.** Minéralisations et Évolution Tectonique de la République Populaire du Congo au cours du Protérozoïque. *IGCP n° 255, Newsletter/ bulletin* 4, 51-56.
- Weecksteen, G., 1957.** Carte géologique de reconnaissance à l'échelle 1/500000, coupure Douala-Est avec notice explicative. *Bulletin de la direction de géologie et des mines, Cameroun*, 69 p
- Whitney, D.L., Evans, B.W., 2010.** Abbreviations for names of rock-forming minerals. 185-187 P.
- Yonta-Ngouné, C., 2010.** Lecontexte géologique des indices de talc de la région de Boumnyebel (chaîne panafricaine d'Afrique Centrale, Cameroun). Thèse de Doctorat Ph. D, Université de Yaoundé I: 221 p +annexes.

Youngue-Fouateu, R., Boli Baboule, Z., Temgoua, E., Bitom, D.L., 1986. Erosion hydrique en milieu urbain : Le cas du site d'oyomabang dans la ville de Yaoundé. Influence de l'homme sur l'érosion : bassins versant, élevage, milieux urbain et rural. Bull du réseau érosion 20(2), 332-34.

ANNEXES

Table 4: Summary table of the different sample collection coordinates.

Sample code	Coordinate system (DMS)	Altitude (m)	Name of the rock sample	Locality
G01	N03°51'21,76" E11°28'14,14"	812±11m	Migmatites	Akouandoue
G02	N03°51'51,31" E11°28'1,3"	818±9m	Migmatites	Carrefour Akouandoue
G03	N03°51'50" E11°27'55"	915±12m	Migmatites	Mezesam I
G04	N03°53'48,57" E11°26'21,32"	832±5m	metadiorites	Leboudi 1 quarry
G05	N03°52'33" E11°24'46,60"	755±5m	metadiorites	Fam-Assi
G06	N03°52'34,10" E11°24'52,2"	740±5m	Migmatites	Fam-Assi
G07	N03°52'30,76"	723±5m	Migmatites	Fam-Assi
G08	N03°52'50,31"	766±4M	Migmatites	Fam-Assi
G09	N03°53'13,61" E11°26'47,78"	776±4m	migmatites	Fam-Assi
G10	N03°51'5,97" E11°27'50,35"	753±4m	Migmatites	Oyomabang
G11	N03°48'47,27' E11°25'57,78	744±5m	Migmatites	Arab contractor
G12	N03°48'23,54" E11°26'13,57"	713 ±4m	Migmatites	Mbadoumou
G13	NO3°47'57,59' E11°26'20,92"	753±4M	Migmatite	Bibong-Bidoum
G14	N03°53'45,35" E11°29'40,45"	799±4M	Migmatites	Mbankolo
G15	N03°53'40,87" E11°28'1,94"	784±4m	metadiorites	Afeumenor
G16	N03°50'39,14" E11°30'19,84"	766±4m	migmatites	Old Mvolye basilica quarry
G17	N03°47'33,51" E11°26'31,27"	704±3m	migmatites	Nsaa
G18	N03°46'40,46" E11°24'47,36"	745±5m	migmatites	Nomayos quarry

Table 5: Foliation planes measurements and some fractures direction

N°	Trend	Dip	Plunge	N°	Trend	Dip	Plunge
1	28	12	ESE	33	41	38	NW
2	26	20	WNW	34	47	34	NW
3	140	66	NE	35	45	40	NW
4	140	18	NE	36	48	40	NW
5	171	12	WSW	37	74	10	SSE
6	152	20	ENE	38	82	10	SSE
7	176	64	ENE	39	85	05	SSE
8	171	62	ENE	40	62	13	SSE
9	39	40	NW	41	72	10	SSE
10	28	19	WNW	42	85	8	SSE
11	26	17	WNW	43	80	8	SSE
12	44	16	NW	44	78	7	SSE
13	47	18	NW	45	76	6	SSE
14	30	17	NW	46	76	6	SSE
15	38	10	NW	47	83	03	SSE
16	18	20	WNW	48	10	14	WNW
17	138	32	NE	49	12	26	WNW
18	135	62	SW	50	17	20	WNW
19	56	30	NW	51	38	10	NW
20	50	36	NW	52	152	60	SW
21	46	40	NW	53	151	29	SW
22	45	37	NW	54	159	40	SW
23	48	38	NE	55	146	30	SW
24	44	39	NW				
25	40	40	NW				
26	39	38	NW				
27	44	33	NW				
28	44	42	NW				
29	43	35	NW				
30	46	44	NW				
31	50	35	NW				
32	49	37	NW				

Some fracture direction	
1	120
2	166
3	10
4	N010E
5	N036E
6	N108E
7	N102E
8	N146E
9	N30E
10	N120E
11	N40E
12	N150E
13	N110E
14	N098E
15	N142E
16	N010E
17	N160E
18	N146E
19	N142E
20	N148E
21	N070E
22	N068E